JPRS-UMS-92-005
26 MARCH 1992

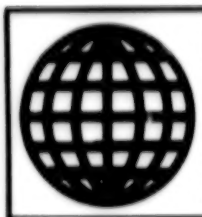

FOREIGN
BROADCAST
INFORMATION
SERVICE

JPRS Report

Science & Technology

Central Eurasia: Materials Science

Science & Technology
Central Eurasia: Materials Science

JPRS-UMS-92-005 26 March 1992

CONTENTS

FERROUS METALS

NONFERROUS METALS, ALLOYS, BRAZES, SOLDERS

NONMETALLIC MATERIALS

PREPARATIONS

TREATMENTS

WELDING, BRAZING, SOLDERING

MISCELLANEOUS

Method of Remote Contactless Monitoring of Changes in Stressed State of Materials

927D0083C Moscow LITEYNOYE PROIZVODSTVO in Russian No 12, Dec 91 pp 9-10

[Article by A.I. Veynik, S.F. Komlik, E.B. Matulis, Engineering Physics Institute at the Belarus Academy of Sciences]

UDC 621.74.08

[Abstract] The properties of the hitherto unknown chronal phenomenon and the possibility of its foundry applications (*Liteynoye proizvodstvo* Nos. 7 & 8, 1991) are examined and illustrated. The principle of the chronal emission generation method in cast iron, steel, and ceramic samples of various shaped is illustrated and the time-frequency relationship during the fracture of samples from pig iron, steel R9, and alundum as well as the dependence of the frequency on time during the sudden relief of load on an alundum pipe are plotted. It is shown that all bodies and processes existing in nature emit chronal fields which affect other bodies, e.g., piezoelectric quartz crystals of a special transducer, and change the pace of all processes in it, making it possible to assess the level of stresses developing in the material. A series of experiments is described in detail and the need for further studies is identified. Figures 6; references 3.

Tribological Evaluation of Thin-Film Copper-Graphite Coatings

927D0034C Minsk TRENIYE I IZNOS in Russian Vol 12 No 7, Sep-Oct 91 pp 843-847

[Article by T.V. Timofeyeva, V.A. Kovtun, and V.B. Shuvalov, Institute of Mechanics of Metal-Polymer Systems, BSSR Academy of Sciences, Gomel]

UDC 621.981:620.22

[Abstract] An experimental study of thin-film copper-graphite coatings on metal substrates was made concerning the dependence of their tribological characteristics on the load pressure and the rubbing speed. The coating material was a mixture of PMS-8 copper power (100-160 μm grain size) and GMP copper-coated graphite granules (100-200 μm size), the total graphite content amounting to 10 wt.%. This mixture was deposited on 0.2 mm thick and 15 mm wide DPRNM copper ribbons and sintered to form 100+/-10 μm thick coatings. Such a coating was tested for performance as lubricant in an SMTs-2 friction machine with a "roller-shoe" pair, a coated copper ribbon lining the shoe and rubbing against a roller. Rollers made of grade-45 plain carbon steel with Rockwell C 44 hardness were used, one with an R_a = 0.3-0.4 μm surface roughness and one with an R_a = 0.10-0.15 μm surface roughness. The contact pressure was varied over the 0.075-0.250 MPa range and the roller speed was varied over the 0.5-1.0 m/s range of linear rubbing velocity. As the measure of the coating wearability, its linear wear rate (μm/h) was selected and removal of the entire 100 μm thick coating within 100 h was selected as the criterion for maximum permissible wear rate. The results of this test indicate that smoothing the roller surface will lengthen the life of such a coating or will maintain its wear rate within the permissible limit at heavier loads and higher speeds. Examination of the rubbing surfaces under a JSM-50A electron microscope has revealed that friction causes formation of a stable boundary layer in the coating. This layer acts as lubricant, but is not continuous while wear only begins. More graphite enters into the friction process and eventually covers almost the entire copper matrix as wear continues. Figures 5; tables 1; references 9.

Neutron and γ-Quanta Emission by Palladium During Impregnation With Gaseous Deuterium

927D0038D Sverdlovsk FIZIKA METALLOV I METALLOVEDENIYE in Russian No 7, Jul 91 pp 176-178

[Article by V.G. Gorodetskiy, B.G. Polosukhin, Ye.M. Sulimov, P.I. Novikov, and V.P. Bychin, Institute of Electrochemistry, Ural Department, USSR Academy of Sciences]

UDC 539:2:539.17

[Abstract] An experimental study of neutron and γ-quanta emission by palladium during its impregnation with gaseous deuterium was made, its purpose being to determine the dependence of both emission flux intensities on the impregnation temperature. Two kinds of palladium specimens were tested: 1) 0.2 mm thick foil of 99.8 wt.% pure Pd weighing 25 g rolled into a 80 mm long cylinder 15 mm in diameter, 2) 80 mm long and 2 mm in diameter wire of 99.9 wt.% pure Pd weighing 6 g. The cylindrical foil specimens were placed in a 12Cr18Ni10Ti-steel flask and the wire specimens were placed in a quartz flask. Each flask was connected to a suction pump for vacuumization and to an injection pump for admission of 99.85 wt.% pure gaseous deuterium under a pressure within the 0.1-0.4 MPa range. Each flask was placed in a heater with a thermocouple for high-precision temperature regulation. The neutron flux emitted by a specimen in two opposite directions symmetrically with respect to the flask was picked up by two parallel plane arrays of 15 CI19N neutron counters, each array placed between two moderator plates of pure polyethylene optimally thick for recording 2 MeV neutrons in the Pd fission spectrum and all counters connected electrically in parallel on the output side. The sensitivity of the recording apparatus to fast neutrons in the 2 MeV energy band was at least 100 pulses/s, upon incidence of one such neutron per cm^2 per second. Thermal neutrons were recorded, after slowdown of fast ones, with an efficiency of about 60 %. The flux of γ-quanta emitted by a specimen in two other opposite directions was picked up by two cylindrical NaI(Tl)

scintillation detectors 63 mm long and 63 mm in diameter, both feeding a common signal to a common FEU-82 photomultiplier. The sensitivity of the recording device to γ-quanta in the 662 keV energy range was 21 pulses/s, upon incidence of one such γ-quantum per cm^2 of detector face area per second, and its efficiency of recording these γ-quanta was about 57 %. The neutron counters and the γ-quanta detectors had been calibrated against a ^{252}Cf-source and a ^{60}Co-source respectively. The preparation of a specimen involved degreasing with alcohol before placement in a flask for degassing under vacuum and simultaneous slow heating to 1000 K. After it had been held at this temperature for 30 min, deuterium was admitted into the flask and the latter with the specimen then slowly cooled to room temperature. The deuterium intake was monitored and thus also the level of palladium impregnation. After impregnation for a 6 h or somewhat longer period, a specimen was subjected to "room temperature - 1000 K - room temperature" cycling while neutrons and γ-quanta emitted by it were being recorded. The readings indicate an emission of not fewer than 2000 neutrons per second and 15,000 γ-quanta per second above the background level at temperatures from 420 K to 570 K, maximum pulse counts being recorded during a 5 s long exposure and pulse counts falling to the respective background levels at temperatures above 570 K. The intensity of neutron emission and the intensity of γ-quanta emission by each specimen were found to be identically temperature-dependent, but the intensity of each emission by Pd wire specimens being more strongly temperature-dependent than that of the corresponding emission by Pd foil specimens. Figures 4; references 3.

Range of Existence of β-Phase in Cu-Al-Zn System

927D0038C Sverdlovsk FIZIKA METALLOV I METALLOVEDENIYE in Russian No 7, Jul 91 pp 161-167

[Article by O.G. Zotov, Yu.N. Koval, S.Yu. Kondratyev, and G.Ya. Yaroslavskiy, Institute of Metal Physics at UkSSR Academy of Sciences and Leningrad State Technical University]

UDC 669.018:620.178

[Abstract] An experimental study of the Cu-Al-Zn system was made concerning the temperature-wt.%(Al,Zn) region of existence of the β-phase, 7.5-10.5 wt.% Al and 0-20 wt.% Zn being known to cover the entire (Al,Zn)- content range of its existence. Three series of these copper alloys with 7.5 wt.% Al, 8.5 wt.% Al, and 10 wt.% Al respectively were produced in an induction furnace with cryolite flux. The true chemical composition of the alloys after homogenizing heat treatment was established by analytical weighing, accurately within +/-0.05 wt.% of each element, and the impurity content was found not to exceed 0.2 wt.%. The temperatures of phase transformation were determined on the basis of dilatometric analysis, also on the basis of metallographic examination, x-ray structural examination, and microhardness test after trial quenches from various temperatures. The results indicate that during slow cooling there occurs reversible eutectoid $\beta \rightarrow \alpha + \gamma$ breakup and, depending on the temperature, either reversible $\beta \rightarrow \beta + \alpha$ or reversible $\beta \rightarrow \beta + \gamma$ transformation. Considering that the temperatures of these two phase transformations depend on the electron concentration, this dependence is evaluated following calculation of the electron concentration and then adequately described by a binomial linear regression equation for the temperature of each transformation. The results are used to construct polythermal sections of the constitution diagram for this ternary system, these sections found to be constitution diagrams of eutectoid alloys very similar to those of the binary Cu-Al system. The data reveal a correlation between the electron concentration and the boundaries of the region within which a stable β- phase exists, martensitic transformation occurring only during quenching from a limited temperature-wt.%(Al,Zn) region of the constitution diagram. They also reveal a quantitative relation between the (Al,Zn)-content in the β-phase and the boundaries of its hardenability range. This relation, expressed in terms of electron concentration and chemical composition, indicates the minimum electron concentration needed for martensitic transformation of the β-phase to occur during quenching in water. Figures 5; tables 1; references 7.

Magnetic, Optical, Magnetooptical Properties and Electronic Structure of Magnetically Hard Fe-Cr-Co Alloys

927D0038B Sverdlovsk FIZIKA METALLOV I METALLOVEDENIYE in Russian No 7, Jul 91 pp 117-122

[Article by Ye.A. Ganyshina, V.S. Gushchin, S.A. Kirov, I.A. Petrunenko, G.P. Samartseva, and V.A. Sein, Moscow State University imeni M.V. Lomonosov]

UDC 669.15'25'26.535.33/34

[Abstract] An experimental study of Fe-Cr-Co alloys for permanent magnets was made concerning the frequency characteristics of their permittivity tensor and the dependence of these characteristics not only on the Co, Fe (transition metals) content but also on both the heat treatment and the thermomagnetic treatment of these alloys. The study involved three cast alloys: 22Cr15Co (22.5 % Cr, 15.0 % Co, 1.5 % Ti, 0.3 % Si), 25Cr15Co (25.0 % Cr, 1.0 % V, 1.0 % Al, 1.0 % Nb), 30Cr22Co (33.0 % Cr, 22.0 % Co, 0.5 % V, 0.5 % Ti, 0.3 % Si, 0.3 % Zr, 0.1 % Ce). They were tested as cast and at various stages of subsequent standard heat treatment: after quenching from 1150°C (22Cr15Co, 25Cr15Co) or 1300°C (30Cr22Co) in water, after thermomagnetic treatment for high coercivity, and after tempering at temperatures within the 620-500°C range. Optical and magnetooptical

properties were measured in reflected light with instruments using a DMR-4 double monochromator. Optical spectra of the refractive index n(hv) and the absorption coefficient k(hv) (h- Planck's constant, ν radiation frequency) were measured by Beattie's polarimetric method over the 3.5-0.5 eV range. Magnetooptical properties were determined on the basis of dynamic measurements of the equatorial Kerr effect in an alternating magnetic field, such a field modulating the magnetization of a specimen and consequently varying the intensity of light reflected by it. The magnet used for this purpose could generate a magnetic field with amplitudes of the order of 400 kA/m. The measurements yielded—in addition to the spectral characteristics of both the refractive index and absorption coefficient, of the equatorial Kerr effect, and of the electrical conductivity, also those of the diagonal components and the nondiagonal components—ε_1', ε_2' of the permittivity tensor $\varepsilon' = \varepsilon_1' = \varepsilon_1' - i\varepsilon_2'$. Metallographic examination revealed that all three alloys in the state as cast had a two-phase structure with the γ-phase uniformly precipitated in the α-phase solid solution. The results of optical and magnetooptical measurements indicate that quenching of these cast alloys has resulted in transformation of their structure into one consisting of the α-phase only, with traces of the γ-phase in some cases, that thermomagnetic treatment has resulted in breakup of the α- phase solid solution into two isomorphous α_1 and α_2 phases with b.c.c. crystal lattices, and that tempering has resulted in formation of a highly disperse structure with an attendant quantitative redistribution of elements leading to (Co,Fe)-enrichment of the α_1-phase and Cr-enrichment of the α_2 phase. Figures 6; references 17.

Problems of Friction and Wear Along Rocket Tracks

927D0034H Minsk TRENIYE I IZNOS in Russian
Vol 12 No 7, Sep-Oct 91 pp 896-903

[Article by V.A. Balakin and O.V. Pereverzeva, Gomel Polytechnic Institute]

UDC 536.12:621.039

[Abstract] Friction and wear along latest rocket flight test tracks are evaluated on the basis of experimental data and theoretical relations. Simulation tests were performed in the multistage launching mode at accelerations of 100-1000 m/s^2, in the free-flight (inertia) mode with a cruise propulsion engine, and in the deceleration mode with a friction brake. Pressure was generated by means of a gas accumulator-compressor with either air type or solid-fuel as the working substance and a cylinder with a piston. Copper and grade-10 plain carbon steel were tested for dependence of the intensity of wear by rail steel during free (constant-velocity) flight on the velocity and on the pressure load. In these tests the velocity was varied over the 120-350 m/s range for copper and over the 150-500 m/s range for the carbon steel while the pressure was varied over the 5-20 MPa range for both. Brake shoes made of the carbon steel were tested for dependence of the friction coefficient on the velocity and on the pressure load. During three brake tests involving deceleration from 150 m/s, 250 m/s, and 500 m/s respectively, measurements were made at several intermediate velocities down to 25 m/s while the pressure was also varied over the 5-20 MPa range. Additional tests were performed concerning the dependence of the intensity of heat release within the contact zone on not only the velocity over the 100-2000 m/s range and on the pressure again over the 5-20 MPa range but also on the friction coefficient over the 0.01-0.04 range. The theoretical analysis of flight simulation for friction and wear evaluation involves the thrust generated by the reaction engine independent of the velocity, the aerodynamic drag force proportional to the velocity squared, and the friction force whose magnitude not only depends on the velocity and on the normal load but also is a function of time since the beginning of motion. Figures 4; tables 3; references 20.

Effect of Tempering and of Heating by Friction on Wear Resistance of Laser-Hardened U8 Steel

927D0034G Minsk TRENIYE I IZNOS in Russian
Vol 12 No 7, Sep-Oct 91 pp 870-878

[Article by A.V. Makarov, L.G. Korshunov, and A.L. Osintseva, Institute of Metal Physics, Ural Department, USSR Academy of Sciences, Sverdlovsk]

UDC 620.18:621.785

[Abstract] An experimental study of laser-hardened and subsequently tempered industrial-grade U8 straight-carbon (0.83 wt.% C) tool steel was made, for the purpose of determining the dependence of its resistance to abrasion and to wear in dry sliding friction on the conditions of tempering and of heating by friction. A batch of 20 mm long square bars (7x7 mm^2) and a batch of 10 mm thick square plates (50x50 mm^2) were first quenched in water from an 810°C furnace temperature, then tempered at 200°C for 2 h, and then ground 0.5 mm deep. One end of a bar and one side of a plate were then etched with aqueous $(NH_4)_2S_2O_8$ solution prior to treatment with an LT1-2M continuous-wave CO_2-laser in a helium jet, the laser radiation forming a rectangular 7x(6-8) mm^2 large spot and the laser power being varied over the 2.8-3.2 kW range. A specimen was passed under the stationary laser beam, its velocity being varied over the 30-50 m/h range and fast heat extraction from below the irradiated surface being facilitated by partial immersion in water. In this way, in one pass a bar was hardened at one end to a 0.8-1.2 mm depth over the entire 7x7 mm^2 area after fusion of a 0.1 m thick surface layer and a 7-8 mm wide zone of a plate was hardened on one side to such a depth with or without fusion of the surface. Some bars were not treated with the laser after having been quench-hardened. All hardened bars and plates were tempered for 2 h, in an oil bath at various temperatures from 75°C to 600°C or in a salt bath at various

temperatures from 250°C to 600°C range, and subsequently cooled in air. Some hardened bars were tempered after having been first additionally cooled to -196°C in liquid nitrogen and some were tempered at 150° for 1-180 min only. The tempering temperature was always held constant, within +/-3°C. Following an x-ray structural examination and microhardness measurements with a TK-2M hardness tester, the working surface of each bar and plate was mechanically ground and electrolytically polished (the 0.1 mm thick fused surface layers thus being removed from the bars) prior to the wear tests. All bars and plates were tested for abrasive wear by 14Al16NM electrocorundum paper and by 81Kr20NM flint paper, with the bar or plate sliding over a clamped sheet of paper. They were also tested for wear in dry sliding friction against a disk of Cr12Mo steel (Rockwell C 62-64 hardness) under a load of 106 N, with the rubbing velocity varied over the 0.05-4.0 m/s range. The duration of this test was 30 min. Tempering at 75°C changed neither the hardness nor the wear resistance of U8 steel, whether laser-hardened or only quench-hardened in water, both having decreased after tempering at higher temperatures. The resistance of both laser-hardened steel and only quench-hardened steel to abrasive wear decreased most appreciably after tempering at temperatures within the 100-250°C range: by a factor of 1.8 to abrasive wear by electrocorundum paper and by a factor of 3.6 to abrasive wear by flint paper. In friction tests at low velocities (0.05-0.10 m/s) heating was insignificant and laser-hardened steel was found to wear much less intensely, by one order of magnitude, than only quench-hardened steel. In friction tests at intermediate velocities (0.28-0.96 m/s) laser-hardened steel was wearing with about the same intensity as only quench-hardened steel after low-temperature tempering, inasmuch as oxide surface layers determining the wear intensity have formed on both steels due to friction. In friction tests at high velocities (1.5-2.7 m/s) seizure caused by heating was found to occur, laser-hardened steel under these conditions wearing less intensely than only quench-hardened steel. At velocities from 2.7 m/s up, with seizure becoming catastrophic, both steels were wearing with a fast increasing intensity. An analysis of the results indicates most resistant to any wear is under-tempered martensite. Figures 5; references 19.

Lengthening Life of Rolling-Contact Bearings by Modification of Their Component Parts With Copper-Base Coatings

927D0034F Minsk TRENIYE I IZNOS in Russian Vol 12 No 7, Sep-Oct 91 pp 862-865

[Article by Yu.I. Kopotya and I.M. Melnichenko, Gomel State University imeni F. Skorina]

UDC 621.822.6

[Abstract] An experimental study of rolling-contact bearings was made which demonstrated the feasibility of lengthening their life expectancy by coating their component parts with copper-base composite material. Fatigue tests were performed on 307 (UR 12) single-row radial ball bearings, their balls and races having been coated each with an about 1 μm thick film of industrial-grade copper-base composite material including some special additives. These bearings were tested for fatigue strength at a speed of 3600 rpm under a radial load of 8500 N, with the inner race under a maximum contact stress of 30-50 MPa. The nominal life under these conditions was 103 h. The duration of a test was determined by fatigue failure, the latter indicated by a sharp rise of the vibration amplitude. Vibrations and noise were measured with a transducer touching the outer race. The probability of failure-free operation was then determined on the basis of the failure probability distribution, its 90 % and 50 % levels, and life distribution histograms. The results of these tests and identical tests performed on plain 307 (UR 12) bearings indicate that such thin plastic coatings lengthen the mean bearing life by 67 %. The surface layer along the groove of the inner race was tested for microhardness after several successive time intervals during a 400 h long running period, the trend of the dependence of its microhardness on the running time indicating how the coating material had modified the characteristics of that surface layer. Its microhardness initially increased almost linearly and much more than in uncoated bearings, evidently due to hardening of the coating and attendant direct deformation of the steel substrate. It continued to increase at a decreasing rate as plastic deformation became gradually destructive, with pores and microcracks building up within microscopically small regions of the steel substrate. The microhardness of the surface layer began to decrease after about 200 h of running time as plastic destruction continued with microdefects merging into microcracks between relatively large carbide grains and brittle fracture of carbides into small particles followed. These carbide particles were found to eventually segregate from particles of the wear product. Factory tests performed on plain and coated 2007124 bearings for agricultural machinery revealed that, while the plain ones failed after 1100 h, the coated ones continued operating much longer. Figures 3; references 5.

Abrasive and Impact-Abrasive Wear of Steels and Alloys in Corrosive Media

927D0034E Minsk TRENIYE I IZNOS in Russian Vol 12 No 7, Sep-Oct 91 pp 855-861

[Article by L.S. Livshits, A.U. Kushekov, and S.M. Levin, Moscow Institute of Petroleum and Natural Gas imeni I.M. Gubkin]

UDC 621.891:620.193

[Abstract] Three plain carbon steels (troostitic-sorbitic grade 20, martensitic grade 45, sorbitic grade 45), three alloy steels (martensitic 20Cr13 with sorbite+Cr_3C_2, austenitic 08Cr18Ni10Ti, martensitic 40Cr13 with

Cr_3C_2), and one nickel alloy (Ni70MoV) were tested for abrasive and impact-abrasive wear under conditions simulating those in the petroleum and natural gas industry. The electromechanical test stand including an electromagnet, a shoe brake, and an electric motor was designed to facilitate not only abrasion by a sliding wheel but also abrasion by a wheel dropping from a height to which it had been lifted. The tests were performed without lubrication, four specimens of each material being so tested. The pressure on the wheel in the sliding tests was varied over the 0.2-2.0 MPa range. The impact energy in the drop tests was varied over the 5-20 J range. Tests were performed in aqueous 3 % NaCl solution and in aqueous 1 N H_2SO_4 solution as well as in air and in water, the duration of each test being 180 min. The results reveal an almost linear pressure dependence of the wear intensity in all media, the slope of the wear-load characteristic depending on both wear resistance and corrosion resistance of the material. While in a noncorrosive medium there is no wear under no load, in a corrosive medium wear begins under no load already. Impact results in a higher wear intensity, evidently attributable not only to a stronger mechanical abrasive action but also to activation of an oxide film removal process with consequent baring of fresh unpassivated surface. Figures 3; tables 2; references 2.

Increasing Wear Resistance of High-Speed and Die Steels by Ionic Nitriding

927D0034D Minsk TRENIYE I IZNOS in Russian
Vol 12 No 7, Sep-Oct 91 pp 848-854

[Article by G.S. Fuks-Rabinovich, V.V. Tikhonychev, N.K. Shaurova, N.V. Kuzmina, A.A. Katsura, V.N. Skvortsov, and S.N. Afanasyev, All-Union Scientific Research and Design Engineering Institute of Electric Crane and Traction Equipment Technology, Moscow]

UDC 621.785.532(73.073)

[Abstract] Ionic nitriding of tool steels for the purpose of increasing their wear resistance was studied experimentally with new equipment which included a bank of electrical resistance heaters. Specimens of two such steels were nitrided, R-6Mo5 (Rockwell C 64-66 hardness) for high-speed cutting tools and Cr12Mo (heat treated to secondary Rockwell C 60-62 hardness) for blanking dies. Ionic nitriding was done with dissociated ammonia gas at 430-500°C temperatures, temperature regulation being facilitated by compound heating. The gas pressure was varied over the 266-660 Pa range and the discharge current being varied over the 3-10 A/m^2 range, the treatment time being varied from 10 min to 6 h. Microstructural examination of nitrided layers was performed under a "Neophot-30" optical microscope with x1000 magnification, "oblique" microsections cut at 5° and 10° angles having been etched with 4 % HNO_3 solution in alcohol. Their phase composition and lattice parameters, also widening of the martensite nitride line, were all determined on the basis of x-ray diffraction analysis in a DRON-3.0 diffractometer. Residual macrostresses were measured by the $\sin^2 \psi$ method with an x-ray tensometer. Microhardness and thickness of the nitrided layers were measured with a PMT-3 hardness tester under a 1 N load. Their toughness was then calculated by the Palmquist method and their plasticity was evaluated on the basis of microindentations. Nitrided Cr12Mo steel was tested for wear in dry sliding friction between a plate of this steel and a roller-ring of U8 steel spinning for 30 min at a speed of 10 rpm, under a Hertz load of 400 MPa simulating typical pressure within the contact zone between punch and die. Nitrided R-6Mo5 steel was tested for wear during lathe operation, various multifacet cutter plates of this steel turning pieces of grade-45 plain carbon steel at a rate of 0.33 mm/rev = 50 m/min for removal of a 2 mm thick layer. On the basis of these tests have been established the conditions of ionic nitriding which will ensure maximum wear resistance of these steels. When cutters made of high-speed steel are nitrided, martensite nitride maximally saturable with nitrogen and sufficiently plastic needs to be formed with high compressive stresses in a short time so as prevent formation of spurious phases. When blanking dies made of high-chromium ledeburite steel are nitrided, martensite nitride needs to be formed more slowly so that it becomes both maximally plastic and very hard with only residual compressive stresses. In this case the martensite nitride is less saturable with nitrogen, owing to formation of intermetallic compounds the amount of which must not exceed 5 %. Figures 2; references 11.

Hydrogen Factor Relating to Wear of Metals in Lubricating Media

927D0034B Minsk TRENIYE I IZNOS in Russian
Vol 12 No 5, Sep-Oct 91 pp 838-842

[Article by L.A. Bronshteyn, Yu.N. Shekhter, Ye.V. Pashkov, and A.Ya. Furman, All-Union Scientific Research Institute of Petroleum Reprocessing, Moscow]

UDC 621.892.099.6

[Abstract] The role of lubricants in hydrogen absorption by metals and the resulting higher intensity of wear by friction was evaluated in an experimental study involving three tests. Four mineral basic lubricants and two synthetic ones (MS-8, M-6, M-9s, IPM-A10; ASV-5, DOS), also ASV-5 with 3 wt.% of a dope (dithiophosphate solution DF-1 or DF-11, PAF-4 containing molybdenum, OTP containing sulfur, TKSF, DFB, MK, MOD) and ASV-5 with 3 wt.% of a corrosion inhibitor (diethanolamide, AKOR-1, SIM, NG-107M, ALOP) were included in the evaluation. For the first test a lubricant coating was deposited on a cantilever plate of 08kp rimmed plain carbon, an aqueous 0.1 M H_2SO_4 solution serving as the electrolyte. The plate was then placed in a special electrochemical cell and made to vibrate flexurally under an alternating pressure load of 150 MPa at a frequency of 500 cpm, the cathode current being monitored throughout the test. The fatigue life of

the plate served as the measure of lubricant effectiveness. The second test was performed in an SMTs-2 friction machine with a roller-shoe pair, a roller of 40Cr alloy steel and a shoe of grade-10 plain carbon steel. For this test the contact pressure was first raised within 1 h stepwise from 1.2 MPa through 1.6 MPa and 2.0 MPa to 2.8 MPa, the pressure being maintained constant at each level for 15 min with the friction pair at rest. The pressure was then maintained for 3 h at the 2.8 MPa level with the roller driven at a speed of 300 rpm, corresponding to a linear velocity of 0.765 m/s, while both the friction moment and the oil temperature were being monitored. Wear was measured by the loss-of-mass method and the amount of absorbed hydrogen was measured by the anodic dissolution method. After this test the shoe was cooled, washed with benzene, weighed, and then placed in a special electrolytic cell with aqueous solution of 12 g/dm^3 KBr and 100 g/dm^3 $NaNO_3$ monoderivative. An anode current of 0.4 A ensured dissolution of a 0.2 mm thick metal layer within 30 min. Gas evolving at the shoe-anode surface which had rubbed against the roller was collected in a microburet, its hydrogen content being then determined with the aid of an LKhM-8MD gas-liquid chromatograph while a Schott filter-separator between the anode space and the cathode space kept out hydrogen evolving at the cathode. The third test, concerning the kinetics of hydrogen absorption by metals during friction, involved direct measurement of the hydrogen flux across a metal membrane in the lubricating medium during friction by a very sensitive new electrochemical method (TEM-2V). An analysis of the data and of the relevant chemical processes indicates that steel can absorb more hydrogen during friction than it can dissolve under static conditions. The principal source of hydrogen is water contained in the lubricant and its absorption by metal is essentially a consequence of corrosion. Under heavy loads at high temperatures, moreover, hydrogen evolves also during oxidation and thermal or tribomechanical decomposition of the lubricant and its components. Even the least effectively wear-reducing basic lubricants contain minimal amounts of water so that hardly any hydrogenation of rubbing surfaces occurs. The hydrogen which does evolve within the high-temperature high-stress contact zone does not, moreover, migrate into the metal but either escapes into the atmosphere or remains trapped in the shavings. Addition of a dope to a basic lubricant, while generally causing the water content to increase, can either stimulate or inhibit hydrogen absorption by a the surface layer of a metal during friction. Tables 2; references 11.

Selection of Tribochemical Suitability Criteria for Aviation Lubricants

927D0034A Minsk TRENIYE I IZNOS in Russian Vol 12 No 5, Sep-Oct 91 pp 833-837

[Article by V.D. Limonchikov, V.M. Kremeshnyy, L.N. Sosulina, and G.M. Gurevich, Central Institute of Aerodynamics imeni N.Ye. Zhukovskiy in Moscow, Riga Higher School of Military Aviation Engineering imeni J. Alksnis, and All-Union Scientific Research Institute of Petroleum Reprocessing in Moscow]

UDC 665.76:621.891

[Abstract] An experimental study of plastic aviation lubricants was made, its purpose being to establish criteria for evaluating their adequacy in shaft-bushing friction pairs on aircraft. Two lubricants, grade 201 (Central Institute of Aviation Fuels and Lubricants) and grade ERA were tested with a friction pair consisting of a shaft (30Ni2CrMnSi steel nitrided, heat treated, chromium-coated) $20f_9$ mm in diameter and a bushing (high-strength 10Al-3Fe-1.5Mn bronze) $20H_9$ mm in diameter. They were tested in a laboratory friction machine simulating the commercial MT-5. Doses of each lubricant weighing 0.035 g were tested for friction reducing and wear reducing action under a moderate 30 MPa constant contact pressure and at a high 0.225 m/s average rubbing velocity, with the temperature of rubbing surfaces allowed to rise from 20°C to 50°C. The amplitude and the frequency of angular oscillations of the rotating shaft were 85° and 1.9 Hz respectively. In the first series of tests were determined the ultimate rubbing "mileage" (km) and the corresponding ultimate lubricant depletion indicators, namely decrease of the amount of dispersing agent and increase of the amount of abraded copper. The amount of dispersing agent was measured by the method of thin-film chromatography. The amount of copper was determined on the basis of x-ray structural analysis in an URS-50IM diffractometer with Cu-line radiation. Wear intensity and thus wear resistance were measured by the loss-of-mass weighing method with a VLR-200 analytical balance. Surface roughness before and after the tests was measured with a Kalibr-296 profilometer. A second series of tests was performed for a study of both lubricant depletion and bronze wear kinetics, the duration of these tests having been set to correspond to various rubbing "mileages" from 0.25 to 0.9 of the ultimate "mileage". On the basis of these tests was then evaluated the dependence of the percentage lubricant depletion α, the friction coefficient f, and the bushing wear intensity I_g (mg/km) on the built up rubbing "mileage" L(km). An analysis of the data for lubricant performance and reliability indicates that ultimate depletion of lubricant and thus need for relubrication are best predicted on the basis of tribochemical criteria such as the amount of metal lost by wear. Figures 4; references 7.

Adhesive Properties of Epoxy Polymers in the Presence of Highly Dispersed Surface-Modified Silicas

927D0078B Moscow LAKOKRASOCHNYYE MATERIALY I IKH PRIMENENIYE in Russian No 6, Nov-Dec 91 pp 21-23

[Abstract of article by S. A. Tishin, B. A. Shipilevskiy, V. A. Tishin, and E. S. Bakayev]

UDC 667.613:539.612:678.643'42'5

[Abstract] Highly dispersed silica fillers were added to an epoxy polymer to determine how the adhesive properties of the polymer would be affected. To make the polymer, bisphenol A-based epoxy resin with a molecular weight of 400 was cured with 10 parts by weight polyethylene polyamine. Three types of silica fillers were used: unmodified A-175 and A-300 Aerosil fillers, TitanAerosil fillers made by the molecular layering of titanium dioxide and simultaneous high-temperature hydrolysis of titanium and silicon chloride vapors, and by making silicon organophillic by replacing surface hydroxyl groups with various types of organic compounds. The fillers had different specific surfaces areas and microparticle surface states. Test patches of the epoxy composition were applied to the surface of a piece of Steel 3, held at room temperature (25°C) for 24 hours, and then heat-treated at 80°C for 3 hours and at 120°C for 8 hours. Standard methodology was used to test normal specimen adhesive strength. Polymer adhesive strength increased regardless of the type of silica added. A concentration of 4 weight fraction A-300 and 6 parts A-175 yielded a peak adhesive strength of about 30 MPa. For the polymers containing the organically modified silicas, maximum strengths between roughly 28 and 38 MPa were reached when silica concentration fell between 4 and 6 weight fraction. The polymers made with titanium aerosil concentrations ranging from 2 to 6 weight fraction had peak strengths of about 30 to about 47 MPa. The highest strength values were associated with the butosil (the 38 MPa mark) and titanium aerosil-36 (47 MPa). The most likely mechanism behind the increase in adhesive strength is a decrease in the concentration of internal stresses and an increase in cohesiveness resulting from additional macromolecular chain packing induced by the surface of the silica filler. Figures 2, tables 1; references 13: Russian.

Choosing Salt Components for Detergents That Simultaneously Pickle and Degrease Aluminum Alloys

927D0078C Moscow LAKOKRASOCHNYYE MATERIALY I IKH PRIMENENIYE in Russian No 6, Nov-Dec 91 pp 27-28

[Abstract of article by V. N. Chernin, L. P. Krykhtina, and V. K. Goydina; All-Union Scientific-Research and Design Institute of Surface-Active Substances of the SintezPAV[Surfactant] Scientific Production Association]

UDC 667.648.12:546.621

[Abstract] Sodium and potassium hydroxides, sodium carbonate, and trisodium phosphate, pyrophosphate, and sodium tripolyphosphate were studied to determine how they affect the pickling action of detergents used to pickle and degrease AMg-2 aluminum alloy strip. The amount of metal consumed and the pickling rate were measured by a method described in another study. A profilograph was used to measure surface roughness. It was found that the pickling rate and surface roughness are optimized (0.08-0.115 g/(m^2 y s) and 1-1.6 μm, respectively) when the detergent is formulated with 0.3% sodium hydroxide, 1 to 1.7% sodium carbonate, 0.5-0.7% of either pyrophosphate or sodium tripolyphosphate, and 0.1% nonionic surfactant (all percentages in terms of mass). Potassium hydroxide can be substituted for sodium hydroxide as long as it does not exceed 50% of the total hydroxide content. A dustless commercial form of the detergent can be produced by combining granulated potassium hydroxide and a liquid solution of caustic soda. Figures 4, tables 1; references 5: Russian.

Encapsulation in Polymer Films and Coatings

927D0078D Moscow LAKOKRASOCHNYYE MATERIALY I IKH PRIMENENIYE in Russian No 6, Nov-Dec 91 pp 29-35

[Abstract of article by A. P. Kondratov]

UDC 667.69:593.219.3

[Abstract] Three advanced processes for encapsulating substances in polymer films and coatings were described in detail. Encapsulation was defined as a process in which particles of a particular substance are encased in a protective coating made from another substance that is physically and chemically inert in regard to the encapsulated substance, thereby isolating the substance particles from the atmosphere (primary purpose) and from one another (secondary purpose). A distinction was made among microencapsulation, encapsulation, and macroencapsulation, with microencapsulation characterized as one of the most promising and fastest-growing areas of chemical technology. Various common applications of encapsulated substances were briefly described. The first process discussed entails the use of rollers, extrusion heads, or similar equipment to apply a layer of either a solution of a polymer composition or a dispersion of an encapsulated substance to a solid surface. A German-patented method of encapsulating insect pheromones was used to illustrate the application of this process. An example of the encapsulation of liquids composed of homogenous polymer solutions was provided by a process patented by the Kurari company of Japan. Finally, the article provided an example of how

an encapsulated substance could be synthesized from two components within a polymer matrix. The descriptions included potential applications of the processes, specific problems associated with a particular process, and the solutions being advanced to overcome these problems. Figures 9; references 18: 16 Russian, 2 Western.

Protective Diamondlike Films on Quartz

927D0070G Moscow FIZIKA I KHIMIYA OBRABOTKI MATERIALOV in Russian No 6, Nov-Dec 91 (manuscript received 11 Mar 90) pp 113-116

[Article by S.M. Klotsman, A.S. Kovsh, L.M. Kovsh, Ye.V. Kuzmina, R.R. Mukhametkhaziyev, S.A. Plotnikov, I.Sh. Trakhtenberg, and L.M. Feygin, Sverdlovsk]

UDC 539.216.2:546.26-162

[Abstract] The authors of the study studied the effect of protective diamondlike films on quartz. The diamondlike films were deposited in a unit equipped with an ion beam sources in the form of a graphite chamber (cathode) in which two copper water-cooled anodes were located. Before the diamondlike films were applied to them, the substrates were cleaned in an ultrasonic alcohol bath and then placed in a vacuum chamber with a vacuum of at least 2×10^{-4} Pa. Both the source and substrate were cleaned in an argon discharge before the diamondlike films were sputtered. The following sputtering conditions were investigated: propane pressure, 8×10^{-3} to 5×10^{-2} Pa; discharge voltage, 1.2 to 2.0 kV; and discharge current, 0.15 to 0.66 A. After the sputtering, the specimens were held in a vacuum for at least 30-40 minutes, after which air was let in. The content of residual gas impurities (oxygen, nitrogen) in the diamondlike films was determined by the method of nuclear reactions on a deuteron beam with an energy of 900 keV and determined to not exceed 0.1%. The optical properties of the diamondlike films were studied by the spectrophotometric method on Hitachi-340 and Beckman-T-1100 spectrophotometers. The thickness (h), refractivity (n), and absorption (k) of the said films were determined in the range from 0.4 to 2.5 μm. The optical constants (n and k) were found to be virtually independent of the sputtering conditions. The value of n was found to depend on the substrate material: The diamondlike films on germanium substrates had a higher refractivity than those on quartz (2.17 +/- 0.06 and 2.02 +/- 0.04, respectively). The absorption of the diamondlike films was found to decrease as the wavelength increased. The rate at which the diamondlike film were deposited onto the germanium substrates was somewhat slower ($\leq$10%) than the rate found in the case of the quartz substrates. When the pressure was kept constant, the deposition rate was found to increase as discharge current increased. The diamondlike films were found to have a pronounced protective effect on the quartz substrates to which they were applied. Specifically, they resulted in a 1.5-fold reduction in the friction coefficient, a severalfold increase in stability when rubbed against abrasive particles, and increased resistance to moisture and heat shock (as well as to heating up to 200°). Figures 3, tables 2; references 6: 5 Russian, 1 Western.

Properties of Polycaproamide-Based Coatings With Polymer Filler

927D0078A Moscow LAKOKRASOCHNYYE MATERIALY I IKH PRIMENENIYE in Russian No 6, Nov-Dec 91 pp 13-14

[Abstract of article by D. I. Pishev, VKhTI, Sophia, Bulgaria, and N. I. Angelova, IPGIV, Vidin, Bulgaria]

UDC 667.613:678.675.126

[Abstract] The use of low-density polyethylene powder as an additive to modify the properties of polycaproamide coatings was studied. Powder compositions produced by dry-mixing polyethylene and polycapromide powder stock were used to apply the coatings, which were sprayed from a fluidized bed onto a metal substrate heated to 593 K and cooled in air or water at 293 K or in silicone oil at 433 K. The powder stock, which had a particle size of 150-250 μm, was produced by cryogenically grinding the granulated form of glossy virgin BDS [Bulgarian Standard] 14259-80 low-density polyethylene with a melting temperature of 490 K and OB-2-102-grade polycaproamide, BDS 10086*72, with a melting temperature of 382 K. The adhesive strength was measured per German Industrial Standard 53232, and mechanical properties per GIS 30016 with the aid of equipment made by the Erickson company. The addition of the polymer in quantities up to 5 wt. % had a positive effect on coating adhesive strength. In coatings that contained between 5-10 wt. % polyethylene, hardness and resistance to abrasion increased, while adhesive strength decreased slightly due to internal stresses arising from crystallization. Impact resistance was lower than in coatings without the filler. It was concluded that adding the polyethylene to the polycapromide improved coating wear resistance without appreciably affecting adhesive strength as long as polyethylene concentration did not exceed 10 wt. %. The improvement in the mechanical properties of the coatings was largely attributed to increased structural homogeneity in the polycaproamide, which resulted from the distribution of the polyethylene in the amorphous and defective regions of the polycaproamide, and to the particular crystallization mechanism of this type of polymer composition. Figures 2; references 7: 6 Russian, 1 Western.

Electric Resistance of $Fe_{0.82}Si_2$-MoO_3-Glass Composites With Eutectoid Transformation in Higher Iron Silicide

927D0076E Kiev POROSHKOVAYA METALLURGIYA in Russian No 12(348), Dec 91 pp 35-39

[Article by S.I. Vecherskiy, F.A. Sidorenko, Urals Polytechnic Institute]

UDC 669.018.9:669.15'782:537.311.3

[Abstract] The effect of the physical and chemical processes occurring during the manufacturing of metal-glass composites on their properties is discussed and the results of an investigation of a model system of $Fe_{0.82}Si_2$-MoO_3-Glass with iron disilicide (leboit) used as the metallic component are presented. The effect of the eutectoid decay in iron disilicide on the electric resistance of the above composition is examined and leboit's contribution to resistance is assessed. To this end, the temperature dependence of resistivity of samples sintered at 1,200K for 15, 30, and 60 min at various annealing temperatures is plotted and the samples' resistivity at 300K as a function of the sintering and annealing duration is summarized. The temperature dependence of resistivity of samples sintered at 1,200K without subsequent heat treatment is approximated and the parameters of linear approximation are cited. The phase composition of the samples is examined by a DRON-3 X-ray diffractometer; the analysis reveals an intensive interaction among components in samples sintered at 1,200K without subsequent annealing resulting in a decrease in the peaks and the development of FeSi and $BaMoO_4$. The formation of the granular structure substantially limits the effect of eutectoid transformation on the composites' resistivity; granular structures forming as a result of the interaction among the components permeate the entire sample volume and form a conducting "grid" which "short-circuits" leboit, so the effect of α-$Fe_{0.82}Si_2$ and the products of its eutectoid decay is substantially lower than in a system with weakly interacting components. Figures 1; tables 2; references 9: 7 Russian; 2 Western.

An Investigation of the Destruction of Composite Materials by Laser Radiation and a Supersonic Nitrogen Flow

927D0070F Moscow FIZIKA I KHIMIYA OBRABOTKI MATERIALOV in Russian No 6, Nov-Dec 91 (manuscript received 13 Jul 90) pp 58-65

[Article by A.A. Betev, V.T. Karpukhin, M.M. Malikov, and N.I. Shalnova, Moscow]

UDC 539.4:678.067

[Abstract] The authors of the study examined the combined effect of laser irradiation and a supersonic nitrogen flow on samples of a composite material with a phenolformaldehyde binder. Test specimens of standard layered carbon-filled plastic with reinforcing fiber and porous chlorosulfonated polyethylene with a filler were subjected to laser radiation (λ = 10.6 μm; W = 10^2-10^4 W/cm^2) falling perpendicular to the specimen surface as the velocity vector of a supersonic nitrogen flow was directed along the same surface at the same time. The time for which both types of effects were used was varied within a rather broad range (3 to 20 seconds in the case of the radiation and 10 to 30 seconds in the case of the nitrogen flow). The experiments were performed on a stand that included a supersonic wind tunnel to blast the specimens and a continuous-wave CO_2 laser with a power up to 20 kW. The nitrogen was heated in a special heat exchanger to 1,300-1,500 K and was accelerated to supersonic speeds in a jet device. When the test specimens were subjected to both the laser irradiation and the hot nitrogen flow, the depth of burnthrough increased sharply. The experiments indicated that the most likely mechanism of the destruction of the test materials that occurs upon the combined effect of laser radiation and a nitrogen flow is one of pyrolysis of the binder due to the effect of the laser irradiation and "deburring" of the surface layer by the supersonic flow. Additional experiments were conducted to examine the separate effects of laser irradiation and blasting with a supersonic nitrogen flow. These experiments indicated that the radiating power and duration of the laser irradiation were most responsible for the sharp increase in depth of burnthrough of the test specimens that was observed. Figures 5; references 5 (Russian).

Improving Grey Cast Iron's Mechanical Properties, Impermeability, and Corrosion Resistance

927D0083F Moscow LITEYNOYE PROIZVODSTVO in Russian No 12, Dec 91 p 23

[Article by M.U. Zhanybekov, Semipalatinsk Reinforcement Works]

UDC 621.74'669.131.6

[Abstract] Pearlitization of the SCh 15 grey cast iron pipeline fittings in order to improve the mechanical properties, impermeability, and corrosion resistance of gate valves is outlined in detail and the smelting procedure and alloying additions and their concentrations are described. The mechanical and operating properties of two types of grey cast iron are summarized and it is shown that cast iron microalloying with boron helps to increase the strength and h' 'ness and decrease the graphite precipitate inclusion length; the use of ferroboron for 6 months made it possible to save more than 35,000 rubles. Furthermore, addition of a small amount of boron (0.02-0.05%) substantially improves the physical, mechanical and operating properties of cast iron. Tables 1; references 1.

Making Complex Cast Iron Ingots by Continuous Casting Method With Differentiated Heat Removal

927D0083A Moscow LITEYNOYE PROIZVODSTVO in Russian No 12, Dec 91 pp 4-6

[Article by V.S. Shumikhin, M.V. Zhelnis, IPL at the Ukrainian Academy of Sciences and Tsentrolit Foundry, Kaunas]

UDC 621.74.002.6:669.13

[Abstract] A report to the Fifty-Eighth International Congress of Foundry Work.rs in Krakow. During continuous horizontal casting of complex ingots, the solidification rates are nonuniform in the transverse direction. The measures proposed for eliminating these differences as well as regulating the heat removal from individual elements of the ingot both in the transverse and longitudinal direction are outlined. They include using composite molds consisting of a graphite molding insert and a sectional water-cooled metal housing and regulating the heat flux from the molten cast iron to the cooling water with the help of liners and coating between the insert and the housing as well as leaving gas vents. The relationship between the heat removal rate and adjusted ingot thickness as a function of the metallostatic head is established and the dependence of the solidifying layer thickness, ingot surface temperature, and solidification rate on the length of the ingot state in the mold, the dependence of the ingot extraction speed on the heat flux ratio on the narrow and wide faces, and the dependence of the heat exchange rate on the change in the gas vent size are plotted. It is shown that the use of the suggested procedures and selection of cooling conditions make it possible to increase the continuous casting process yield and produce more than 150 standard sized of complex-shaped ingots. Software and instructions for computer analysis and design are available. Figures 4; tables 1.

Effect of Pulsing Sintering Waste Gas Exhaust Condition on Sintering Process

927D0082A Moscow IZVESTIYA VYSSHIKH UCHEBNYKH ZAVEDENIY: CHERNAYA METALLURGIYA in Russian No 9, Sep 91 pp 5-7

[Article by Ye.F. Vegman, A.N. Pyrikov, A.R. Zhak, S.D. Filimonov, Moscow Institute of Steel and Alloys]

UDC 622.785.001.5

[Abstract] The use of the pulsing gas motion condition in the sintered layer—one of the reserves for intensifying the sintering process—is analyzed and the sintering process of a burden which is similar in composition to that of the Cherepovets Integrated Iron and Steel Works and consists of iron ore concentrates of the Olenegorsk and Kovdor Ore Dressing Combines, coke breeze from Pechora basin coal, and limestone is investigated in detail. The pulsing sintering gas exhaust condition was developed by a mechanical pulser installed in the gas vent; the pulser was turned on between the first and fourth minute after the completion of the sinter ignition; the pulsing operation duration was also varied. The effect of the pulsing condition on the usable sinter yield, non-sintered fines yield, vertical sintering rate, and specific output of the sintering unit is summarized and the effect of the pulsing duration on the total sintering duration, vertical sintering rate, and specific yield is plotted. An analysis demonstrates that sintering of the charge, whose composition corresponds to the Cherepovets Integrated Iron and Steel Works sinter, in a pulsing mode at a 4 Hz pulsing frequency makes it possible to increase the vertical sintering rate and the specific yield of the sintering unit by 30-40% at the same total sinter yield and quality. Figures 2; tables 1; references 5.

Delayed Fracture of Maraging Steels

927D0038F Sverdlovsk FIZIKA METALLOV I METALLOVEDENIYE in Russian, No 7, Jul 91 pp 5-11

[Article by I.S. Toydorova, V.V. Zabilskiy, and V.I. Sarrak, Institute of Engineering Physics, Ural Department, USSR Academy of Sciences]

UDC 539.374:669.15-194

[Abstract] Theoretical and experimental research done so far on delayed fracture of maraging steels, namely brittle and predominantly intergranular fracture after incomplete aging under a static load within a certain

temperature range, is comprehensively reviewed with emphasis on the kinetics of such a fracture and on the effect on it of alloying elements as well as of the medium in these steels have been tested. The review covers data pertaining to Ni-Co-Mo steels (Ni18Co16Mo4Ti, Ni18Co15Mo7Ti, Ni18Co13Mo4Ti2, Ni18Co12Mo4Ti2, Ni18Co11Mo4Ti, Ni18Co11Mo3Ti, Ni18Co9Mo5Ti, Ni18Co8Mo5Ti, Ni17Co15Mo6Ti, Ni14Co15Mo7, Ni14Co10Mo10, Ni13Co15Mo10, Ni13Co12Mo4Ti), Ni-Cr-Mo steels (Ni12Cr3Mo2Ti, Ni14Cr3Mo2Ti, Ni12Cr3Mo2Ti), Ni-Cr steels (Ni10Cr3Ti), Ni-Mo steels (Ni18Mo4TiAl), and Ni-Ti steels (Ni20Ti2, Ni15Ti2, Ni10Ti2). They were aged at temperatures ranging from 300°C to 575°C for periods of time ranging from about 1 min to about 100 h. They were tested for rate of crack growth during aging, also for ultimate strength and percent elongation under tension. These tests were performed under vacuum, in air, and in a hydrogen atmosphere with temperatures varied in some cases (N18Co12Mo4Ti2 steel) as widely as from -80°C to +160°C. The results reveal that the proneness of these maraging steels to delayed fracture depends on their chemical composition: especially on the Ti-content, less on the Co-content, and almost not at all on the Mo-content. Such a fracture was found to occur after incomplete aging at temperatures within the 410-450°C range, with maximum proneness to embrittlement after aging at 410°C for about 28 h. The results of electrical resistance measurements indicate that embrittlement of these steels is due to precipitation of intermetallic compounds such as Ni_3Ti with a f.c.c. crystal lattice during the initial aging stage. Delayed fracture of steel specimens with an already initiated fatigue crack was found to occur only in air and in a hydrogen atmosphere, not under vacuum. Figures 7, references 26.

Corrosion-Resistant Nitrided Austenitic Steel

927D0038E Sverdlovsk FIZIKA METALLOV I METALLOVEDENIYE in Russian No 7, Jul 91 pp 179-183

[Article by I.I. Kositsyna, V.V. Sagaradze, O.N. Khakimova, and Yu.I. Filippov, Institute of Metal Physics, Ural Department, USSR Academy of Sciences]

UDC 669.15'26'74-194

[Abstract] An experimental study of 04Cr18Mn15V2Mo2 aging austenitic steel was made involving mechanical and corrosion tests after it has been surface hardened by nitriding instead of carburizing, this steel than containing 0.4 wt.% N besides 0.04 % C so that carbonitrides could have formed. The steel was produced in an induction furnace. Ingots weighing 10 kg were forged and rolled into 10x10 mm^2 blank bars. These were quenched from temperatures covering the 1000-1250°C range and then aged at temperatures covering the 600-700°C range for 1-20 h at each. Structural examination by the method of thin foils was performed under a JEM-200CX transmission electron microscope and fractography was performed under a JEM-U3 scanning electron microscope. Tensile tests were performed by standard methods on round bars 3 mm in diameter. Tests for corrosion cracking in aqueous 3.5 % NaCl solution were performed on 60 mm long 10x10 mm^2 cantilever bars with an already formed 3 mm-deep fatigue crack and under a bending load, these tests lasting for 2800 h. The results indicate that this steel case hardened by nitriding is, owing to dispersion hardening, a high-strength steel with a yield strength $\sigma_{0.2\%} \geq 850$ MPa and a percentage elongation $\delta \geq 25$ %. It retains a high corrosion resistance in aqueous 3.5 % NaCl solution under bending stresses up to 1000 MPa. Figures 3; tables 1; references 10.

Dependence of Internal Friction in Austenitic Steel on Conditions of Deformation and Heat Treatment

927D0038G Sverdlovsk FIZIKA METALLOV I METALLOVEDENIYE in Russian No 7, Jul 91 pp 184-187

[Article by V.A. Pavlov, M.V. Popov, V.P. Ketova, V.S. Vakhrusheva, S.V. Atanasov, and V.I. Shalayev, Institute of Metal Physics, Ural Department, USSR Academy of Sciences]

UDC 669.15'24'26'-195

[Abstract] An experimental study was made concerning internal friction in austenitic steel after cold working with or without high-temperature annealing. Tubes of industrial-grade 02Ni15Cr16 steel, 200 mm long and 6.9 mm in diameter, were cold rolled in a mill with two pairs of cylinders sufficiently close one behind the other to ensure interaction of the two respective stress and strain fields. Internal friction during vibrations at a frequency in the 2800 Hz band was measured after plastic deformation to a high level of true strain ($\varepsilon = 5.9$) and then after final annealing at 1000° for 1 h. Some tubes had been cold rolled without intermediate annealing between passes, others with one intermediate annealing heat treatment at 1050°C or with three such intermediate heat treatments. All tubes were tested for internal friction at temperatures covering the 20-700°C range and the temperature dependence of Q^{-1} (ratio of energy dissipated per vibration cycle to 2π times average energy stored) was found to include several "grain boundary" peaks about successively higher temperatures, their number as well as their heights and widths depending on the number of intermediate heat treatments: two peaks after cold rolling without intermediate heat treatment, three peaks after cold rolling with one intermediate heat treatment, four peaks after cold rolling with three intermediate heat treatments. Cold rolling in a standard mill with standard heat treatments such as only final annealing at 1200°C for 4 h is shown to ensure a more stable state of stress and strain with only one "grain boundary" peak of internal friction about 470°C. Cold

rolling in a two-row mill with final annealing at 1200°C for 4 h and no intermediate annealing is shown to ensure even more stability, by producing most nearly perfect grain boundaries and thus impeding relaxation, so that internal friction passes through only one "grain boundary" peak about 575°C and a thus even higher temperature. Figures 2; references 11.

Effect of Screw Rolling Conditions on Wear of Piercing Mandrels

927D0082E Moscow IZVESTIYA VYSSHIKH UCHEBNYKH ZAVEDENIY. CHERNAYA METALLURGIYA in Russian No 9, Sep 91 pp 48-50

[Article by N.M. Vavilkin, V.A. Popov, A.M. Stepashin, Moscow Institute of Steel and Alloys]

UDC 621.774.35

[Abstract] The issue of increasing the strength of piercing mandrels in making hollow products with a small inside diameter by the screw rolling method is addressed and an attempt is made to determine the effect of screw rolling conditions on the wear of piercing mandrels with a small diameter. The study is performed in a MISiS-130D screw rolling mill with barrel-shaped rolls using blanks from corrosion-resistant steel 40Kh13. The piercing mandrel rod is made from the EP-437B nickel-based high-temperature alloy. Three-to-five blanks are pierced in each point of the factor space, then the value of wear per pass is averaged. The effect of the roller feed angle on the piercing mandrel rod, the effect of the piercing mandrel rod extension beyond the roller neck on wear, and the dependence of the roller spin rate on the piercing mandrel wear is examined and plotted. Experiments show that the blank temperature has an ambiguous effect on wear and should be determined separately for each piercing condition. They also demonstrate that in order to decrease the piercing mandrel wear, it is necessary to increase the feed angle, speed up the roller spin, and decrease the piercing mandrel tip extension beyond the roller neck as much as possible. In general, the mandrel wear increases with the billet temperature. Figures 4; tables 1; references 6

Results of Statistical Analysis of Smelting Method's Effect on Steel Properties

927D0082D Moscow IZVESTIYA VYSSHIKH UCHEBNYKH ZAVEDENIY. CHERNAYA METALLURGIYA in Russian No 9, Sep 91 pp 28-31

[Article by L.A. Kuznetsov, A.M. Korneyev, V.V. Ryabov, Lipetsk Polytechnic Institute]

UDC 621.771.06

[Abstract] The results of a statistical analysis of the effect of steel making process parameters on the quality of steel are presented; to this end, process data on 719 coils of steel produced by standard technology according to GOST 9045—80 are used in the study. The yield point, ultimate strength, elongation, HRB hardness, Erichsen indentation depth, and the probability of producing surface finish I or II for each coil are used as output data and their correspondence to GOST 9045—80 is used as the quality criteria. The probability of producing the required properties for given scrap volume ranges and the probability of producing the required qualities for given silicon concentration ranges in pig iron are summarized and the dependence of the probability of producing steel which meets the requirements imposed on the mechanical properties on the oxygen blasting duration range and the amount of manganese added is plotted. The joint distribution of the amount of added lime and yield strength is summarized. This distribution paints the most complete picture of the statistical interrelation of various factors and makes it possible to estimate the level of output parameter values at various levels of the particular factor under study. The level of output properties is largely determined by the ranges of given process factors. These ranges are not equal in magnitude or the number of experiments which fall within them, so the problem of selecting the optimum range boundaries for each process factor which would maximize the probability of attaining the requisite output parameters remains urgent. Figures 1; tables 3; references 2.

Nonmetallic Inclusion Composition at Nucleation Moment During Steel Deoxidation by Aluminum

927D0082C Moscow IZVESTIYA VYSSHIKH UCHEBNYKH ZAVEDENIY. CHERNAYA METALLURGIYA in Russian No 9, Sep 91 pp 20-22

[Article by A.I. Preobrazhenskiy, A.F. Vishkarev, Yu.I. Nebosov, A.V. Dub, Moscow Institute of Steel and Alloys]

UDC 669.046.554

[Abstract] Conventional concepts of the deoxidation process are reviewed and their validity is questioned, consequently, the conditions of oxide phase formation at the stage of aluminum dissolution are investigated assuming that there are no substrates facilitating the oxide phase nucleation present on the deoxidizing agent surface. The oxide phase nucleation equation is derived and analyzed and the most likely composition of the oxide phase nucleus consisting of a FeO-Al_2O_3 perfect solution is calculated. The change in free energy during the critical nucleus formation with various FeO concentrations and the change in free energy during the formation of critical nucleus with the most likely composition in the aluminum dissolution zone are plotted. The conclusion is drawn that regardless of whether or not there is an oxide film on the surface of aluminum or whether it is added in the liquid or solid state into the melt, local oversaturation spots sufficient for uniform oxide phase nucleation may develop at the initial deoxidation stage. The thermodynamic model of the deoxidation product

formation at the aluminum dissolution stage demonstrates that the formation of oxide with a high FeO concentration is most likely; the results also attest that the melt oxidation degree has a dominant effect on the deoxidizing agent emulsification. Figures 2; references 5: 4 Russian; 1 Western.

Steel-Making Pig Iron Desiliconization During Interaction With Solid Oxidants

927D0082B Moscow IZVESTIYA VYSSHIKH UCHEBNYKH ZAVEDENIY: CHERNAYA METALLURGIYA in Russian No 9, Sep 91 pp 8-10

[Article by V.I. Shatokha, A.A. Gimmelfarb, V.M. Snagovskiy, O.V. Sotsenko, Yu.P. Martynov, Dnepropetrovsk Metallurgical Institute]

UDC 669.162.267.64

[Abstract] The importance of finding efficient reagents for removing silicon from molten pig iron and lowering its concentration to below that of steel-making pig iron in order to develop economical out-of-furnace refining methods and ensure specified cast iron composition and properties is stressed. The efficiency of pig iron desiliconization by rolling mill scale, iron ore concentrate, oxide and carbonate manganese ore, and chromate nickel ore was evaluated. To assess the effect of the resulting slag composition on the outcome of desiliconization, the reagent was mixed with lime and calcium fluoride in some experiments. The desiliconization efficiency was assessed by two indicators: the absolute change in the silicon content in pig iron and the ratio of this indicator to the specific rate. The experimental conditions, the chemical composition of pig iron and slag, and the desiliconization efficiency are summarized and the effect of the slag basicity on the silicon and manganese distribution between pig iron and slag during the mill scale and iron ore concentrate (ZhRK) treatment and the effect of the silicon content in pig iron on the proportion of area occupied by white, grey, and mottled cast iron in the casting fracture are plotted. The results confirm that pig iron refining out of furnace with the help of iron ore materials makes it possible to decrease the silicon concentration in steel-making pig iron to 0.3%, thus considerably increasing its chilling and expanding its applications. Figures 2; tables 3; references 4: 3 Russian; 1 Western.

Gaseous Phase Monitoring in Investigations of Equilibrium in Systems Typical of Pyrometallurgy of Heavy Nonferrous Metals

927D0084A Sverdlovsk RASPLAVY in Russian No 5, Sep-Oct 91 pp 9-13

[Article by I.E. Makhov, S.V. Mikhaylov, A.V. Tarasov, Gintsvetmet Institute, Moscow]

UDC 669.4:541.6

[Abstract] The role of the gaseous phase in general and partial pressure in particular in the system of its principal components—oxygen and sulfur—at all stages of the pyrometallurgical process is discussed and the issues of monitoring and controlling partial oxygen and sulfur pressures in examining the matte-slag-gas system are considered. A procedure for calculating the equilibria in the gaseous phase is developed on the basis of the method of minimizing the system's free energy; using the procedure, a number of gas mixtures used in the experiments is investigated and the applicability range of each of them is determined. Logarithmic partial pressure diagrams of binary and ternary gas mixtures with and without SO_2 are plotted and the behavior of the oxygen and sulfur pressure in the SO_2-Ar and SO_2 systems with an addition of sulfur in the form of the S_2 gas is examined. The method of controlling the gaseous phase with the help of SO_2-Ar and SO_2-N_2 mixtures is analyzed in detail and it is demonstrated that the partial pressures of oxygen and sulfur in the system can be controlled by manipulating the SO_2:Ar(N_2) ratio. It is noted that for safety's sake, it expedient to use the explosive gases (CH_4, CO, and H_2S) contained in ternary systems in a mixture with inert gases, e.g., nitrogen, rather than in a pure form. Figures 4; references 13: 3 Russian, 10 Western.

Processing of Secondary Lead-Containing Raw Material

927D0084B Sverdlovsk RASPLAVY in Russian No 5 Sep-Oct 91 pp 14-21

[Article by G.F. Kazantsev, N.M. Barbin, L.Ye Ivanovskiy, Electrochemistry Institute at the Urals Branch of the USSR Academy of Sciences]

UDC 669.714.2:669.21/235.42

[Abstract] It is argued that since lead-acid battery manufacturers are the leading consumers of lead and the demand for lead batteries continues to rise while spent lead batteries pose a serious environmental and aesthetic threat to society, the issue of battery lead recovery dominates the field of secondary lead refining in general. Ways of refining secondary lead raw materials are considered and the conclusion is drawn that pyrometallurgical (blast smelting, smelting in rotary kilns, and smelting in KEPAL-ZhV units) and hydrometallurgical methods as well as recovery from ionic solutions are all suitable, but the latter method is more ecologically clean than the first two. The proposed technology is recommended for small and medium-sized secondary lead raw material refining volumes and is protected by patents. References 25: 17 Russian, 8 Western.

Estimating Short-Range Order Parameter of Binary 3*d*-Metal Melts With Ge and Al

927D0084C Sverdlovsk RASPLAVY in Russian No 5, Sep-Oct 91 pp 22-25

[Article by Ye.S. Levin, P.V. Geld, Urals Polytechnic Institute imeni S.M. Kirov]

UDC 669.783:669.715'1'24'25

[Abstract] Methods of estimating the close-range order parameters of 3*d*-transition metals and their melts with germanium and aluminum which are characterized by structural microinhomogeneities are considered and it is shown that data on the enthalpy of formation, hydrogen solubility, and molar volumes sensitive to the change in the close-range order structure are especially convenient for these purposes. To examine the close-range order structure, X-ray and electron scattering curves are plotted and compared to the diffraction characteristics of crystal samples; radial atomic distribution is calculated and analyzed; and intensity curves established on the basis of various hypothetical structural models are analyzed theoretically and compared to experimental curves. As a result, the concentration dependence of the close-range order parameters in binary melts of chromium, iron, cobalt, and nickel with germanium and aluminum is established. It is shown that the knowledge of the close-range order parameter η and its dependence on the composition makes it possible to predict the behavior patterns of other properties. Tables 3; references 6.

Electrodeposition of Germanium From Tungstate-Germanate Melts

927D0084D Sverdlovsk RASPLAVY in Russian No 5, Sep-Oct 91 pp 39-43

[Article by K.P. Tarasova, A.N. Baraboshkin, A.Yu. Khvatov, Z.S. Martemyanova, S.A. Ganeyev, N.L. Oparina, Electrochemistry Institute at the Urals Branch of the USSR Academy of Sciences]

UDC 541.135.3:546.286

[Abstract] Production of germanium by electrolytic deposition is discussed and the possibility of producing germanium coats by electrolyzing tungstate melts with additions of germanium oxide compounds is considered. To this end, the products deposited on the cathode during the electrolysis of Na_2WO_4-Na_2GeO_3-WO_3 at an 850-900°C temperature in an atmosphere of air on nickel, molybdenum, tungsten, and graphite substrates is

investigated in an Alundum container. A soluble germanium anode is used for this purpose. A radiographic analysis of the cathode residues makes it possible to delineate the concentration domains of electrochemical tungsten and germanium deposition. A DRON-3 X-ray diffractometer, a Neofot-2 metallographic microscope, and a Camebax X-ray microanalyzer are used in the study. Experimental data point towards poor germanium-containing salt dissolution in tungstate melts and indicate that in a pure form, germanium is deposited only from tungstate-germanate melts which do not contain tungsten trioxide or contain only small quantities of it while tungsten is deposited from melts with a high tungsten trioxide concentration. Figures 2; references 13: 7 Russian, 6 Western.

Corrosion-Electrochemical Behavior of Fe-Al Alloys in Molten Alkali Metal Carbonates

927D0084E Sverdlovsk RASPLAVY in Russian No 5, Sep-Oct 91 pp 50-55

[Article by V.I. Yelkina, V.Ya. Kudyakov,, A.A. Pankratov, O.P. Penyagina, V.D. Antonov, V.G. Zyryanov, Electrochemistry Institute at the Urals Branch of the USSR Academy of Sciences]

UDC 160.193.43

[Abstract] The task of selecting corrosion-resistant materials in order to design fuel elements with molten alkali metal carbonates is addressed and the behavior of binary alloys of iron with aluminum in molten alkali metal carbonates is investigated. The corrosion and electrochemical behavior of the alloys is examined in a hermetically sealed quartz cell in a carbon dioxide atmosphere over the melt in an Alundum crucible. Anode polarization curves of Fe-Al melts in a molten eutectic mixture of $LiCO_3$, $NaCO_3$, and KCO_3 at various temperatures and mass fractions of aluminum are plotted with the help a PI-50-1 potentiostat and LKD-4 XY-plotter; the surfaces, structure, and composition of the corrosion products forming on the surface of Fe-Al alloys are examined by methods of chemical analysis, radiography, and electron probe X-ray spectral microanalysis (RSMA) using a DRON-4 unit, a Camebax X-ray microanalyzer, a STAD-1 diffractometer, and an electron diffractometer. The studies make it possible to draw the conclusion that Fe-Al melts containing more than 10% aluminum by mass may be used as structural materials in contact with molten alkali metal carbonates. The authors are grateful to L.V. Smirnov and the Precision Alloys Lab at the Institute of Physics of Metals at the Urals Department of the USSR Academy of Sciences for preparing the materials for the study. Figures 4; tables 2; references 9: 7 Russian; 2 Western.

Nickel and Nickel-Based Alloy Aluminizing in Chloride-Fluoride Melts Using Liquid Metal Sublayer

927D0084F Sverdlovsk RASPLAVY in Russian No 5, Sep-Oct 91 pp 63-68

[Article by Z.N. Protsenko, B.V. Podafa, O.G. Zarubitskiy, Sumy State Teachers College imeni A.S. Makarenko]

UDC 541.135.3.621.793.4

[Abstract] Aluminizing—the principal method of protecting high-temperature nickel alloys from high-temperature gas corrosion—is discussed and the results of an investigation of the electrode processes occurring during the alloying of aluminum on a nickel cathode are presented. The study is carried out by plotting timed volt-ampere characteristics and examining the effect of various parameters of the saturation process on the rate of formation and the chemical and phase composition of the coat. The mechanism of nickel aluminide formation during the electrochemical aluminum reduction from a chloride-fluoride salt electrolyte is analyzed and the process of electrochemical saturation of nickel and nickel-based alloys with aluminum through a liquid tin sublayer is studied. The optimum parameters of the diffusive saturation of nickel and nickel-based alloys with aluminum which ensure the development of a uniform diffusion layer on the basis of the NiAl phase and good physical and mechanical properties of the end product are established. The outcome of lab tests of the refractory properties of diffuse aluminized coats on nickel and ZhS6K alloy is described. The tests confirm that nickel and nickel alloy aluminizing through a liquid metal tin sublayer produces uniform coats with a high heat resistance and ductility. Figures 4; tables 1; references 14: 13 Russian, 1 Western.

High-Voltage Behavior of Molten Lithium Sulfate and α-Li_2SO_4 Solid Electrolyte

927D0084G Sverdlovsk RASPLAVY in Russian No 5, Sep-Oct 91 pp 91-95

[Article by R.M. Guseynov, S.M. Gadzhiyev, V.D. Prisyazhnyy, Dagestan State Teachers College, Makhachkala, Dagestan State University, and Institute of General and Inorganic Chemistry at the Ukrainian Academy of Sciences, Kiev]

UDC 541.135.3:537.52

[Abstract] The behavior of molten salts and solid electrolytes in strong electric fields (SEP) is indicative of their structure and properties; consequently, the high-voltage behavior of molten lithium sulfate and the corresponding α-Li_2SO_4 electrolyte under 10^{-6} s-long voltage pulses with a 1.5-5.0 kV amplitude within a 675-932°C temperature range is investigated. The study reveals a high-voltage activation of the electrolyte and

the melt whereby their conductivity increases under the effect of a strong electric field. The process of excess conductivity relaxation induced by the electric field is discovered and analyzed and the relaxation lifetime of nonequilibrium charge carriers in the molten salt and α-Li_2SO_4 solid electrolyte is determined. The conclusion is drawn that the physical and chemical properties of electrolytes can be controlled by manipulating the strong electric fields applied to them. Figures 1; tables 3; references 3.

Surface Composition and Properties of Binary Metallic Melts of Fe, Co, and Ni With Cu

927D0084H Sverdlovsk RASPLAVY in Russian No 5, Sep-Oct 91 pp 111-115

[Article by V.I. Nizhenko, L.I. Floka, G.P. Khilya, Institute of Materials Science Problems imeni I.N. Frantsevich at the Ukrainian Academy of Sciences, Kiev]

UDC 541.183:669.15'24'25-154

[Abstract] The importance of understanding the principal patterns of the behavior of surface composition and properties as a function of conditions in order to enhance the impregnation of refractory frames of composite materials with a liquid metal melt or sintering them in the presence of the liquid phase is emphasized and the role of the concentration dependence of surface tension and molar volumes of metallic systems is discussed. The composition and thermodynamic activity of components on the surface of Fe-Cu, Co-Cu, and Ni-Cu melts and the Gibbs energy of solution formation on the surface, and excess Gibbs energy are investigated; to this end, the surface of the binary melt on the boundary with its own vapor is considered as a layer of finite thickness and the minimum possible surface thickness is determined. The surface tension and molar volume of Fe-Cu, Co-Cu, and Ni-Cu melts as a function of the second component concentration are summarized and the dependence of the surface composition on the melt composition in these binary systems are plotted at various temperatures. It is shown that the above melts are systems with a positive deviation from Raoult's law and are characterized by a polyatomic surface model whereby the surface thickness increases with deviation from ideal behavior. Figures 3; tables 1; references 8: 6 Russian, 2 Western.

Optical Properties of Liquid Cerium

927D0084I Sverdlovsk RASPLAVY in Russian No 5, Sep-Oct 91 pp 115-117

[Article by L.A. Akashev, V.I. Kononenko, Chemistry Institute at the Urals Branch of the USSR Academy of Sciences, Sverdlovsk]

UDC 669.1:535.331

[Abstract] The lack of published data on the optical properties of cerium in the liquid state is noted and the results of an examination of liquid cerium's optical properties in the 0.42-2 μm spectrum band at a 1,173K temperature are presented. The optical constants were measured by J.R. Beatie's method using a LEF-3M ellipsometer. The unit developed for measuring the optical properties of metals and alloys at high temperatures and in the liquid state is described and the dependence of the refractive index and absorptance on the wavelength is investigated and tabulated. The dependence of the optical conductivity of liquid cerium on the photon energy, the dependence of liquid cerium's reflectance on the photon energy, and the variance curves of the carrier concentration, relaxation frequency, and direct current conductivity calculated in the hybridized *s-d*-band for cerium are plotted. The lack of theoretical data on the electron structure and density of states near Fermi's level and on the optical properties of liquid rare earth metals makes it impossible to compare the experimental results to theoretical data. Figures 3; references 10: 6 Russian; 4 Western.

Production of Powders of Light Metals (Aluminum, Magnesium, and Alloys Based on Them)

927D0100C Moscow TSVETNYYE METALLY in Russian No 9, Sep 91 pp 77-78

[Article by B.R. Osipov]

[Abstract] In the Soviet Union the creation of light metal powders has been inextricably connected with the activity of the State Scientific Research and Design Institute of Aluminum [Giproalyumiya] and All-Union Scientific Research and Design Institute of the Aluminum, Magnesium, and Electrode Industries [VAMI]. B.P. Golubev, N.N. Ivanov-Skoblikov, G.M. Vorobyev, M.M. Sorokin, B.R. Osipov, and I.N. Ivanov are among those who have made a great contribution to the domestic production of aluminum and magnesium powders. Soviet production of light metal powders, which are important to the defense industry, began in 1935. The VAMI has been a leader in research on the production of magnesium powders since the mid-thirties, and its associates (including V.I. Apraksin) have been instrumental in developing new processes for producing magnesium chips by the technique of rapid milling of ring-shaped magnesium blanks to produce powder. In the late 1930's the VAMI collaborated with the All-Union Scientific Research and Design Institute for Machining Useful Minerals [Mekhanobr] and the Central Boiler Turbine Scientific Research, Planning, and Design Institute imeni I.I. Polzunov to develop a technology to produce aluminum and aluminum alloy powders suitable for pyrotechnics. The new technology was based on a method of simultaneous ejection and pulverization of liquid aluminum. When construction of the Kamensk Magnesium Plant (which was to produce magnesium by

the silicothermal method) was interrupted by World War II, a set of shops that had already been completed were put into operation. During World War II they operated as an independent plant that retained the name Kamensk Magnesium Plant. From 1941 to 1945, the plant was staffed by workers from the VAMI and Giproalyuminiy and by a group of young specialists who transferred to the VAMI after the war. In the USSR, the years 1941-1945 marked the launch of full-scale industrial production of the following: aluminum powders produced by the technique of ejection pulverization of melts, pyrotechnic and pigment aluminum powders, powders of aluminum-magnesium alloys, and magnesium powder directly from BF-3 mills. Pyrotechnic powders and powders of secondary aluminum were also produced at the plant, and safety measures and standards regulating production of all of the stated types of powders were introduced. In the postwar era development of light metal powders continued at a rapid pace in the direction of expanding commercial production. The GNIIKhTEOS [not further identified] and its associates A.S. Sakhiyev, V.V. Vavilov, and V.G. Gerlivanov made significant contributions to the development of a process for creating aluminum powders with spherical particles (type ASD powder). New shops designed by the VAMI were introduced to produce the new powder. Other new developments included processes to produce the following: type APS (the system Al-Al_2O_3) powder, spherical highly disperse powders of aluminum and its alloys, type SAS-1 powders of aluminosilicon alloys, and granulated aluminum alloys. The following types of equipment were either newly developed or updated significantly: melting and pulverizing units, new types of pulverization assemblies, high-capacity grinding and separating units for dry pulverization of aluminum, and type KVTs-500 centrifugal gas classifiers to separate highly disperse powders. Quality control methods and equipment have also been improved significantly. Figure 1.

Results of Work To Recover Red Mud From Alumina Production

927D0100B Moscow TSVETNYYE METALLY in Russian No 9, Sep 91 pp 71-75

[Article by V.A. Utkov, V.V. Meshin (Nikolayevsk Alumina Plant), Yu.I. Shmigidin, S.I. Petrov, and S.A. Nikolayev]

UDC 669.712.002.68.002.8(100)

[Abstract] The seriousness of the problem of recovering red mud at the Nikolayevsk Alumina Plant was noted in the 1984 USSR Council of Ministers decree regarding construction of the plant, which stipulated that the appropriate institutes (including the All-Union Scientific Research and Design Industry of the Aluminum, Magnesium, and Electrode Industries [VAMI]) take the measures necessary to develop a no-waste technology capable of delivering 400,000 tons of red mud per year by 1991-1995. The plant's operating mud storage will be full by the year 2000 and is being filled at a rate close to its design rate. Finding the space for a new mud storage is problematic, and pumping the red mud into the sea as is done in France would entail enormous expenses and major construction and would also result in the irrevcoverable loss of the red mud itself. In both the USSR and abroad large-tonnage tests related to recovering red mud are being held up by the lack of industrial facilities to prepare, ship, and transport the red mud. For these reasons, what has been termed the world's first "main industrial installation" to prepared red mud for shipment to users at a rate of 20,000 t/y has been constructed at the Nikolayevsk Alumina Plant. The new unit contains the following: an FPAKM-25 filter-press, a crusher, a mixer, a sieve, conveyers, hoppers, mixers, an alumina shop washer, a gondola, and stacks. The new installation was used to produce a new material, namely, a ferroalumina mud/flux capable of passing freely throughout the equipment of the process flow of a sintering plant without getting hung up, clogging, or adhering to surfaces. The new mud/flux was subjected to tests at the Zaporozhstal Metallurgy Combine. The new preparation and shipping installation has also produced enough recovered red mud to enable two potential users of recovered red mud (i.e., the Zaporozhstal Metallurgy Combine and Serov Metallurgy Combine imeni Ilich) to test different versions of sintering blast furnace processes using recovered mud. The new installation has also made enough recovered red mud available to test the feasibility of using it in construction materials. The Nikolayevsk Alumina Plant is receiving numerous requests for red mud for various construction purposes and has requested that the VAMI finalize plans to bring the red mud recovery installation up to full capacity in 1991-1992. Figures 5, tables 4; references 8 (Russian).

Solving Ecological Problems in the Subsector

927D0100A Moscow TSVETNYYE METALLY in Russian No 9, Sep 91 pp 67-68

[Article by V.I. Smola, V.S. Burkat, V.P. Nikiforov, and A.I. Polin]

UDC 669.713.074

[Abstract] The aluminum industry is an important source of atmospheric pollutants. Specifically, the production of alumina, aluminum, silicon, and fluoride salts involves the generation and release of a large amount of dust, hydrogen fluoride, fluorine-containing salts, sulfurous anhydride, carbon monoxide, tarry cuts, and other wastes. Aluminum enterprises are responsible for about 18% of all wastes produced by nonferrous metallurgy enterprises and about 5.3% of all wastes generated by enterprises under the jurisdiction of the USSR Ministry of Metallurgy. About 75% of the said wastes come from the six largest aluminum producers, namely, the AGK [not further identified, possibly Achinsk Alumina Plant], Krasnoyarsk Aluminum Plant, Bratsk Aluminum Plant,

Irkutsk Aluminum Plant, and Novokuznetsk Aluminum Plant. Overall, the amounts of waste generated by aluminum plants is decreasing. The waste generated in 1990 was 27.5% less than that generated in 1980, for example. Impurities in the atmosphere surrounding the country's largest aluminum producers are still about the minimum permissible concentrations, however. Three types of electrolyzers are currently being used in the industry, specifically, electrolyzers with a continuous self-baking anode and side current supply, electrolyzers with a continuous self-baking anode and top current supply, and electrolyzers with periodically replaceable prebaked anodes. The latter are the most acceptable from the standpoint of meeting sanitary-hygiene requirements because they consume fewer fluoride salts and do not release tarry cuts when burned. The main reasons for the large level of wastes released from aluminum enterprises are inadequate sealing of production units and a low level of technological discipline. In an effort to reduce the gross emissions of pollutants a system has been developed to automatically feed aluminum to electrolyzers. The new system significantly reduces the amounts of fluoride compounds and resins released, cuts down on the amounts of heat and dust discharged into the atmosphere, and reduces gross emissions of fluorine by reducing the duration of the operation of electrolyzers with an open electrolyte. The new automatic alumina feed system has been fully developed and introduced at facilities with electrolyzers with side current supply, is now being introduced at facilities with electrolyzers with baked anodes, and is being readied for introduction with electrolyzers with top current supply. All of the said electrolyzer series have been equipped with the Aluminiy automated technological process control system, and a new automated technological process control system called Elektroliz has been developed and is now being introduced. Because the stability of the electrolysis process is largely dictated by the quality of the primary material, a set of measures is being introduced to correct and optimize electrolytes and electrolysis conditions. Specialists at the subsector's enterprises and the All-Union Scientific Research and Design Institute of the Aluminum, Magnesium, and Electrode Industries [VAMI] are working to improve the efficiency of gas scrubbing and removal so as to reduce toxic emissions into the air basins surrounding plants. Several new gas-scrubbing methods and devices have been developed and introduced at the Bratsk, Krasnoyarsk, and Novokuznetsk aluminum plants. The new system is said to scrub up to 96% of the dust, 98% of the hydrogen fluoride, and 95% of the sulfurous anhydride generated in the aluminum production process. A prototype dry gas scrubber is now being tested at the Bratsk Aluminum Plant, and the foam devices in place at the Bratsk, Irkutsk, and Novokuznetsk plants are now being updated and having foam stabilizers added. Back-up devices, draft equipment, pumps, and even smokestacks are being widely introduced to increase the scrubbing equipment efficiency. Specialists from the VAMI have also collaborated with specialists from the aluminum subsector to inventory the pollutants released by aluminum enterprises and have developed a program of measures to reduce such emissions by the year 2000. The program is expected to cut aluminum production-related pollution to half of its 1990 level by the year 2000. Figure 1.

Sintering Intensification of Loess Loam-Based Ceramic Bodies

927D0091F Moscow STEKLO I KERAMIKA in Russian No 9, Sep 91 pp 19-21

[Article by V.S. Binckauskas, A.S. Vlasov, Samarkand State Architectural Engineering Institute imeni M. Ulugbek and Moscow Chemical Engineering Institute imeni D.I. Mendeleyev]

UDC 666.3.015.4

[Abstract] The urgency of increasing the production of ceramic building materials from the easily available clays, e.g., loess loams, and the negative effect of calcites contained in them are discussed and an attempt is made to quantify the effect of phosphorus-containing compounds on the sintering efficiency of ceramic body containing loess loam and kaolinite clay. Ceramic bodies containing loess loam from the Khadzhigaydash deposit and kaolinite clay from the Prosyanaya deposit, phosphorite from the Karatau deposit, and orthophosphoric acid are analyzed. The numerical value of the apparent activation energy is calculated in order to estimate the effectiveness of the sintering enhancers. Differential thermal analysis curves and the dependence of water absorption and uniaxial compression strength of roasted samples and of the apparent activation energy on the phosphorite concentration in the burden are plotted. It is noted that the addition of orthophosphoric acid considerably improves the mechanical properties of roasted samples made from a ceramic body on the basis of loess loam. The results make it possible to speculate that phosphorus-containing compounds, e.g., phosphorite and orthophosphoric acid, help to decrease the apparent sintering activation energy of the ceramic body and enhance the silicate formation and calcite dissociation processes in it, thus improving the physical and mechanical properties of low-grade multicarbonate loess loam-based ceramics and expanding their applications. Figures 2; tables 1; references 5.

Preparation of Electrochemically Treated Glass for Metallizing

927D0091E Moscow STEKLO I KERAMIKA in Russian No 9, Sep 91 pp 17-18

[Article by L.A. Samsonova, S.Ya. Shulov, Ye.F. Panteleyev, T.N. Mostovaya, G.I. Maksimova, Tekhstroysteklo Scientific Production Association]

UDC 666.162.056

[Abstract] The production cycle of preparing thermally polished glass (TPS) for metallizing, which includes electrochemical treatment with tin and prepolishing, is discussed and an attempt is made to formulate recommendations for mirror glass-making enterprises for developing the methods of prepolishing the electrochemically treated glass which increase the resulting mirrors' operating characteristics to the utmost. The prepolishing procedure is outlined and kinetic etching curves as well as the dependence of the spectral transmission of an electrochemically tinted glass on a 400 nm wavelength on the etching depth and the dependence of transmission on the duration of the unit surface contact with the polishing machine and the etching depth are plotted. The water resistance of polished glass and the metallized layer peeling are examined. The study demonstrates that electrochemical treatment of the surface of thermally polished glass by an anode tin melt improves the operating properties of metallized (aluminized) glass if the preliminary polishing condition ensures the integrity of the modified layer. In making mirrors, it is expedient to select the prepolishing condition with the help of a standard set of electrochemically tinted glass. Figures 3; tables 2; references 7.

Increasing Strength and Specific Impact Elasticity of Glass Ceramics by Combined Hardening Method

927D0091D Moscow STEKLO I KERAMIKA in Russian No 9, Sep 91 pp 14-16

[Article by V.N. Dubovik, A.M. Raykhel, O.A. Nepomnyashchiy, V.I. Pokolenko, L.G. Ivchenko, L.M. Iotkovskaya, Scientific Research Institute of Automotive Glass]

UDC 666.263.2

[Abstract] Various methods of measuring the specific impact elasticity of glass-based products are outlined and the expediency of testing samples of various standard sizes in order to obtain comparable tests data is recognized. The bending strength and specific impact elasticity of the AS-418 and AS-023 commercial glass ceramics (spodumene and high-lithium, respectively) developed at the Production Association of Automotive Glass as a function of hardening methods and conditions are investigated and the results are tabulated. The samples are hardened by a combined method of etching the surface layer to a 300 μm depth and treating them in an ion exchange melt at a 500-600°C temperature for 1-21 h. High-strength impact-resistant materials are produced as a result. The highest hardening efficiency is attained by using glass ceramics with a 775°C solidification temperature. The methods make it possible to expand glass ceramics applications to mechanical and chemical engineering, radio electronics, geological prospecting, and consumer goods and ensure the structural strength and reliability of ceramic glass products under diverse operating conditions, especially under the effect of considerable static and dynamic loads. Tables 6.

Development of Methods and Hardening Technology of Glass Ceramic Products for Structural Purposes

927D0091C Moscow STEKLO I KERAMIKA in Russian No 9, Sep 91 p 13

[Article by V.M. Gomon, V.N. Dubrovik, A.M. Raykhel, V.I. Pokolenko, Production Association of Automotive Glass and Scientific Research Institute of Automotive Glass]

UDC 666.263.2

[Abstract] The method and process of hardening structural products from the AS-418 spodumene glass ceramic developed and implemented at the Production Association of Automotive Glass are summarized; an increase in contact impact resistance and, consequently, in the operating reliability of the product is used as the hardening efficiency criterion. The procedure used to determine the product resistance is outlined. The glass ceramic products are hardened by a combined methods which includes etching to a 100 μm depth and an ion exchange treatment in an electric furnace with internal heating. Breaking strength tests of the products are described; the tests show that due to the combined hardening, the critical impact force increases by 2.5-3.5 times and reaches 23,000 N and 27,000 N, respectively, for two samples while the number of intact samples increases by 35-40%.

Production Characteristics of Cordierite Glass Ceramics Suitable for Hardening

927D0091B Moscow STEKLO I KERAMIKA in Russian No 9, Sep 91 pp 11-13

[Article by Z.L. Zhuryari, T.A. Rozhnova, V.M. Cheban, G.N. Shmatko, Scientific Research Institute of Automotive Glass]

UDC 666.263.2.548.5

[Abstract] The effect of composition and optimum synthesis conditions of cordierite glass ceramics enabling their subsequent hardening is discussed and the range of compositions of glass ceramics, the patterns of their formation, and methods of controlling their structure development are investigated. Glass ceramics containing oxides of magnesium, manganese, aluminum, silicon, and titanium with a 54.0-63.0% concentration of SiO_2 produced by founding at 1,580°C, annealing at 650°C, and solidification at 1,170°C are used in the study and their thermograms and mineral formation during crystallization are plotted. The microstructure and defect structure of glass ceramics are examined under an electron microscope. The study shows that glass ceramics which are suitable for subsequent hardening and have a low structural defectiveness can be synthesized at an elevated coherence degree of the aluminum-silicon-oxygen frame, i.e., $MO:Al_2O_3 \leq 0.1$ ratio, and a SiO_2 content of >59.0%. Thus, by manipulating the synthesis parameters of the material it is possible to control its structural defects; the outcome of the analysis is used to develop a commercial method of producing products from cordierite glass ceramics suitable for subsequent hardening. Figures 4; references 2.

Hardening of Glass Ceramics

927D0091A Moscow STEKLO I KERAMIKA in Russian No 9, Sep 91 pp 9-11

[Article by V.M. Gomon, V.N. Dubovik, A.M. Raykhel, O.A. Nepomnyashchiy, V.I. Pokolenko, L.G. Ivchenko, L.M. Iotkovskaya, Production Association of Automotive Glass and Scientific Research Institute of Automotive Glass]

UDC 666.263.2

[Abstract] The role of defects in the development of strength properties of brittle structural materials and the need for fluoroscope nondestructive testing methods of structural glass ceramics which makes it possible to detect intermediate-sized defects are emphasized. It is shown that the strength of defective glass ceramics changes with changes in their surface defectiveness, so such glass ceramics can be hardened by treating their surface defects. The design and hardening efficiency of AS-418, AS-370, and AS-380 commercial glass ceramics containing oxides of lithium, aluminum, silicon, titanium, potassium, magnesium, and manganese are evaluated. The efficiency of the simplest and most popular hardening methods such as etching and ion exchange treatment is assessed and special attention is given to surface hardening by carburizing and carbonitriding. The compressive stresses developing on the surface as a result of these methods of surface hardening are examined. Various combined methods, e.g., carburizing with preliminary etching, are considered and their efficiency is evaluated. The thermal coefficient of linear expansion (TKLR) of various glass ceramics and its effect on their properties are discussed. Exceptional efficiency of the carburizing method due to the combined effect of two processes, ion exchange and carbon saturation, is noted. References 7.

New Types of Refractories for Ferrous Metallurgy

927D0080F Moscow OGNEUPORY in Russian No 1, Jan 92 pp 32-36

[Article by G.I. Kuznetsov, A.A. Kortel, V.G. Borisov, A.M. Akselrod, Yu.Ye. Pivinskiy, All-Union Institute of Refractory Materials]

UDC 666.76:669.02/.09

[Abstract] The expanding assortment and increased production of highly efficient refractories for advanced metallurgical processes made possible by new scientific development of the All-Union Institute of Refractory

Materials in recent years, i.e., fused magnesia refractories for converters, corundum- and graphite-, quartz-, and zirconium-containing refractories for continuous casting machines (MNLZ) and refractory gates for new types of continuous casting machines, ceramic concrete for cast-in-situ linings of metallurgical units, are summarized. The composition of these refractory materials, carbon content, apparent density, open porosity, and compressive strength at various temperatures are listed and principal characteristics are examined. Examples of successful operation of the new refractory materials in the USSR and abroad are cited and areas of future research are identified. Tables 6.

Study of Southeastern Ukrainian Quartzite Suitability for Making Silica Refractories

927D0080E Moscow OGNEUPORY in Russian No 1, Jan 92 pp 25-27

[Article by L.G. Sizintseva, V.I. Drozd, Ukrainian Scientific Research Institute of Refractory Materials]

UDC 666.762.2 (477)

[Abstract] An attempt to expand the raw material base of the silica refractory production prompted a study of the suitability of southeastern Ukrainian quartzites for this purpose, particularly from the Dnepropetrovsk and Donetsk areas. The quartzites were investigated using a procedure developed at the Ukrainian Scientific Research Institute of Refractory Materials; the method makes it possible to derive data on their technological properties on the basis of an exhaustive lab examination which includes physical, chemical, and mineralogical analyses, an analysis of the amount of impurities, and other tests. Five samples are studied; their chemical composition and refractoriness are summarized and their microstructure is examined under a transmitted light microscope. As a result, the physical and chemical properties of quartzites and refractory samples on their basis before and after roasting are examined and tabulated. Quartzites from the Vasilkovka deposit are found to be a suitable raw material for silica refractories for noncrucial applications while the same quartzites mixed with those from the Tarasovskiy deposit are suitable for silica refractories used in noncrucial parts of thermal units, such as coke oven regenerators. Figures 2; tables 2; references 2.

Effect of Certain Factors on Spin Casting of Oxide Ceramics

927D0080D Moscow OGNEUPORY in Russian No 1, Jan 92 pp 22-24

[Article by Yu.M. Mosin, I.A. Zakharov, Ye.O. Lavrova, M.A. Voynova, Moscow Chemical Engineering Institute]

UDC 666.762:621.74.042.001.4

[Abstract] Two methods of centrifugal casting of ceramics—with solid and perforated rotors—are considered and the effect of various factors on spin casting is investigated; in particular, the effect of hydrodynamic conditions, sedimentation duration, and the process rate and duration are examined. The concentration dependence of the casting suspension viscosity and the dependence of the solid phase particle velocity on the volume fraction of the solid phase in the suspension are derived and Reynolds numbers for various sedimentation conditions of individual corundum particle are plotted. The effect of the mold filling degree and corundum concentration in the suspension on the billet wall thickness and the effect of the granulometric content and casting conditions on the density of moist zirconium dioxide residues are examined. An analysis shows that during spin casting, sedimentation occurs in a laminar condition and sedimentation of large fractions occurs during the mold spin acceleration. The principal factor affecting the density of finely dispersed billets is the spinning duration while for systems containing coarse fillers, centrifugal acceleration is the principal factor. The billet wall thickness can be controlled by manipulating the solid phase concentration in the suspension and the mold filling degree. Figures 2; tables 2; references 11.

Straining Characteristics of Ceramics Under Heating

927D0080C Moscow OGNEUPORY in Russian No 1, Jan 92 pp 15-19

[Article by G.A. Gogotsi, D.Yu. Ostrovoy, IPP at the Ukrainian Academy of Sciences]

UDC 666.762.93.017:620.163.3

[Abstract] The inadequacy of ceramics specifications listing only the strength characteristics at constant loading and straining rates for today's ceramics used for making elements of heat exchangers, internal combustion engines, turbines, cutting tools, etc., necessitated an investigation of the features of mechanical behavior of ceramics as a function of the straining rate. The device developed for this purpose on the basis of the standard U-10-1 breaking tester and the testing procedure are described. Strain and creep diagrams of various types of ceramics, the temperature dependence of the ultimate strength, the dependence of the bending strength on the straining rate, and the effect of the amount of alloying oxide additions on the mechanical characteristics of ceramics are plotted. The density, speed of ultrasonic vibrations, dynamic modulus of elasticity, bending strength, ultimate strain, and static modulus of elasticity of the SN-1, SN-2, and A-1 ceramics are summarized and the microstructure of ceramics sample fractures is examined microscopically. The conclusions are drawn that in selecting ceramic materials, it is necessary to know their strain diagrams under real operating temperatures; that ceramics must be tested at various straining

rates due to the activation of creep and subcritical crack growth processes; and that at high temperatures, the maximum operating loads must be lower than those causing the appearance of discontinuities. Figures 10; tables 1; references 10: 6 Russian, 4 Western.

Zr, Y, and Ce Oxide-Based Ceramics With Elevated Electric Conductivity

927D0080B Moscow OGNEUPORY in Russian No 1, Jan 92 p 7

[Article by A.I. Snegirev, M.G. Zuyev, V.I. Pivovarova, VostIO]

UDC 666.762.52:621.3.028

[Abstract] The electric conductivity of zirconium, yttrium- and cerium-containing oxide ceramics used as highly refractory conducting material in high-temperature power plants or as heating elements is investigated in order to find ways of further increasing the electric conductivity. After diffusion annealing, the ceramics were subjected to a physical and chemical treatment by molten low-melting P_2O_5-V_2O_5-N_2O glass. The charge composition for founding the P_2O_5-V_2O_5-N_2O glass is examined and the temperature dependence of electric resistivity of ceramics before and after the physical and chemical treatment is plotted. No chemical interaction was observed between the glass and ceramic components. Electric conductivity was measured by a four-probe method and revealed that of the three compositions tested, two had an electric conductivity increase within the entire 500-2,000K range and one—at up to 1,390K. The proposed technology is recommended for producing traditional ceramics with an elevated electric conductivity. Figures 2; references 5

Thermostable Composites Based on Three-Component Binding Suspension

927D0080A Moscow OGNEUPORY in Russian No 1, Jan 92 pp 4-7

[Article by I.I. Nemets, N.S. Belmaz, L.N. Semykina, BTISM]

UDC 666.974.2:666.762.2

[Abstract] The need for composite materials which operate efficiently in an anisotropic temperature field and maintain their mechanical strength and structural integrity prompted an interest in producing multiphase refractory highly concentrated ceramic binding suspensions (VKVS) and ceramic concretes on their basis and examining their properties. The solid phase composition of the binding suspensions are summarized and the properties of casting made on their basis are investigated. Quartz sand with a 98% SiO_2 content, refractory industry scrap, and unstabilized TsRO-1 zirconium dioxide with a 99.5% ZrO_2 content are used as the raw materials for making the three-phase ceramic suspension. The microstructure of ceramic concrete is examined microscopically and the effect of pH on the suspension viscosity and casting properties and the dependence of the bending strength on the roasting temperature are plotted. An analysis shows that the development of a gel-like coat on the particle surface which ensures binding and volume stability of casting with temperature can be facilitated by combining the process of wet mechanical grinding of the three-component mixture and topochemical interaction among its particles. The optimum suspension pH ensuring the maximum bending strength of 4-5 N/mm^2 and the lowest porosity of 18-19% is established: 9.4-10.5. A molding material composition is developed for making ceramics-based concrete with a 28 N/mm^2 bending strength and a heat resistance of 54 cycles of 1,300°C in water. Figures 3; tables 3; references 6.

Bioresistant Polymer Cement Based on Pulverized Binder

927D0079D Moscow STROITELNYYE MATERIALY in Russian No 12, Dec 91 pp 19-20

[Abstract of article by N. I. Osminin, Candidate of the Technical Sciences, and I. M. Tishchenko, engineer, Odessa Civil Engineering Institute]

UDC 666.972.16

[Abstract] The Odessa Civil Engineering Institute has developed a process for producing a cement based on a pulverized binder made by simultaneously grinding portland cement and sand of average grain size (M_k = 2.4) in a 1:1 ratio until the powder has the desired specific surface (4500 cm^2/g for the cement used to make the concrete test specimens). A compound additive consisting of furfural, which acts as a biocide, and ATsF-3M water-soluble acetone formaldehyde resin in a weakly alkaline solution is mixed into the cement, which requires 10-15% less water than the control cement. The test specimens were made from a stiff mixture of the experimental cement, using a water/cement ratio of 0.25. The cone upsetting of the specimens was 1.5 cm. In comparison with the control specimens, the bioresistance number of the concrete specimens made from the modified cement dropped from 5 to 0, water absorption fell from 6.7 to 2.1, freeze resistance increased from 500 to 700 cycles, the chemical resistance factor increased from 0.4 to 0.6-0.7 (when the specimens were immersed in a corrosive solution), and ultimate compressive and bending strengths over a 28-day period increased from 56 to 70 and from 6.8 to 9.2 MPa, respectively. Over 3 months, compressive strength increased to 87 MPa due to the long-term effect of the final polymerization of the additive, which promotes greater cohesiveness among the cement components. Tables 1

Frost Resistance of Asbestos-Cement Piling Pipe

927D0079C Moscow STROITELNYYE MATERIALY in Russian No 12, Dec 91 pp 14-15, 18-19

[Abstract of article by M. I. Mezhogskikh, A. A. Kiselev, A. L. Pakhomov, and I. V. Matskiv, engineers, All-Union Scientific Research Institute of Specialized Construction Design Engineering (Ukhtin branch)]

UDC 666.961—462:620.17

[Abstract] Asbestos-cement specimens were tested for frost resistance using two methods recommended in State Standard 10060—87. The specimens were obtained by using a diamond disk to saw piling pipe made by the Korkinsk combine into cubes 41x41x41 mm. The pipe, which had a wall thickness of 41 mm, was made from asbestos cement that had aged for 9 months. Protective coatings were applied to some of the specimens, which were either immersed or given two coats of paint while they were still naturally damp (10-11%). Specimen temperature was 20-22°C, coating temperature was 20 to 35°C. The average initial density of the cement was 1.85 g/cm^3, and water absorption was 15.8%. Depending on the method used, the specimens were subjected to 400 or 95 freezing/thawing cycles at temperatures down to -18°C or -52°C while immersed in tap water or a 5-% solution of sodium chloride. Regardless of the test method used, the specimens completely retained their shape and appearance. The average value for compressive strength remained virtually unchanged, falling between 38.4 to 50.2 MPa, and the specimens had no significant loss of mass. None of the coatings except for the anticorrosive grease provided enough protection from water saturation, nor did they affect strength one way or the other. The large variance in average compressive strength was explained by the uniformity coefficient of the material, which ranged from 0.65 to 1.35. Asbestos concrete is a highly frost-resistant material equivalent to F2500-grade material and can be recommended for use as a piling material in regions with extensive permafrost. It can be used without a protective coating, but if it is coated, the anticorrosive grease is recommended. The inhomogeneity of asbestos cement should be taken into account when using it as a frost-resistant material. Figures 3, tables 1; references 22: Russian.

Energy-Saving Process for Making Gypsum Materials From Industrial Waste Containing Gypsum

927D0079A Moscow STROITELNYYE MATERIALY in Russian No 12, Dec 91 pp 6-8

[Abstract of article by V. V. Ivanitskiy, Candidate of the Technical Sciences, All-Union Scientific Production Association of Wall and Binding Materials]

UDC 666.91.002.2.004.8

[Abstract] A new energy-saving "wet" process for making gypsum materials was described step by step. Instead of the conventional dry, powdered binder, the wet process uses the fresh, moist, semi-finished product that comes directly from the autoclave processing of raw materials obtained from gypsum-bearing industrial waste. During all stages of the process, from preparing the raw material to manufacturing the final product, the moisture content is at a maximum, which is 3-30% for the process materials, and 10-15% for the final products. Since the rate at which the autoclave product hardens depends primarily on the surface activation of the centers of solution, the addition of chemical additives to this material while it is in the mixing and activating machine approximates the effect of powdered gypsum binder on the hardening process. The new process is used to make wallboard 390+/-4 mm in length, 190+/-3 mm wide, and 188+/-4 mm in height with a compressive strength of 3.5-9 MPa, 14-17% porosity, less than 14% water absorption, a softening factor greater than 0.55, and freeze resistance of more than 35 cycles. In comparison with the conventional process, the wet process results in a 1.7- to 2.6-fold savings in fuel that would otherwise be spent on drying the semi-finished product prior to processing it into gypsum-based products. Capital expenditures are reduced two- to three-fold because of the elimination of dust-removal equipment. Overall production costs are reduced about two-fold. The process is also environmentally safe. Figures 1, tables 2, references 2: Russian.

Electric Field Gradients in $YBa_2Cu_3O_7$

927D0038A Sverdlovsk FIZIKA METALLOV I METALLOVEDENIYE in Russian No 7, Jul 91 pp 12-15

[Article by N.I. Medvedeva, S.A. Turzhevskiy, and V.A. Gubanov, Institute of Chemistry, Ural Department, USSR Academy of Sciences]

UDC (546.562+538.945):538.915

[Abstract] Calculations by the LMTO (linear combination of muffing tin orbitals) method pertaining to the electronic structure, the chemical Cu-O bonds, and the tensor of electric field gradients in the $YBa_2Cu_3O_7$ crystal lattice have yielded the energy of covalent interactions and the population of orbital-orbital bonds. The results of these calculations, based on the LMTO representation of a strong link, include the asymmetry of 01 and 04 positions, the frequencies of nuclear quadrupole resonance on ^{63}Cu nuclei, the populations (per one spin) of 3d-orbitals of Cu1 and Cu2 copper atoms, the populations (per spin) of 2p orbitals of O1 and 04 oxygen atoms, and the energy of covalent Cu-O interaction within the various Cu-O atom pairs. The values of these parameters, which agree fairly well with experimentally obtained values, confirm the theoretical proposition that the high-frequency resonance line refers to a Cu2 atom and the low-frequency resonance line refers to a Cu1 atom. The electric field gradient associated with a Cu2 atom is determined by the difference between the populations of orbitals d [z] and d [x^2-y^2], while the electric

field gradient associated with a Cu1 atom is determined principally by the nondiagonal population and thus hybridization of these two orbitals. Tables 4; references 17.

Effect of Process Factors on Structure Formation and Properties of Hot-Compacted Silicon Nitride Ceramics

927D0076H Kiev POROSHKOVAYA METALLURGIYA in Russian No 12(348), Dec 91 pp 61-67

[Article by V.B. Vinokurov, V.A. Melnikova, L.F. Ochkas, Yu.G. Tkachenko, O.A. Babiy, Institute of Materials Science Problems at the Ukrainian Academy of Sciences]

UDC 620.187:66.762+548.53

[Abstract] Numerous factors affecting the properties of ceramic materials—the granulometric and chemical composition of powders, their sintering conditions, and the structure of compact products, etc.—are discussed and attention is focused on the effect of the granulometric composition of powders and their grinding conditions on the range of particle dimensions, binding phase distribution, and mechanical properties of silicon nitride-based ceramics. The sample preparation procedure and instruments used to measure the particle size distribution are described, the characteristics of the powders under study and the properties of hot-compacted samples made from them are summarized, and spectra of constituent elements are recorded. It is demonstrated that during hot compaction, grinding of iron in the amount of 4.2-11.5% by mass does not reduce the flexural strength of ceramics at room temperature; moreover, iron dissolves in the oxide binder and partially forms finely dispersed silicide inclusions. The maximum bending strength of 490 MPa is attained at a 6.8% iron concentration and a median particle size of 0.45 μm. Consequently, β-Si_3N_4 ceramic contamination with iron is permissible in structural materials operating at room temperatures. Figures 6; tables 2; references 7: 4 Russian; 3 Western.

Reinforced Concrete and Environment

927D0093A Moscow BETON I ZHELEZOBETON in Russian No 10(439), Oct 91 pp 2-3

[Article by F.M. Ivanov, Scientific Research Institute of Reinforced Concrete]

UDC 691.328.001

[Abstract] The multifaceted interaction of reinforced concrete with the environment is considered from the viewpoint of its role as a barrier between the environment and various toxic substances it is called upon to contain and from the viewpoint of its role as a source of contamination due to various fillers, cements, or chemical agents added to it. The admixtures are capable of slowly releasing toxic substances into the atmosphere. Moreover, for many years reinforced concrete has been used as an absorber of toxic waste which is otherwise difficult to process or dispose of. In addition, the byproducts and waste of reinforced concrete production itself may also be harmful for the environment. Measures aimed at reducing the negative environmental impact of these factors are outlined and the need for further studies is emphasized. References 5: 3 Russian, 2 Western.

Full-Scale Investigation of Pile Concrete Hardening in Winter

927D0093F Moscow BETON I ZHELEZOBETON in Russian No 10(439), Oct 91 pp 22-24

[Article by B.A. Krylov, A.A. Dedyukhov, Scientific Research Institute of Reinforced Concrete]

UDC 666.972.167

[Abstract] The importance of predicting the hardening of concrete piles in cold climate regions where the soil temperature varies greatly with depth and the soil is seasonally frozen is stressed and the results of such a study conducted in Izhevsk in Feb-Mar 90 in four 3-m-long round piles with a 0.5 m diameter and five 3-m-long concrete fragments with a 0.15x0.15 m cross section are reported. The temperature varies from -10.7°C at the top of the pile to +5.3°C at the bottom. The piles are made from class V15 concrete using brand 400 cement from the Gornyy Zavod plant. The kinetics of the concrete pile strength in contact with seasonally frozen soil at a -0.05 m level, the integral porosity distribution in the pile cross section at the -0.05 m level, the kinetics of concrete fragment strength in contact with seasonally frozen soil at various depths, and the integral concrete porosity distribution in the height of the longitudinal pile fragment are plotted. An analysis shows that the concrete strength increases and its pore structure develops in contact with seasonally frozen soil differently at different depths; these processes are affected predominantly by the concrete mix stratification at the initial hardening period and the cooling action of the soil within the freezing layer. These factors result in a deficit of strength at the top of the pile, especially in contact with the soil, and facilitate the destructive processes accompanied by an increase in the integral at the top of the pile and, as a result, a decrease in its frost resistance. The need to decrease the concrete mix stratification and reduce the thermal action of the soil is emphasized. Figures 4; tables 1.

Production Line for Making Thin-Walled Prestressed Articles

927D0093E Moscow BETON I ZHELEZOBETON in Russian No 10(439), Oct 91 pp 18-20

[Article by A.V. Motin, G.I. Igoshin, Ryazan Branch of the Stroyindustriya Special Design Office]

UDC 69.024.26

[Abstract] A contractor design of a production line and the necessary equipment and accessories for making thin-walled prestressed articles using a prestressing bed method developed at the Ryazan Branch of the Stroyindustriya Special Design Office under the technical guidance of the Scientific Research Institute of Reinforced Concrete is discussed and the line's technical and economic indicators are summarized. The anticipated annual output is 71,000 m^2 or 2,672 m^3 based on 262 working days with seven workers and two shifts per day. The consumption of concrete, cement, and metal as well as labor outlays for 1 m^2 panel are computed. The fabrication and prestressing procedures which do not require the use of formwork are described in detail. The fist phase of the production line operation demonstrated that in order to decrease shipping costs, it is expedient to assemble the elements into large panels on site. The production line has been in operation since 1988 at the Ryazanstroy Association reinforced concrete plant. Figures 1; tables 1; references 1.

Steel-Concrete Elements With Grooved Reinforcement

927D0093D Moscow BETON I ZHELEZOBETON in Russian No 10(439), Oct 91 pp 12-14

[Article by I.I. Karkhut, A.I. Gavrilyak, I.I. Luchko, Lvov Polytechnic Institute and Physics and Mechanics Institute at the Ukrainian Academy of Sciences]

UDC 624.012.454

[Abstract] The studies aimed at examining the steel-concrete structures used at nuclear power plants and water works conducted at the Lvov Polytechnic Institute and the Physics and Mechanics Institute at the Ukrainian Academy of Sciences are summarized; they involve measuring the strength and deformability of sheet reinforcement with a periodic profile and its joint performance in the reinforced concrete cross section under the effect of operational thermal and force loads in nuclear power plant structures and heat storage tanks. The design of linear steel-concrete elements and the testing layout are presented and the reinforcement strain and bond stress distribution in the anchorage length are plotted. Portland cement from the Nikolayev plant is used to make class V25 concrete and steel-concrete samples are loaded until they fail. An analysis demonstrates that the reinforcement sheets with a grooved profile ensure reliable joint operation of concrete and reinforcement sheets in the steel-concrete element cross section at all loading stages, up to failure, and are a new and efficient type of reinforcement which makes it possible to save both high-strength reinforcement material and concrete. Figures 2; tables 1; references 2.

Concrete Strain Anisotropy Development Under Axial Compression

927D0093C Moscow BETON I ZHELEZOBETON in Russian No 10(439), Oct 91 pp 9-11

[Article by V.P. Mitrofanov, O.A. Dovzhenko, Poltava Civil Engineering Institute]

UDC 666.972.017:539.4

[Abstract] It is speculated that microcracks develop in concrete prior to its failure; to verify this model, prismatic concrete samples are subjected to axial compression tests at a 29.7 MPa load. Resistor strain gauges and piezoelectric transducers are used to measure the longitudinal and lateral strain and a UP-10M instrument is used to measure the ultrasound propagation time in the prismatic samples' three directions. The dependence of the longitudinal and mean lateral ultrasound velocity on the stress level and the dependence of the longitudinal and mean lateral strain on the stress level are plotted. The proposed method treats concrete as an orthotropically strained material: at low strain levels, concrete can be regarded as isotropic material while at high levels is acquires anisotropy which increases up to the moment of failure due to the development of a system of oriented cracks. Figures 4; references 5.

Effect of Temperature and Time on Stresses in Congealed Concrete Under Thermal Cycling

927D0093B Moscow BETON I ZHELEZOBETON in Russian No 10(439), Oct 91 pp 7-9

[Article by V.N. Benkov, Ye.S. Sergeyeva, Siberian Department of All-Union Scientific Research Institute of Hydraulic Engineering]

UDC 69.059.22:551.524.37

[Abstract] The effect of the temperature and exposure on the stresses developing in congealed concrete at low temperatures which determine the freeze-induced concrete failure is discussed and methods of determining these stresses are considered and it is shown that an indirect method based on measuring the material's loss of strength as a result of multiple freezing and thawing cycles is the most reliable and representative. A formula for assessing the mean effective internal stresses developing in the material during one freezing cycle is derived on the basis of the kinetic theory of rock strength. Experiments for determining the effect of temperature and exposure are conducted; to this end, concrete samples are subjected to multiple freezing and thawing and their chipping tensile strength is measured after 230 days. The dependence of the tensile strength on exposure time is plotted. For concrete containing Krasnoyarsk Plant portland cement, a decrease in the freezing temperature from -10°C to -20°C increases the effective mean stresses by 27%; this is attributed to the role of smaller pores which become active as well as an increase in the stresses resulting from the difference in the components' coefficients of linear expansion. It is noted that the above approach is sufficiently general and promising for predicting the freeze failure of concrete under natural conditions. Figures 2, tables 2, references 4.

Microporosity of Powders Produced by Centrifugal Spraying

927D0076A Kiev POROSHKOVAYA METALLURGIYA in Russian No 12(348), Dec 91 pp 1-7

[Article by V.Ya. Koshelev, V.T. Musiyenko, All-Union Institute of Light Alloys]

UDC 621.762

[Abstract] The shortcomings and advantages of existing methods of making refractory alloy powders are considered and attention is focused on the most promising one—plasma jet spraying of the rapidly spinning melting billet end (PREP). The gas porosity of nickel-based refractory alloy powders produced by the PREP is investigated; the experiments are conducted in a special unit in a medium of high-purity helium and argon mixture with less than 0.0005% oxygen by volume. The resulting powders are separated into -200+160, -160+100, and -100 μm fractions and embedded in polystyrene. To determine the number of porous particles and gas pocket dimensions, microsections are prepared and examined under binocular and electron microscopes. The effect of the billet spinning velocity on the powder porosity and the effect of the granule size on the pore diameter at various rotation speeds are plotted and the drop formation mechanism is analyzed. The bulk microporosity of metal samples compacted from the powder as a function of rotation speed is summarized. The results show that the character of molten metal film flow on the billet end during the spraying is determined by its spinning speed, the largest number of porous particles is in the large fraction powder while the lowest is in the fine powder with a less than 100 μm fraction. The effect of the He concentration in the medium on the number of porous particles is established. The pore size virtually does not depend on the production conditions. It is recommended that -100 μm fraction powders produced at a 35-40 m/s billet speed be used in order to ensure the lowest microporosity of compacted products. Figures 4, tables 2, references 4

Structure and Properties of Palladium- and Stainless Steel-Based Bilayer Powder Membranes

927D0076G Kiev POROSHKOVAYA METALLURGIYA in Russian No 12(348), Dec 91 pp 56-61

[Article by V.P. Georgiyev, P.Ya. Zlatkov, V.M. Kaptsevich, V.V. Savich, V.K. Sheleg, Cermet Economic Association and Scientific Instrument-Making Production Association (Bulgaria) and Belarus Republican Scientific Production Association of Powder Metallurgy]

UDC 621.762

[Abstract] Special requirements of the so-called pure technologies, i.e., microelectronics, optics, and chemical and pharmaceutical industries, where gases containing less than one hundredth percent of impurities are used as protective atmospheres, media, and reagents are addressed and the process of making bilayer palladium membranes on a porous corrosion-resistant steel (PKS) base is examined. To this end, various fractions of powders produced by atomizing the composition in water are used to make the membrane base, the steel porosity is measured by hydrostatic weighing, the permeability factor is determined by COMECON standard SEV ST2291-90, and the lateral bending strength is measured by COMECON standard SEV ST4654-84. Disc-shaped study samples are made by the traditional compaction and sintering method. The dependence of the permeability factor and lateral flexural strength on the powder stainless steel porosity is plotted and the effect of sintering temperature, compaction pressure, and PKS porosity on the purification efficiency is investigated. The microstructures and fractograms of bilayer membranes sintered at various temperatures are examined and the cohesive strength of the palladium layer to the powder stainless steel base as a function of sintering temperature is summarized. The collapsing pressure of membranes made by three different methods is investigated. The results of the experiment show that two-layered membranes produced by powder metallurgy methods and consisting of a permeable stainless steel powder base and a compact palladium layer exceed those used today with respect to mechanical strength and purity and should therefore be used in industrial equipment for fine purification of hydrogen (to remove oxygen). Figures 7, tables 2, references 6: 4 Russian, 2 Western

Atomized Powder-Based Structural Powder Low-Alloyed Steels

927D0076F Kiev POROSHKOVAYA METALLURGIYA in Russian No 12(348), Dec 91 pp 40-46

[Article by V.N. Klimenko, S.G. Napara-Volgina, L.N. Kostyrko, V.V. Mizyuk, Institute of Materials Science Problems at the Ukrainian Academy of Sciences]

UDC 621.762.8

[Abstract] The use of atomized powders alloyed beforehand for improving the physical and mechanical properties of structural materials is discussed and the properties of the KhGNM low-alloyed structural steels manufactured by the Tulachermet scientific production association and KhGM (Sumiron-4100 S) produced by the Sumitomo corporation in Japan, i.e., materials with a similar chemical composition produced on the basis of powders atomized by water and oil, respectively, are compared in order to establish the effect of the initial raw material characteristics and the atomization method on the properties of the end product. The chemical composition and production method of the powders under study are summarized and the shape of their

particles is examined under a microscope. The microstructure of sintered KhGNM and KhGM materials made from a burden with various graphite concentrations is examined and compared. The dependence of the carbon concentration in sintered materials on the basis of atomized KhGNM and KhGM powders on the sintering temperature and graphite concentration in the burden and the dependence of the density of sintered materials on the basis of atomized KhGNM and KhGM powders on the sintering temperature is summarized. An analysis confirms that atomized KhGNM and KhGM powders may be used for making structural materials with a high level of physical and mechanical properties both by hot die forging and single compaction and sintering and demonstrates the advantages of low alloyed powders atomized with oil over those atomized with water: the former reach a higher level of mechanical characteristics at lower sintering temperatures and make it possible to control a specified carbon content in the materials after sintering. Figures 5, tables 3, references 9.

Permeable Materials From Fiber-Like Rapidly Quenched Particles

927D0076D Kiev POROSHKOVAYA METALLURGIYA in Russian No 12(348), Dec 91 pp 26-29

[Article by L.I. Chernyshev, N.N. Kuzmenko, L.D. Kulak, A.G. Kostornov, Institute of Materials Science Problems at the Ukrainian Academy of Sciences]

UDC 621.762

[Abstract] The high cost of existing methods of production of porous permeable fibrous materials from thin wires and the need to develop new ways of making them from, e.g., rapidly quenched powders with a high particle size anisotropy are discussed and data on the properties of fiber-like materials made from rapidly quenched powders of stainless steel Kh18N9T produced by spraying liquid drops of molten metal upon a cooled substrate (these materials are often referred to as quasifibers) are presented and compared to the properties of traditional fibrous porous materials of the same composition. The structure of porous materials from sprayed and traditional fibers is examined under a microscope and the effect of porosity on the volume shrinkage during sintering, sag during bending, bending strength, pore size, and gas permeability coefficient of quasifiber porous materials is examined and plotted. The hydrodynamic and physical-mechanical properties of permeable materials made from traditional fibers and quasifibers with a length of 3-4 μm, a width of 0.1-0.5 mm, and a thickness of 10-20 μm are summarized. It is demonstrated that the hydrodynamic and mechanical properties of permeable materials from quasifibers are close to those made from 20 μm thin fibers yet are much cheaper to produce; consequently, in making porous permeable materials, it is recommended that quasifibers produced by spraying be used as raw materials. Figures 2, tables 1, references 4.

Chrome-Plating Features and Properties of Highly Porous Mo-Cu Composites

927D0076C Kiev POROSHKOVAYA METALLURGIYA in Russian No 12(348), Dec 91 pp 14-17

[Article by A.G. Kostornov, V.P. Semenets, Institute of Materials Science Problems at the Ukrainian Academy of Sciences]

UDC 621.762

[Abstract] The use of molybdenum-copper composite materials in contact with high-temperature gas flows—as porous interelectrode inserts (MEV) for plasmatrons—is considered and an attempt is made to determine the effect of the chrome-plating conditions, i.e., the temperature and exposure duration, and the properties of the Mo-Cu composite material samples (the porosity and composition) on the characteristics of the chrome-plating process and the properties of the product. Prismatic samples produced by compaction of powder mixtures of molybdenum (TU 48-19-316—80), 20-30% PME-1 electrolytic copper, 3-10% PNE-1 electrolytic nickel, and urea as a pore-forming agent are used in the experiment. The dependence of the samples' resistivity on the porosity of Mo-Cu composites with and without the addition of nickel after sintering at 1,000°C and after chrome-plating under the same conditions, the dependence of the weight gain, volumetric changes, and resistivity of Mo-Cu composites after sintering and chrome-plating at various temperatures on their porosity, the effect of the chrome-plating process duration in the absence of liquid phase on the weight gain and volumetric changes in porous Mo-Cu compositions, and the dependence of the weight gain and volumetric changes on the porosity of Mo-Cu compositions are plotted. The effect of chrome-plating on the strength of Mo-Cu composites is examined under impact bending and the dependence of the impact bending strength on the Mo-Cu composition porosity after chrome-plating is plotted. An analysis shows that the properties improve in the presence of the liquid phase and remain virtually constant with an increase in the amount of copper during the solid-phase chrome-plating of sintered composites; properties deteriorate in the presence of nickel which interacts with copper. Figures 6; references 5: 4 Russian; 1 Western.

Optimization of Liquid Metal Dispersion Process in 'Free' and 'Limited' Discharge Jet Sprayers

927D0076B Kiev POROSHKOVAYA METALLURGIYA in Russian No 12(348), Dec 91 pp 7-13

[Article by V.M. Blekherov, All-Union Scientific Research Institute of Metallurgical Machine-Building]

UDC 621.762.224

[Abstract] Since the propellant gas pressure, rate, temperature, and origin are the diagnostic variables in the production of metal powders by gas jet spraying of molten metals and also determine the principal energy outlays of the method, optimization of these parameters makes it possible to utilize additional reserves for improving the equipment performance and reducing the cost of powder production. Design drawings of both free and limited discharge jet sprayers and their respective jets are presented and the relationship between the critical velocity and specific rate of the propellant gas on the dispersion degree of the resulting powder is examined. The dependence of the flow characteristics in the atomization zone and specific gas rate on the pressure in the jet sprayer and the dependence of the specific gas rate on its temperature on the jet sprayer inlet are summarized and the results of the spraying of Armco-iron by a limited discharge jet sprayer with nitrogen serving as the propellant gas are tabulated. An analysis shows that the knowledge of jet sprayer parameters may be used to manipulate the spraying process so as to ensure specified powder characteristics with minimal energy outlays. The effect of various process parameters on the granulometric composition of the resulting power is established. Figures 2, tables 2; references 3.

Increasing Effectiveness of Rod Manufacture in Heated Equipment

927D0032B Moscow LITEYNOYE PROIZVODSTVO in Russian No 6, Jun 91 pp 22-23

[Article by S. I. Koltunov, E. P. Orlovskiy, V. K. Kuzovkov, G. P. Smirnov, O. V. Krilova, Scientific-Production Association of the Scientific Research Institute of Tractors and Agricultural Machinery]

UDC 621.743.06.073.42.54:628.512

[Abstract] The most effective method of reducing the time required for curing of rods and improving their strength is vacuum treatment of the rods in heated equipment. The essence of the method involves installation of a system of vents or slots which are connected to a vacuum pump, drawing off the toxic gases and water vapor evolved during the curing of the rods. Laboratory studies indicate an increase in rod heating rate of 6-12 times, in strength of 1.5-2 times and in moisture removal rate of 4-10 times in comparison to the tradition process. Figures 2.

Accessory for Model 042 M Instrument to Determine Gas Permeability of Dry Specimens

927D0032C Moscow LITEYNOYE PROIZVODSTVO in Russian No 6, Jun 91 pp 23-24

[Article by A. A. Stryuchenko, V. M. Kompanichenko, IPL, Ukrainian Academy of Sciences]

UDC 621.74.045

[Abstract] Difficulties arise in determining the gas permeability of a molding mixture in the dry state in assuring reliable sealing of the dry specimen on the side surface of the sleeve. Devices now used to seal the side surfaces of dry specimens with sleeves are unreliable. The authors' institute has developed a new accessory device for the 042 M instrument completely eliminating the problems of known devices. It consists of a multipart sleeve, receiver, elastic plastic pipes, three-way valves and hand pump. The major advantages of the device are its design simplicity, reliability, possibility of testing dry specimens of different heights and significant decrease in time expended in testing.

Classification and Application of Continuous Casting Methods

927D0032D Moscow LITEYNOYE PROIZVODSTVO in Russian No 6, Jun 91 pp 24-28

[Article by Ye. I. Marukovich, V. I. Tutov, V. A. Grinberg, Mogilev Department, Institute of Physics and Technology, Belorussian Academy of Sciences, Belorussian Polytechnical Institute]

UDC 621.746.047.001

[Abstract] Continuous casting is easily automated and produces products which are in high demand. This article presents a system for classifying various continuous casting processes in order to allow the most appropriate process to be selected for manufacture of a given product. It is concluded that continuous casting methods with horizontal process axis have a number of advantages making them most efficient for the production of machine building blanks. The use of crystallizers with metal cooling sleeves increases durability and productivity, while expanding the range of application of the process. Continuous casting quality can be improved by such processes as modifying the casting material, gas-pulse treatment of the melt before entry into the crystallizer, plasma and magnetodynamic effects, vibration and suspension casting. The classification system which has been developed will allow the selection of the most effective continuous casting method in each specific case. Figures 2; References 9: 8 Russian 1 Western.

Design of Chill Mold Ventilation System

927D0032E Moscow LITEYNOYE PROIZVODSTVO in Russian No 6, Jun 91 pp 28-29

[Article by V. S. Cerebro, I. Kh. Tarasov, NIISL Scientific-Production Association]

UDC 621.74.019.043

[Abstract] The method here suggested for designing a chill mold ventilation system allows a sharp reduction in losses due to rejection of castings by eliminating the

conditions of formation of exogenous defects. The essence of the method is defined by the mathematical model used for a chill mold in the casting stage. Numerous physical and numerical experiments were performed, indicating that the predictions of the theory and experimental data agree satisfactorily. An example of determining the diameter of a rod ventilation system is presented.

Program-Goal Design of Casting Processes

927D0032A Moscow LITEYNOYE PROIZVODSTVO in Russian No 6, Jun 91 pp 13-14

[Article by B. L. Kuznetsov, Kamsk Polytechnical Institute]

UDC 621.74.001.63

[Abstract] Improvement in the production of castings will require mastery of methods borrowed from the theory of operations research and mathematical-economic modeling, as well as special methods capable of acting as flexible elements to mate factors having different nature and dimension, in order to allow automatic process control and computer-assisted design techniques to be applied to the production of castings. Elements of program-goal design were developed in 1974-1980 at the KamAZ Motor Vehicle Plant casting shop as a part of the process of intensifying casting of cast iron in superhigh power electric furnaces. The program includes five subsystems: metallurgical melting technology; electric melting technology; organizational; electromechanical; and overall management. The program included research and design operations. As a result, a new course on casting machines and processes has been developed for the Kamsk Polytechnical Institute.

Increasing Quality of Castings Produced by Chill Mold Casting

927D0032F Moscow LITEYNOYE PROIZVODSTVO in Russian No 6, Jun 91 pp 29

[Article by A. V. Lapshin, Rybinskiy Institute of Aviation Technology]

UDC 621.74.043:669.715

[Abstract] A study was made of the possibility of increasing casting quality by increasing the rate of solidification by the use of water-cooled steel inserts in a chill mold. A comparison of the mechanical properties and process characteristics indicates that the new process has definite advantages over traditional methods. Problems include the danger of appearance of condensate on the cooled chill mold surfaces, which occurs if the mold is continuously cooled. If cooling is interrupted from the moment a casting is extracted until the start of the next pour, condensate is not formed.

Reinforcing Shell Forms With Foamed Pearlite

927D0032G Moscow LITEYNOYE PROIZVODSTVO in Russian No 6, Jun 91 pp 30-31

[Article by G. I. Timofeyev, I. G. Sapchenko, A. I. Yevstigneyev, Gorkiy and Komsomolsk-na-Amure Polytechnical Institutes]

UDC 621.74.045

[Abstract] Pearlite is an igneous rock close to granite in its chemical composition containing at least 1% water. When heated it foams and forms a light porous material widely used as a concrete filler. The process of manufacturing shell forms reinforced with foamed pearlite in the intermediate layer is similar to the traditional process of shell manufacture. Reinforcing molds with foamed pearlite is found to increase the strength of the molds both before and after heating and the crack formation resistance after thermal shock. Cracks formed by deformation are stopped in the reinforced layer, which prevents the propagation of cracks. References 4: Russian.

Production of Cast Dies

927D0083G Moscow LITEYNOYE PROIZVODSTVO in Russian No 12, Dec 91 pp 23-24

[Article by Ye.N. Vishnyakova, V.P. Prikhodko, V.V. Korobeynik, E.F. Mordvinov, A.A. Malkov, Ukrainian Scientific Research Institute of Metallurgy and Zavod imeni Malyshev]

UDC 621.74.002.6:669.14

[Abstract] The advantages of using cast forging dies instead of forged dies, particularly the possibility of considerably extending their service life and lowering production costs due to the improved characteristics of cast steel, are outlined. The process of making cast forging dies from steel 5Kh2NMF, 4KhSMF, and 5Kh3M by permanent mold casting is described and the properties of cast blanks are summarized. The cast die testing procedure and test results are presented. The results show that the mean endurance of a batch of cast dies from steel 5Kh3M with an HB 352-388 hardness after tempering exceeds that of forged dies by an average of 76% although at an HB 415 hardness, dies sometimes fail prematurely due to cracks in the bottom. The economic impact from replacing 800 sets of forged dies with cast at the Zavod imeni Malyshev production association is 1,308,000 rubles.

Effect of Dispersion on Sintering of Atomized High-Speed Steel Powders

927D0088A Kiev POROSHKOVAYA METALLURGIYA in Russian No 10(346), Oct 91 pp 11-15

[Article by R.A. Andriyevskiy, N.K. Kasmamytov, Physics Institute at the Kyrgyzstan Republic Academy of Sciences]

UDC 621.762

[Abstract] The urgency of developing the sintering conditions of high-speed steel (BS) powders whose physical, mechanical, and operational properties are comparable to those of hot deformed materials is recognized and a series of experiments conducted with atomized high-speed steel powders produced by the Dneprostal Plant is described. The microstructure of the powders and sintered steel R12M3K5F2 is examined microscopically, revealing internal pores which affect the pycnometric density. The chemical composition of high-speed steel powders is summarized and the dependence of the electric resistivity and relative density of sintered steels R12M3K5F2, 10R6M5, and R12MF5 on temperature is plotted. The microhardness of steel R12M3K5F2 powders before and after sintering as a function of the sintering temperature and particle diameter is investigated. The conclusion is drawn that the redistribution of metallic components during the sintering of alloyed steels due to a difference in their diffusive mobility—the diffusion segregation phenomenon—should be taken into account due to its possible effect on the physical, mechanical, and chemical properties of sintered bodies. Peculiar sintering behavior near the liquid phase initiation temperature is noted. An increase in microhardness in the contact necking zone is attributed to a more intensive carbon influx to these areas. The authors are grateful to V.P. Makarov and V.A. Pavlov for help. Figures 3; tables 2; references 13: 10 Russian, 3 Western.

Heat Treatment and Properties of 10R6M5-MP High-Speed Steel Produced From Gas-Atomized Powder Using High Hydrostatic Pressures

927D0088B Kiev POROSHKOVAYA METALLURGIYA in Russian No 10(346), Oct 91 pp 17-21

[Article by V.Z. Spuskanyuk, V.S. Tyutenko, Yu.A. Darda, T.V. Ploskogolovaya, A.V. Zavgorodnyaya, A.I. Sorokina, N.P. Chumakov, Donetsk Engineering Physics Institute at the Ukrainian Academy of Sciences]

UDC 621.762.4

[Abstract] The high quality of sintered high-speed steel due to the fine-grain structure of the material with uniformly distributed carbides and the high purity of the initial gas-atomized powders prompted their extensive production and studies aimed at improving the process. The effect of heat treatment on the properties of high-speed steel 10R6M5-MP produced from gas-atomized powder under a high hydrostatic pressure is investigated and the microstructure of hot compacted samples from steel 10R6M5-MP is examined under a microscope. The dependence of the HRC hardness, grain index, HRC hardness after tempering, heat resistance, bending strength, and impact elasticity of steel 10R6M5-MP on the hardening temperature and the properties of standard and high-speed steels heat treated under optimal conditions are examined and tabulated. The study demonstrates that compaction by hydrostatic pressure of a powder blank preformed by vacuum sintering to a 0.88-0.90 theoretical density makes it possible to produce rods and sections by the hot compaction method without using shells with a close to 100% quality. The properties of 10R6M5-MP products thus made are better than those of standard steel R6M5; the use of the method makes is possible to increase the endurance of cutting tools made from hot compacted rods by 1.6-2.0 times compared to steel 10R6M5-MP. Figures 2; tables 2; references 10.

Physicochemical Aspects of Detonation Coatings' Adhesive Bond Formation: I. Vulnerability to Erosion During Deposition

927D0088C Kiev POROSHKOVAYA METALLURGIYA in Russian No 10(346), Oct 91 pp 22-27

[Article by S.N. Buravova, A.A. Goncharov, Yu.N. Kiselev, E.A. Mironov, Yu.P. Fedko, Structural Macrokinetics Institute at the USSR Academy of Sciences, State Scientific Research Energy Institute, and Scientific Research Institute of Automotive Engineering]

UDC 621.793.7

[Abstract] The effect of the parameters of the topochemical reaction occurring between the base material and the powder being sprayed onto it on the adhesion bond strength between them is discussed and the adhesive bond strength formation of the (mostly) oxide detonation-deposited coatings is investigated stage by stage. To this end, preliminary abrasive jet surface preparation for spraying and the principal experimental factors accompanying the erosion wear of the surface under the effect of the flux of particles are analyzed. The interaction of particles with the base, i.e., the shock waves in the obstacle, bow and tail characteristics of the relief waves generated by the lateral faces of the particle, and the axial loosened material channel is examined and the dependence of the individual particle crater depth, axial loosened channel penetration depth, and the depth at which the shock wave degenerates into an elastic wave on the Mach number is plotted. The surface relief after the treatment by a particle flux is examined under a microscope. The erosion wear results in the formation of a jagged relief with a damaged subsurface layer whose structure is nonuniform and contains alternating strengthened and loosened segments. The appearance of spalling is noted. Figures 5; references 15: 12 Russian, 3 Western.

Certain Properties of Aluminum Nitride Compacts Produced by Shock Wave Loading

927D0088D Kiev POROSHKOVAYA METALLURGIYA in Russian No 10(346), Oct 91 pp 27-32

[Article by V.D. Andreyev, V.A. Lukash, M.N. Voloshin, A.I. Markov, Yu.I. Sozin, S.N. Dub, Superhard Materials Institute at the Ukrainian Academy of Sciences]

UDC 621.762

[Abstract] Published studies of shock wave loading of aluminum nitride powders aimed at ascertaining the possibility of activating them beforehand by explosion treatment before hot compaction and examining the capabilities of explosive compaction of AlN with and without preliminary heating are reviewed and the structure and properties of compacted aluminum nitride items produced by the explosion method without preheating are investigated. Commercial AlN powders with a less than 200 μm grain size containing 64.6% Al, 29.9% N, 4.2% O, 0.5-0.8% C, 0.5-0.65% Fe, and traces of Si and Mn loaded in steel containers are studied. The loading conditions and density of the resulting compacts of four batches as a function of the initial powder density and peak pressure are summarized and the fractures and microsections of compacts are examined under a microscope. The mosaic block size, lattice distortions, and dislocation density are investigated by X-ray structural tests. The material achieved 96% of theoretical density value; a considerable degree of mosaic block dispersion and a significant lattice microdistortion growth are noted. The dislocation density is increased by one-to-two orders of magnitude. All compacts are black in color. The crack resistance of AlN ceramics ranges from 3.4 to 5.8 MPa x $m^{1/2}$. The experiments confirm the possibility of producing AlN ceramics with a high crack resistance. Figures 4; tables 2; references 13: 3 Russian, 10 Western.

Mechanical Behavior of ZrO_2-Based Ceramics

927D0088E Kiev POROSHKOVAYA METALLURGIYA in Russian No 10(346), Oct 91 pp 51-56

[Article by G.A. Gogotsi, Strength Problems Institute at the Ukrainian Academy of Sciences]

UDC 666.76.01+621.48

[Abstract] The mechanical behavior of tough zirconium dioxide-based phase transition-hardened ceramics under loading is investigated. To this end, the ceramic index, brittleness modulus, density, ultrasonic vibration propagation velocity, Vickers hardness, bending strength, dynamic and static moduli of elasticity, ultimate strain, and notch sensitivity index of zirconia ceramics are studied as a function of the stabilizing additive. The strain diagram of brittle and relatively brittle ceramics and the dependence of sag and acoustic emission on the force applied are plotted. The behavior of relative brittleness with temperature is analyzed and ceramic material fractures are examined under a microscope. The results show that ceramics stabilized by yttrium oxide are linearly elastic until fracture while those stabilized by magnesium oxide are brittle; consequently, these ceramics' resistance to cracking and other properties differ. It is noted that the findings should not be interpreted solely by traditional concepts of the effect of phase transitions in zirconium dioxide on its mechanical behavior. Figures 6; tables 1; references 14: 6 Russian, 8 Western.

Systems To Extract Castings From Chill Molds

927D0104D Moscow LITEYNOYE PROIZVODSTVO in Russian No 11, Nov 91 pp 23-25

[Article by V.N. Yanchenko, I.Kh. Tarasov, and V.A. Kryuchatov, NIISL [not further identified] Scientific Production Association]

UDC 621.747.51

[Abstract] The experience that has been gained in designing chill molds demonstrates that one-third or more of all the design work that goes into developing such molds involves developing systems to extract castings from the working planes of the chill molds and removing the metal cores from the castings. Lever intensifiers may be recommended to increase the force applied when power operators are used to extract castings. Two-stage pushing can also significantly reduce the amount of power required of power operators used for casting extraction. Pushers are the most wear-prone components of a chill mold. Because they must be replaced so frequently, quick-detachable pushers are recommended. The use of gas pushing is another way of increasing the reliability of a chill mold's pushing mechanism. A chill mold has been developed that does not rely on pushers to extract castings. This sharply reduces the wear on the print sections of the core because the core prints do not come into contact with the shaping plates during the entire extraction period. Moreover, the molten metal does not come into contact with the guide element joint, and the number of parts moving relative to one another is kept to a minimum. In the case of castings requiring the use of a bottom, a chill mold design in which the bottom consists of two parts (moving and stationary parts) is recommended. Another area where problems arise when chill molds are designed is that of designing the guide sections of chill molds with large-diameter moving metal cores. The optimal length of such guides is 1.5 to 2 times the diameter of the core, which increases the chill mold's dimensions significantly. In such cases it is advisable to supply the core with an extension piece so that the core can be configured in the half-mold with a gap. The size of this gap should be selected so as to eliminate any flash and compensate for superheating in reaction to the nest. A guide surface of the required length can be created by using the extension piece, which may be secured to the mold body on the rear surface of the plate. Figures 5; references 9 (Russian)

An Equipment Set for Continuous and Periodic Monitoring of Casting Process Temperature

927D0104C Moscow LITEYNOYE PROIZVODSTVO in Russian No 11, Nov 91 pp 20-21

[Article by L.F. Zhukov, B.D. Kikish, V.M. Geyko, S.V. Kucherenko, and V.V. Drozdovskiy, Casting Problems Institute, Ukraine Academy of Sciences]

UDC 621.745.56:681.5.08

[Abstract] Temperature is critical to the casting process. It determines the quality of cast products and the costs of producing them. For this reason, associates at the Casting Problems Institute collaborated with a number of organizations to develop an equipment set for continuous and periodic monitoring of the temperature of metal in furnaces, ladles, and other units involved in the casting process. Two types of portable thermometers to measure short-immersion (10 to 30 seconds) temperature have been created. The immersible thermometers have a self-contained electric power supply and are capable of measurement, memory, and digital visual display of the temperature of molten metal. The first type of thermometer consists of a thermoelectric heat transducer and electronic unit to compensate for the temperature of the free ends, amplify the thermoelectromotive force, and linearize the thermoelectric characteristics of the thermometer, as well as convert the linearized analog signal into digital form and display it. The second type of thermometer is an optical thermometer that consists of an immersible model of thermodynamically equilibrious radiation in the form of a refractory terminal and lens-lightguide pyrometric converter. The electronic unit of the lightguide thermometer amplifies, linearizes, converts (from analog to digital form), and displays the output signal of the converter and compensates (i.e., provides thermal compensation) for its radiation detector. Both types of thermometers may be used together with automatic potentiometers when necessary. Systems with several modifications of the thermometers have been developed for continuous temperature monitoring. Depending on the individual conditions, the systems may be modified to include additional transducers and auxiliary devices for contactless or lightguide thermometry of metals, alloys, and other objects in various types of furnaces. The thermometers may be used with a manual or microprocessor automatic scaling module. The electronic portion of the microprocessor system has eight channels for continuous monitoring, recording, and digital display of the temperatures of four objects. Prototypes of the systems are now being introduced into industry in several versions. The new equipment has been demonstrated to operate under industrial conditions with an error of ≤1%. The new measuring techniques and devices have been awarded inventor's certificates in patents in the USSR, Bulgaria, the United States, Japan, Germany, Great Britain, Sweden, Canada, and Australia and are slated to be put into series production this year.

Intensification of the Continuous Horizontal Casting of Cast Iron by Blasting With Inert Gas

927D0104B Moscow LITEYNOYE PROIZVODSTVO in Russian No 11, Nov 91 pp 14-15

[Article by Ye.I. Marukovich, A.P. Melnikov, and E.B Ten, Mogilev Department, Physics Engineering Institute, Belarus Academy of Sciences, and Moscow Institute of Steel and Alloys]

UDC 621.746.047

[Abstract] A study examined the effectiveness of blasting a cast iron melt with inert gas. A model A-99 continuous horizontal casting unit was used for the casting and nitrogen or argon used as the inert gas. The gas was fed in in a cyclic regimen corresponding to the drawing of the blank. This made it possible to intensify the process of forming the casting. The gas stream acted so that when the ingot was stopped and the initial skin was forming, the hotter melt would not travel from the metal reservoir to the crystallizer cavity. As the blank was being drawn, a portion of the melt that was partially cooled by blasted gas entered the crystallizer. The convective flows of the melt in the system "metal reservoir-crystallizer" was adjusted to increase the productivity of the process. The gas stream "screened" the entrance to the crystallizer, impeding the natural flow of the melt to and from the crystallizer, thereby weakening the intensity of lengthwise heat transfer from the superheated melt in the metal reservoir to the colder metal in the crystallizer. This reduced the amount of heat entering the crystallizer from the metal reservoir and resulted in more rapid formation of a hard skin on the cast iron. This in turn created the requisites for reducing the duration of the stoppage and the duration of the blank-drawing cycle. The efficiency of gas treatment of cast iron before the entrance to the crystallizer was found to increase as the area of the cross section of the blank being produced was increased. Blasting cast iron with nitrogen was found to improve its mechanical properties (ultimate strength, yield strength, relative elongation, and constriction). This increase in the strength properties of cast iron blasted with nitrogen was attributed to the reduction in the size of the eutectic grain that results from the blasting. Overall, the technique of blasting cast iron blanks with inert gas was found to boost process productivity by a factor of 1.4 to 1.6. Figures 3; references 6 (Russian).

Synthesis of Cast Hard Alloys

927D0104A Moscow LITEYNOYE PROIZVODSTVO in Russian No 11, Nov 91 pp 5-6

[Article by Yu.Yu. Zhiguts, Machining Accessories Special Design Office, Beregovo]

UDC 621.74:669.018.25

[Abstract] Hard alloys and carbide steels are generally produced by powder metallurgy methods. Producing cast hard metal alloys is difficult because of their highly refractory nature. The creation of the theory and practice of self-propagating high-temperature synthesis has provided new hope with respect to producing cast carbide steels. In view of these facts, the authors of this article considered the problem of manufacturing a tungsten-cobalt hard alloy. Specifically, they consider a combined "hybrid" process in which mixtures of powders and carbides are burned (as when carbides, borides, and silicides are produced). The process occurs in two stages: reduction from an oxide (a metallothermic reaction) and

self-propagating high-temperature synthesis. Because no additional power supply is required, the process may be implemented in the simplest reactors, and cast products may be obtained from the starting components of the metal mixture in a single stage. The authors repeated a previously published experiment in which a cast hard alloy was synthesized by using tungsten oxide (WO_3), metallic cobalt or its oxides (CoO, Co_2O_3, and Co_3O_4), commercial-grade aluminum (types PA-2 and PA-4), and carbon (in the form of graphite powder or carbon black). A thermit match was used to initiate the reaction. The content of aluminum in the starting mixture was varied from 16.0 to 19.5% (17.% being the stoichiometric quantity). Increasing the aluminum content in the metallothermic mixture was found to increase the yield of alloy from the starting mixture and to result in a slight increase in the amount of residual aluminum in the alloy (0.1 to 0.2%). Further increases in the amount of aluminum in the starting mixture were not found to change either the yield of alloy or the content of residual aluminum. Cast solid alloys of the types VK3, VK4, VK6, VK8, VK10, VK15, and VK20 alloy were synthesized analogously. Using metallic cobalt instead of its oxides was found to result in the appearance of a large number of drops of solidified alloy in the slag. Adding Co_2O_3 or Co_3O_4 instead of CoO was found to increase the yield of alloy somewhat. The cast solid alloy synthesis was quite different from that produced by powder metallurgy in that it lacked porosity and free carbon and thus possessed differences at the levels of microstructure and mechanical properties. The grain size of the tungsten carbide synthesis by the new technique was larger, and the cast alloys were harder than their counterparts produced by powder metallurgy methods. The heat conduction of the cast alloys was 15 to 25% higher than that of analogous alloys produced by the powder metallurgy technique, which is one of the reasons behind the improved cutting properties of cast hard plates. Figure 1; references 4 (Russian).

Filters for High Temperature Melts

927D0083D Moscow LITEYNOYE PROIZVODSTVO in Russian No 12, Dec 91 pp 11-12

[Article by Yu.A. Selivanov, E.V. Azarov, Odessa Polytechnic Institute]

UDC 621.745.56:669.14

[Abstract] The use of filters makes it possible to separate the slag inclusions and gas from the molten metal flow, increase the uniformity of the metal's mechanical properties, and decrease the cutting tool wear during the machining of the resulting castings. The three principal types of filters—screen, granular, and ceramic—used for this purpose are described and the methods of making them are outlined. The dependence of the quantity and release rate of volatile components on the melt treatment duration is plotted and the mechanical properties and number of machining operations per casting with and without filtering are summarized. It is shown that highly porous carbon is the best material for developing highly porous carbide filter materials for high-temperature melts. Experiments show that the best silicon carbide coats on filters are produced on carbon-carbon composite materials on a polyurethane base. The microstructure of the carbon material is examined under a microscope. An analysis also reveals that silicon deposition from the vapor phase on a vitreous carbon substrate is an efficient means of producing highly porous silicon carbide filters and that the strongest materials are produced at a 2,000-2,200°C temperature. Figures 2; tables 1; references 1.

Induction Hardening of Base Parts of Heavy and Unique Machine Tools

927D0083B Moscow LITEYNOYE PROIZVODSTVO in Russian No 12, Dec 91 pp 6-9

[Article by A.A. Agrayev, G.V. Glukhov, I.Ye. Illarionov, Ulyanovsk Heavy Machine Tool Plant and Chuvash State University]

UDC 621.747.58

[Abstract] The method of strengthening the slide guides of cast iron and steel base parts of unique and heavy machine tools by high-frequency induction hardening performed in model 206S machine with a traveling gantry, one or two 100 kW, 8 kHz generators, and a workbench for the hardened parts developed at the production association of the Ulyanovsk Machine Tool Plant is described. The optimum cast iron structure for the slide guides is established and the relationship between the pearlite structure and flaky graphite distribution is plotted. The cracking mechanism during the induction hardening of castings is examined and data on the casting dimensions and distortions are summarized. The dependence of the casting distortion on the stiffness coefficient is plotted and the straightening procedure is outlined. The economic impact from increasing the original life alone exceeds 0.3 million rubles a year for parts of vertical knee-type milling machines. Figures 4; tables 1; references 6.

On Selecting Laser Treatment Conditions of Ni-P Coats on Tool Steels

927D0082K Moscow IZVESTIYA VYSSHIKH UCHEBNYKH ZAVEDENIY: CHERNAYA METALLURGIYA in Russian No 9, Sep 91 pp 82-85

[Article by G.I. Brover, Ye.A. Katsnelson, V.N. Varavka, V.T. Loginov, G.Ye. Trofimov, V.D. Kritin, Rostov-na-Donu Institute of Agricultural Machinery Industry]

UDC 621.785:669.14.018.29

[Abstract] The importance of the adhesive bond strength of chemically applied Ni-P coats and their hardness in agricultural machinery is discussed and the results of an investigation of Ni-P coats are reported. The coats under study did not have the required strength of bonding to the base metal and thus necessitated heat treatment; a preliminary analysis revealed that laser heat treatment is the most efficient for this purpose. A series of experiments was conducted in order to optimize the laser irradiation conditions and establish their effect on the structure and principal properties of Ni-P coats. To this end, the phase and structure of coats on alloyed steels 9KhS, Kh12M, and R18 were studied by methods of X-ray structural and metallographic analyses after laser hardening in order to establish the morphological characteristics of the irradiated zones under various conditions. The dependence of the irradiated Ni-P surface hardness on these brands of steel on the radiation power density is examined and the diffraction patterns of chemically applied Ni-P coats on steel U8 before and after laser irradiation under various conditions are plotted. The results show that laser heat treatment without bulk heating to 400°C beforehand increases the coat hardness at high irradiation power densities while laser irradiation following bulk preheating makes it possible to maintain high hardness only at low irradiation densities. Laser processing generally increases the bonding strength due to the development of a continuous series of Ni-Fe solid solutions in the transition zones. Figures 3; references 2.

Measuring Certain Properties of Powder Ti and its Alloy With Mo During Phase Transformations

927D0082J Moscow IZVESTIYA VYSSHIKH UCHEBNYKH ZAVEDENIY: CHERNAYA METALLURGIYA in Russian No 9, Sep 91 pp 80-82

[Article by A.A. Nuzhdin, Moscow Institute of Fine Chemical Technology imeni M.V. Lomonosov]

UDC 669.018.095

[Abstract] The processes accompanying polymorphous transformations in metals and alloys are discussed and changes in the coefficient of thermal expansion (KTR) and volumetric phenomena occurring during phase transitions in powder titanium and its alloy containing 29.5% molybdenum are investigated using the dilatometry method with the help of a Leitz dilatometer. Samples from the PTES-1 titanium powder were made by compaction at normal or high temperatures by conventional methods while samples from powder alloys were made by compacting titanium and molybdenum granules produced beforehand with subsequent extended diffusion annealing and sintering. The modulus of elongation and shear modulus were measured and the modulus of dilatation was determined on their basis. The studies show that residual porosity does not significantly affect the temperature behavior of the coefficient of thermal expansion of powder titanium and Ti-Mo alloy while an abrupt change in the value of the thermal coefficient of expansion is observed during phase transitions. Volumetric effects depend largely on the sample porosity and cooling rate; this is attributed to the temperature-induced stress. During the heating of the materials under study, phase transitions are accompanied by an increase in the parameter determined by the product of the volumetric coefficient of thermal expansion and the modulus of compression. The results are consistent with the findings of other researchers. Figures 3; references 7.

Dependence of Mechanical Properties of Steel 08YuT on Cooling Rate

927D0082I Moscow IZVESTIYA VYSSHIKH UCHEBNYKH ZAVEDENIY: CHERNAYA METALLURGIYA in Russian No 9, Sep 91 pp 78-80

[Article by S.V. Bobyr, O.M. Shapovalova, Dnepropetrovsk State University]

UDC 669.017.539.41.5

[Abstract] The effect of the chemical composition and various process parameters on the mechanical properties of steel are discussed and attention is focused on the effect of the cooling rate during the $\gamma \rightarrow \alpha$ transformation in steel 08YuT on its mechanical properties. The investigation is carried out both theoretically and experimentally; in so doing, the dependence of the yield point, ultimate strength, and elongation of cylindrical samples from steel 08YuT on the cooling rate, the dependence of the dislocation density on the equivalent grain size, the dependence of the equivalent grain size of steel 08YuT and 08ps on the cooling rate, and the dependence of the yield strength on the dislocation density and cooling rate are plotted. A comparison shows that steel 08YuT has a smaller equivalent grain at the same cooling rate and, as a result, better strength properties. It is established that at low cooling rates, the ferrite grain size in steel 08YuT changes by the logarithmic law. Figures 2; references 7.

Structure and Texture Inhomogeneity of Fe-Si Alloys Quenched in Liquid State

927D0082H Moscow IZVESTIYA VYSSHIKH UCHEBNYKH ZAVEDENIY: CHERNAYA METALLURGIYA in Russian No 9, Sep 91 pp 75-78

[Article by M.V. Anisimova, S.S. Golovanenko, L.I. Labed, G.A. Nuzhdin, Ye.I. Polyak, Moscow Institute of Steel and Alloys]

UDC 669.018.524.85

[Abstract] The method of producing thin sheet materials by quenching in the liquid state making it possible to eliminate a considerable number of rolling process stages is considered; in addition, rapidly quenched sheets have an increased cold rolling ductility which is especially important for high-silicon electrical sheet steel or Fe-Si-Al alloys. The structure and texture of rapidly quenched sheets differ considerably from those of sheets of the same thickness and composition produced by other methods; consequently, the structure and texture inhomogeneity of cast sheets and its changes under the effect of temperature- and strain-induced factors which do not equalize the cross-sectional structure distribution are investigated. Alloys of iron with 3-5% Si produced by quenching in the liquid state are used in the experiments. The structure of rapidly quenched silicon steel immediately after solidification with symmetric and asymmetric grain configurations is examined and pole figures of cast and annealed fine-crystalline Fe+5% Si strips are plotted. The dependence of the intensity and scattering angle of the texture component, mean grain size, and microhardness on the annealing temperature of the Fe+5% Si fine-crystalline strips is examined. The study reveals that immediately after the solidification by quenching, the strip from high-silicon electrical sheet steel has a high cold-work degree leading to primary recrystallization of the cast sheets during heating. The liquid state quenched Fe-Si alloy strip has a highly nonuniform cross-sectional structure and texture due to its nonequilibrium state. The cubic texture most favorable to magnetic properties is concentrated at the central part of the strip; this structure can be weakened by annealing. Figures 4; tables 1; references 3: 1 Russian; 2 Western.

Mechanism of the Hardening of Metals During the Ultradeep Penetration of High-Speed Particles

927D0070A Moscow FIZIKA I KHIMIYA OBRABOTKI MATERIALOV in Russian No 6, Nov-Dec 91 (manuscript received 9 Aug 89) pp 19-24

[Article by V.F. Nozdrin, S.M. Usherenko, and S.I. Gubenko, Dnepropetrovsk]

UDC 534.2:621.385.833

[Abstract] The authors of the study examined the mechanism of the hardening of Armco iron and molybdenum metals during the ultradeep penetration of high-speed

particles. Specimens of Armco iron and molybdenum were forged and annealed prior to the high-speed treatment. Particles of Si_3N_4 or Ti together with TiB_2 ranging in size from 40 to 125 μm were used as a striker. The target was treated with a high-speed steam of active medium produced by using the energy of an explosive to throw the plate. The particles were accelerated to a speed of 2 km/s, and the pressure upon collision with the target exceeded 15 GPa. An EMV-100 B transmission electron microscope was used to study the microstructure of the test specimens before and after the explosive treatment. Blanks for foils 0.3 to 0.4 mm thick were cut from the specimens by the electric spark method. The blanks cut were perpendicular and parallel to the specimens' axes at a depth of 5 to 7 mm from the surface. Mechanical polishing with diamond pastes followed by electrochemical polishing in an electrolyte consisting of orthophosphoric acid (640 ml) and chromic anhydride (120 g) at a temperature of 70 to 80°C and a voltage of 6 to 8 V was used to make the blanks thinner. The microstructural studies of the Armco iron revealed the presence of thin channels in the foils made from the lengthwise blanks. The channels found in the foils made from the crosswise blanks were in the form of oval holes. The channels contained particles demonstrated to be a powder material. The particles were often surrounded by spiderlike extinction contours. The zone directly adjacent to the metal matrix did not contain the conventional fine-structure elements, i.e., dislocations, stack faults, or microtwins. A thin metal layer on the channel surface was found to be in an amorphous state that was likely caused by fusion of a thin layer of metal due to heating by friction generated as the particles moved or else by the development of a very high degree of plastic deformation. The fine structure of the metal far from the channels and particles exhibited a very low degree of deformation. Directly adjacent to the thin surface layer of the channel with an amorphous structure was a zone with a highly fragmented structure characterized by a high density of dislocations. Dark, narrow, small bands located strictly parallel to the grain boundaries, i.e., zones of localized deformation, were discovered against the background of the fragmented and cellular dislocation structure. A set of highly curved twins was also discovered to have formed in the same zones after the explosive treatment. The same structural zones were observed in the molybdenum foils. Shock waves propagated from particles inward into the metal's bulk were found to result in strong plastic deformation along the entire trajectory of their motion as well as in braking (arrest) sites. The plastic deformation occurring upon an explosive effect was found to have the following distinctive features: 1) a sharp increase in the number of dislocation sources and slip systems and 2) an increase in the growth rate of the dislocations developed by the nonconservative motion of the dislocations with small steps that in turn resulted in an increase in the number of point defects. The interaction of the dislocations at a high rate of speed was found to result in flare-ups of stresses. The deformation decreased gradually farther from the channels and particles. The transition from one deformation zone to another appeared similar to phase transitions from one dislocation phase to another. The plastic deformation discovered was local in nature and high-speed. Rotation and twin components were found to play a big role in the development of deformation. Figures 3; references 10 (Russian).

The Effect of γ- and Electron Irradiation on the Optical Properties of Barium-Sodium Niobate ($Ba_2NaNb_5O_{15}$) Crystals

927D0070C Moscow FIZIKA I KHIMIYA OBRABOTKI MATERIALOV in Russian No 6, Nov-Dec 91 (manuscript received 15 May 90) pp 39-42

[Article by S.A. Baryshev, G.A. Yermakov, V.N. Karasev, V.P. Nosov, and S.V. Protasova, Moscow]

UDC 535.34:621

[Abstract] The authors of the study examined the effect of γ- and electron irradiation on the process of the twinning of barium-sodium niobate crystals and on the optical loss coefficient in crystals at the wavelength of a neodymium laser (1.064 nm). The barium-sodium niobate crystals used were grown from a melt by the Czochralski method. The crystals were in the shape of parallelepipeds measuring 12 x 5.0 x 2.5 mm along the X, Y, and Z axes. The crystals were irradiated as specified with a γ-quanta energy of 1.25 MeV. The temperature of the specimens did not exceed 30°C. The irradiated specimens underwent a twinning process that included heating to a temperature of 260-300°C, holding at that temperature under a load applied perpendicular to the (100) plane of a tetragonal cell of the crystal, and cooling (while still under a load) to room temperature. Nonirradiated control specimens were subjected to the same twinning process. The refractivity gradient was measured before and after twinning along the direction (010) at λ = 632.8 nm, and the transmission coefficients at λ = 532 and 1,064 nm were measured. The experiments performed confirmed that γ-irradiation has a significant effect on the twinning process. The magnitude of the uniaxial mechanical load applied to the preirradiated specimens was only a third to a half that applied to the nonirradiated crystals so as to exclude the possibility of mechanical fracture of the crystals during the twinning process. The refractivity gradient of the irradiated crystals after twinning did not exceed 10^{-5}, whereas that for the nonirradiated crystals was between 10^{-4} and 10^{-3}. The time for which the irradiated crystals were held under a mechanical load was also considerably (by a factor of 3 to 5) less than that used in the case of the nonirradiated control specimens. Measurements of transmissivity at λ = 532.8 nm demonstrated that preliminary γ-irradiation and subsequent thermomechanical treatment of barium-sodium niobate crystals reduces their optical irradiation sensitivity in the dose range of 10^2 to 10^6 Gy by 10%. The same effect was achieved by heat treatment in air at T = 650°C for 5 to 15 hours. In all cases, the transmissivity at λ = 1,064 nm remained

virtually unchanged from the starting values. From their results, the authors concluded that preliminary γ-irradiation of barium-sodium niobate crystals evidently changes the state of the defect centers impeding the motion of twin boundaries and thus accelerates the twinning process. In the second half of their study, the authors subjected barium-sodium niobate crystals measuring 10.0 x 5.0 x 3.5 mm along the X, Y, and Z axes to electron irradiation in the flux range from 10^{10} to 10^{15} electrons/cm^2 with a power of 1 to 10 MeV. After irradiation the specimens were subjected to heat treatment at temperatures from 50 to 250°C for various holding times. The optical loss coefficient of the test specimens ranged from 0.01 to 0.5 cm^{-1}. In cases where the length of the free electron run (R) was not greater than the crystal's dimension in the direction of the irradiation, the optical uniformity of the crystals dropped significantly: It exceeded 0.2 cm^{-1}. When it was greater, however, the absorbed dose was absorbed evenly throughout the entire crystal. Subsequent heat treatment made it possible to reinforce the effect achieved and to burn off the radiation defects occurring during irradiation. Figure 1, table 1; references 12: 10 Russian, 2 Western.

The Formation of $Mg_{32}(Al, Zn)_{49}$ and Al-Mg-Zn Phases in an Aluminum-Magnesium-Zinc Unsaturated Solid Solution During Electron Irradiation in a Diffraction Channeling Mode

927D0070D Moscow FIZIKA I KHIMIYA OBRABOTKI MATERIALOV in Russian No 6, Nov-Dec 91 (manuscript received 28 Sep 90) pp 50-52

[Article by V.V. Ivanov, V.M. Lazorenko, and Yu.M Platov, Moscow]

UDC 621.791.85:620.18

[Abstract] The authors of the study examined the formation of $Mg_{32}(Al, Zn)_{49}$ and Al-Mg-Zn phases in an alloy consisting of aluminum, 1% (atomic) Zn, and 0.06% (atomic) Mg when subjected to electron irradiation in a high-voltage microscope. Foils of the said alloy with a thickness of 0.2 mm were annealed in air at a temperature of 550°C for 2 hours. The specimens were thinned in an electrolyte consisting of 20% $HClO_4$ and 80% C_2H_5OH at a temperature of -60°C. The foils were then irradiated in a JEM-1000 high-voltage electron microscope by electrons with an energy of 1 MeV at temperatures of 20 to 150°C. The irradiation was implemented with an intensity of 6.2 x 10^{18} cm^{-2} x s^{-1} in a channeling mode where the electron beam was virtually parallel to planes of the type (111), (100), and (110) and passed along the axis of the crystal's zone. Irradiation in a channeling mode as described was found to result in the decomposition of the solid solution and the formation of two phases: $Mg_{32}(Al, Zn)_{49}$ and Al-Mg-Zn and a phase consisting of 20% (by weight) Al, 40% (by weight) Mg, and 40% (by weight) Zn. Unlike in the case of neutron irradiation, the appearance of an additional Al-Mg-Zn phase upon electron irradiation may be connected with the high content of Mg in the starting alloy. After analyzing their results, the authors concluded that they can only speculate as to the mechanisms of the formation of the $Mg_{32}(Al, Zn)_{49}$ and Al-Mg-Zn phases. They hypothesized that the mechanism at work was either a segregation mechanism analogous to the formation of a phase during neutron irradiation or else a spin decomposition mechanism. They concluded by stating that the phase transformations occurring in unsaturated solid solutions during neutron irradiation may be modeled by electron irradiation in a diffraction channeling direction. Figure 1, table 1; references 5: 3 Russian, 2 Western.

Electroerosion-Laser Alloying of High-Chromium Steels by Tungstenless Electrodes

927D0070H Moscow FIZIKA I KHIMIYA OBRABOTKI MATERIALOV in Russian No 6, Nov-Dec 91 (manuscript received 23 Oct 90) pp 124-129

[Article by V.S. Kovalenko, I.A. Podchernyayeva, L.D. Kinkina, and R.K. Ivashchenko, Kiev]

UDC 535.211:669.017

[Abstract] The authors of the study examined the process of combined electroerosion-laser alloying of high-chromium corrosion-resistant steels (Cr12Mo and Cr12V) by using tungstenless electrode materials based on titanium carbide, titanium boride, and zirconium nitride. The effectiveness of these tungstenless electrode materials was compared with that of the hard alloy VK8. Specimens of the two aforesaid steels measuring 15 x 15 x 5 mm were first coated with an electroerosion coating on an Elitron-21 unit. The alloyed layers were 15 +/- 5 μm thick and had a continuity of 80-90% in the case of the VK8 versus 60-70% in the case of the tungstenless alloys. Next, the specimens' surfaces were irradiated with a solid-state laser operating at a wavelength of 1.06 μm with a radiating power of 0.2 kW and beam diameter of 500 μm. The specimens were moved at rates varying from 165 to 750 mm/min. The degree of overlap of the paths was 0.3. Helium was blown coaxially with the laser beam to prevent oxidation of the surface in the area being treated. The tribotechnical characteristic of the test specimens were determined on an MT-58 friction-testing machine. The specimens were also subjected to metallographic and micromechanical analyses. The treatment regimen used resulted in the formation of two zones on the high-chromium steels tested. The first zone, i.e., a melt zone, was formed by laser fusion of the surface. It contained dendrites elongated in the direction of the heat abstraction that are characteristic of crystallization from a melt. This zone was 30 to 100 μm thick and had a microhardness of 8.00 +/- 0.30 GPa, which corresponds to the maximum microhardness of Cr12Mo steel attainable by laser hardening from a liquid state. The second zone, i.e., a heat-affected zone, was found to be 100 to 250 μm thick and have a microhardness of 13.00 +/- 0.50 GPa. It also had a lower relative wear

when compared with the initial alloyed layer and the main layer. The depth of the zone with improved physicomechanical properties was found to be linearly dependent on the laser's radiating power. Figures 3, table 1; references 7 (Russian).

Acoustic Shock Effects in Crystals During Ion Irradiation

927D0070E Moscow FIZIKA I KHIMIYA OBRABOTKI MATERIALOV in Russian No 6, Nov-Dec 91 (manuscript received 14 May 90) pp 53-55

[Article by P.V. Pavlov, Yu.A. Semin, V.D. Skupov, and D.I. Tetelbaun, Gorkiy]

UDC 539.1.043:620.18

[Abstract] The authors of the study analyzed and attempted to systematize the generation of elastic waves in crystals by an ion beam. They identified several microscopic and macroscopic mechanisms of the occurrence of elastic (acoustic) waves during ion irradiation. Specifically, they drew a distinction between the effects of pulsed and continuous irradiation and identified the following sources of elastic waves: 1) cascades of atomic displacements caused by local dilation or a thermal effect or else by restructuring of radiation defects in cascades, as well as the radiationless recombination of pair-generated charge carriers, and 2) elementary acts involving point defects (e.g., recombinations of Frenkel pairs). They went on to offer several pieces of evidence confirming that elastic waves generated by an ion beam may induce structural (and property) changes in solids (crystals) far beyond the boundaries of the ions' run. Finally, they concluded with the point that these effects are more pronounced in structurally imperfect crystals and close to a crystal's surface (including that surface opposite the irradiated surface). Figures 2; references 21: 19 Russian, 2 Western.

Sets of Rotation Effect Functions in the Problem of Forecasting the Stability of Materials and Instruments in Ionizing Radiation Fields

927D0070B Moscow FIZIKA I KHIMIYA OBRABOTKI MATERIALOV in Russian No 6, Nov-Dec 91 (manuscript received 14 May 90) pp 33-38

[Article by V.I. Ostroumov, G.G. Solovyev, and A.I. Trufanov, Irkutsk, Moscow, and Leningrad]

UDC 539.1.043

[Abstract] The radiation fields governing the operating conditions of equipment located aboard spacecraft are characterized by a complex particle component and significant variations in the differential density of particle fluxes. These fields must be given consideration when designing testing and measuring equipment and instruments that can completely recreate conditions on earth when used on board spacecraft. In an effort to advance work on this problem, the authors of the study formulated the problem of expanding the set of problems that can be solved by using an approach based on the concept of a radiation effect function. They derived a series of formulas designed to consider the effect that fluence and intensity of irradiation have on the stability of instruments and materials. The authors then proceeded to incorporate these equations into a model of the radiation processes occurring in materials with a shock mechanism of damage. The model was based on the equivalence of the contributions that the first atoms to be knocked off make to the changes in the properties of the said materials as they are irradiated. On the basis of their proposed model, the authors demonstrated that the radiation effect function approach to forecasting radiation stability may be used to solve a wide range of practically important problems. This includes many problems that are critical in the science of the materials used in spacecraft, where it is often necessary to consider broad ranges of variations in fluence and bombarding-particle flux density, as well as the problem of simultaneous irradiation by different sources. The radiation-effect function approach may also be used when working with data obtained in ground experiments on readily available and more economical equipment. Figure 1; references 11 (Russian).

Metallographic Model for Predicting Austenite Thermokinetic Transformation Diagrams

927D0027E Moscow METALLOVEDENIYE I OBRABOTKA METALLOV in Russian No 6, Jun 91 pp 18-20

[Article by I. Tamura, N. Komatsubara, and K. Kunshige, Japan]

UDC 669.017.3:001.891.573

[Abstract] A model of phase transformation based on laws of thermodynamics as well as on metallographic theory of crystal nucleation and growth has been constructed for austenite, including also the kinetics of ferrite, pearlite, and bainite transformations. This model is more adequate for predicting nonisothermal and thus thermokinetic phase transformation diagrams, considering that the additivity law applicable to isothermal transformation is not valid here and that experimental determination of the transformation rate for use of empirical formulas in not easy. The metallographic model covers four kinds of diffusive transformations during continuous cooling and uses simple relations for calculating the volume fractions of respective phases after any given time interval. These transformations are: 1) austenite → polygonal granular ferrite, calculations based on periodic solution to equations of sublattice model and on the assumption of ferrite nucleating at austenite grain boundaries; 2) polygonal ferrite → Widmanstatten lamellar ferrite, calculations based on the assumption of both nucleating under identical conditions; 3) pearlite → bainite, pearlite formed from either

polygonal or lamellar ferrite. Practical application of this model is demonstrated on steel containing 0.14 % C, 1.5 % Mn and 0.2 % Si. The effect of latent heat Q_L on the cooling rate dT/dt is evaluated analytically, the temperature rise due to latent heat is calculated according to the relation $dT/dx = Q_L/c_p$ (dx- volume fraction of new phase formed within time δt; c_p- specific heat under constant pressure), and the temperature during time interval t = i is estimated as $T_i = T_{i-1} + dT_Q + dT$ (T_{i-1}- temperature during preceding time interval i-1; dT_Q- temperature fall due to cooling), disregarding the internal temperature gradient. Figures 2; references 15.

Pretransformation State of Iron Alloys

927D0027B Moscow METALLOVEDENIYE I TERMICHESKAYA OBRABOTKA METALLOV in Russian No 6, Jun 91 pp 7-10

[Article by A.P. Gulyayev, Central Scientific Research Institute of Ferrous Metallurgy imeni I.P. Bardin]

UDC 669.14:669.017.3

[Abstract] Following a review of γ→α - α→γ phase transformations and recrystallization in accordance with the Fe-C constitution diagram, which has been refined since D.K. Chernov's discovery (in 1868) of solid-state processes in steel and their dependence on the carbon content, the anomaly of two different diagrams for the high-carbon (> 6.7 % C) range is examined and found to be apparent only. One and the same diagram is shown to explain that cementite in pure Fe-Ni-C and other iron alloys with a lower than < 0.1 % Si content will not break up into a liquid phase and graphite, inasmuch as only in ternary alloys containing enough graphitizing agents such as silicon will graphite form and coexist with residual cementite. The fact that cementite is an unstable and not exactly stoichiometric Fe_3C compound which in such ternary alloys does not, however, break up below 1250°C is indicated by a homogeneity range on this diagram. The diagram need not indicate internal changes in solid-solution phases, however, because these changes do not cover ranges of different phases. Solid solutions usually extend along lines of change from one phase composition to another, thus characterizing the preparedness of existing phases to undergo transformation and thus their pretransformation state. There are, more precisely, two such states along the solidus: preliquefaction and pretransformation. The preliquefaction state is demonstrated on a heat-resistant Fe-Ni alloy, structural changes occurring over the 800-1350°C temperature range being reflected by the temperature dependence of its strength and ductility (ultimate strength decreases monotonically as temperature rises, while percentage elongation peaks to maximum at 1200°C). The pretransformation state is demonstrated on R-W18 high-speed tool steel, which exhibits subcritical superplasticity below the A_{c1}-point but not immediately above it within the α→γ transformation range (characterized by decreasing plasticity). The pretransformation state is also demonstrated on low-carbon (< 0.3 % C) steels, with a higher plasticity not only below but also above the A_{c1}-point. This increase of plasticity is caused by increasing diffusive mobility of atoms. During fast heating only, moreover, pearlite-to-austenite transformation is followed by a temperature range of stability preceding an intense α→γ transformation with attendant buildup of more carbon-free austenite than corresponding to phase equilibrium. Superplasticity exhibited by low-carbon steels during fast heating is thus only apparently and not really inconsistent with the concept of subcritical superplasticity, if that stability range is regarded as a pretransformation range of subcritical superplasticity. Figures 7; references 11.

Improving Coarse-Grain Structure of Steel by Corrective Heat Treatment (Chernov's b-Point)

927D0027A Moscow METALLOVEDENIYE I TERMICHESKAYA OBRABOTKA METALLOV in Russian No 6, Jun 91 pp 6-7

[Article by V.D. Sadovskiy (deceased), Institute of Metal Physics, Ural Department, USSR Academy of Sciences]

UDC 621.785:620.186.8

[Abstract] Recrystallization of austenite from coarse grain to fine grain by heat treatment of steel at a temperature above Chernov's b-point following α→γ transformation is considered, a distinction being drawn between that b-point and Osmond's A_{c3}-point at which austenitic transformation has been completed. The proposed and experimentally demonstrated recrystallizing heat treatment is to proceed in two stages, inasmuch as α → γ martensite-to-austenite transformation may not necessarily result in a smaller grain size, inasmuch as in the first stage austenite forms with a structure identical to its original one. Grain size-reduction and reorientation then occur in the second stage as a result of spontaneous recrystallization triggered by residual structural imperfections. The two stages differ in terms of their kinetics, the α → γ temperature range being almost independent of the heating rate while the recrystallization temperature range can be widened by faster heating or narrowed by slow heating. While the α → γ transformation takes place without a decrease of grain size, the grain size is decreased as the temperature is raised further or the heating time is lengthened. In this way the b-point and the A_{c3}-point cease of coincide and the b-point moves away from the A_{c3}-point, especially far away when very fast heating suppresses recrystallization of austenite over the entire temperature range up to the melting point (at which the b-point vanishes). The two points can coincide when there is sufficient time for the austenite to recrystallize during the α → γ transformation, or they can differ by tens or even hundreds of degrees. Recrystallization and phase transformation thus become separate processes during both very fast heating and very slow heating, the A_{c3}-point remaining a fixed one. It is noteworthy that recrystallization of austenite is

strongly stimulated by prior plastic deformation so that preliminary cold working and subsequent fast heating by a laser beam, for instance, will result in an ultrafine structure with 1-2 μm diameter grains. Figures 2; references 2.

Theory of Alloying High-Speed Tool Steels

927D0027C Moscow METALLOVEDENIYE I TERMICHESKAYA OBRABOTKA METALLOV in Russian No 6, Jun 91 pp 10-14

[Article by L.S. Kremnev, Moscow Institute of Machine Tool and Tool Design]

UDC 669.14.252.3

[Abstract] The problem of alloying high-speed tool steels is analyzed from the standpoint of their hardenability and grindability, considering that the classical R-W18 and the R-W6Mo5 steels are hardened principally due to precipitation of Me_6C carbides during tempering at 560°C. It is shown that in order to ensure a minimum 62-63 Rockwell C hardness by precipitation of one such carbide, namely Fe_4W_2C in steel with 0.7-0.8 % C or $Fe_4(W,V)_2C$ in steel with 0.8-0.9 % C, it is necessary to add approximately 18 % W in the first case and 12-13 % W + 1.5-2.0 % V in the second case. A comparative examination of the two R-W18 and R-W12 steels reveals that the volume fraction of carbide is the same in both, but that increasing the tungsten content increases the weight fraction of carbide. The solubility of vanadium in the Fe_4Me_2C is maximum in the R-W12 steel, the volume fraction of this carbide-solvent decreasing as the tungsten content is decreased below 12 wt.% W or increased above 13 wt.%. This trend is comprehensively depicted on the V_{ss}/V_{st}-W diagram describing the dependence of the V_{ss}/V_{st} ratio (V_{ss}- wt.% V in solid solution, V_{st}- wt.% V in quenched steel) over the 7-18 % W range. The dependence of the grindability factor K on the W + Mo content is depicted on diagrams for W + 1.5 wt.% Mo high-speed tool steels, including some which contain vanadium and some which do not. The theory and principles of alloying are extended to other steels such as R-W6Mo5Cr4V2, R-W2Mo5, W11Mo5V, W11Mo7Cr23Co, and ledeburite (Fe-C + 5.5 % Mo) steels on the basis of their constitution diagrams. The performance of these variously alloyed steels is then analyzed on the basis of their microstructural examination as well as on the basis of diagrams depicting the dependence of their Vickers hardness on the test temperature and diagrams depicting the kinetics of tool-wedge wear during cutting, initial wear at an almost constant low rate being followed by fast wear at a rate which increases up to a catastrophic level due to softening of the solid solution (small grains precipitating along boundaries of originally existing ones) as well as due to development of pores and cracks during creep. Figures 7; references 14.

Phase Equilibria in Fe-N-C System

927D0027D Moscow METALLOVEDENIYE I TERMICHESKAYA OBRABOTKA METALLOV in Russian No 6, Jun 91 pp 14-17

[Article by R.D. Rusev, Bulgaria]

UDC 669.017.3:669.14

[Abstract] Phase equilibria in the ternary Fe-N-C systems are analyzed, for a comprehensive interpretation of the carbonitriding process. The analysis is based on the constitution diagrams of both binary Fe-C and Fe-N systems as well as on isothermal sections of Langenscheid's Fe-N-C constitution diagram and on known crystallographic characteristics of the various phases. Considering that the isothermal sections of that Fe-N-C constitution diagram are topologically correct, two series of polythermal sections of this diagram are constructed in accordance with the reaction-diffusion mechanism of carbonitride layer formation: eight T - % N sections (T = 450-750°C, 0-12 % N) for eight different fixed carbon contents (0.1 %, 0.2 %, 0.35 %, 0.45 %, 0.6 %, 0.8 %) and six T - % N sections (T = 450-720°C, 0-10 % N) for six different fixed C:N ratios (1:10, 1:8, 1:5, 1:3, 1:2, 1:1). These sections indicate essential differences between a carbonitride layer and a nitride layer, already minute amounts of carbon causing appreciable changes in the phase composition. The six major items characterizing a carbonitride layer are: 1) favorable conditions for formation of two-phase zones by reaction; 2) individual one-phase and two-phase regions with smoother and more diffuse boundaries; 3) only cementite (Cm = Fe_3C) entering α + Cm, γ' + Cm, ε + Cm zones involved in phase equilibria when carbon content is up to 2 % C or when C:N = 1; 4) a thermodynamically unstable intermediate "transition" layer forms between "white" and diffusion layers as the carbonitride formation temperature rises and carbon content in the layer increases; 5) cementite content in the various zones depends on conditions of phase equilibrium and its content in steel thus changes upon formation of ε + Cm, γ + Cm, γ' + Cm, α + Cm two-phase zones (which agrees with experimental data indicating formation of cementite in the "white" layer in low-carbon steels and decarburization of the diffusion layer near the "white" layer in medium-carbon and high-carbon steels); 6) secondary phase reactions take place as the degree of saturation increases during cooling, metastability of the three ε, γ, and α phases making it possible for one peritectoid and four eutectoid reactions producing a carbonitride layer to occur. Figures 3; references 9.

New Phosphatizing Materials for Cold Metal Straining

927D0112C Moscow KUZNECHNO-SHTAMPOVOCHNOYE PROIZVODSTVO in Russian No 9, Sep 91 pp 7-8

[Article by V.A. Chmayevskiy, A.V. Kapralov]

UDC 621.794.62:669.1.69

[Abstract] The use of phosphate coats as backing layers in cold metal straining, especially in cold forging and deep drawing, and the requirements imposed on the phosphate films used for this purpose are discussed. The new phosphatizing materials developed by the Buy chemical plant, the KTsF-51 and NK-11, are examined and their effect on the metal and die surface is compared to that of the traditional KFE-1 phosphatizing composition; the effect of the phosphatizing solution composition on the wear resistance properties of the coat produced by KFE-1, KTsF-51, and NK-11 is plotted. An analysis shows that the KFTs-51 and NK-11 solutions result in somewhat lower mass of the coats and better physical and mechanical properties than KFE-1; the new coats have a higher density and corrosion resistance. Figures 1; tables 1; references 11: 7 Russian, 4 Western.

Unit for Rotational Extrusion by Inclined Die

927D0112F Moscow
KUZNECHNO-SHTAMPOVOCHNOYE PROIZVODSTVO in Russian No 9, Sep 91 pp 23-24

[Article by V.F. Stepanov, I.Yu. Suzdaltsev, Yu.A. Sokolov]

UDC 621.531.792

[Abstract] Specifications of a kinematic-type mechanism for rotational extrusion by inclined dies first described in *Kuznechno-shtampovochnoye proizvodstvo* No. 19, 1978 are cited, its schematic diagram is presented, and its operation is explained in detail. The unit is driven by a 4.0 kW electric motor and develops an axial pressure of 30 kN. The unit is mounted on the table of a vertical drilling machine. The principle of double metal flow focus localization—due to the tool incline and to its eccentric position relative to the part—is utilized. The machined parts have an ISO accuracy class 8 and a surface roughness of 0.65-1.1. Figures 1; references 2.

Mechanized Process Complexes for Orbital Forming of Hollow and Tube Items

927D0112E Moscow
KUZNECHNO-SHTAMPOVOCHNOYE PROIZVODSTVO in Russian No 9, Sep 91 pp 21-22

[Article by N.A. Koryakin, A.A. Kolupayev, F.S. Kokin, I.D. Galimov]

UDC 621.77.3:658.011.56.002.2

[Abstract] Three types of process complexes used for orbital forming (ShO) of hollow and tube-like items—rotary lines with an orbital forming drive in each tool block, orbital forming complexes for medium and large-size blanks, and complexes for medium-size blanks utilizing specialized PKW-100A and PKW-200 die forging presses—are discussed. One of the first orbital forming complexes developed at the Izhevsk Mechanical Institute is examined in detail and its principal specifications are cited. The complex utilizes the P0440ShO, P2940ShO, P7836, P7834, PA7834, and Mueller presses which develop a force of 2,500 to 10,000 kN with a punch rate of up 0.5 to 95 mm/s. The blank installation and removal procedures are outlined. The complexes can be easily retooled and meet the main demand of today's technology—ensure succession with respect to the principal parameters of forge shops which do not have to be modified substantially when switching from one product to another. Figures 1; tables 2; references 2.

Using Mathematical Methods to Select Alloy Which Extends Tool Life During Plastic Metal Working

927D0112D Moscow
KUZNECHNO-SHTAMPOVOCHNOYE PROIZVODSTVO in Russian No 9, Sep 91 pp 8-9

[Article by V.A. Falkovskiy, Yu.V. Rudakov, M.V. Kuralina, N.Yu. Matyushina]

UDC 621.73.073.002.3:669.018.25

[Abstract] Experimental data which indicate that groups S, KS, and K high-temperature carbide-based hard alloys ensure the longest tool service life at various plastic metal working operations, i.e., upsetting, die forging, stamping, drawing, and rolling, are discussed and an attempt is made to control the carbide phase concentration and grinding duration as well as the alloy composition in order to select the optimum alloy brand which ensures the longest tool life. To this end, experimental data are processed on a computer (EVM) by the linear regression analysis method and analytical expressions are derived for selecting the alloy. The mathematical procedure is illustrated using the example of selecting the VK20 alloy for a blanking die. The sensitivity of the WC-Co solid solution's mechanical properties to a change in the cobalt concentration and the carbide phase grain size is plotted. The results show that the equations derived on the computer by the linear regression analysis method are indeed suitable for determining the sensitivity of the principal mechanical properties, primarily antifriction, of WC-Co solid solutions to changes in the cobalt concentration and carbide phase grain size. Figures 1.

Effect of Forging Process Parameters on Titanium Alloy Billet Quality

927D0112A Moscow
KUZNECHNO-SHTAMPOVOCHNOYE PROIZVODSTVO in Russian No 9, Sep 91 pp 4-5

[Article by S.A. Mashekov, V.A. Petrov, A.V. Kotelkin, V.K. Vorontsov (deceased)]

UDC 621.73.002.63.004.12

[Abstract] The shortcomings of existing methods of producing blanks from titanium alloys with a fine grain structure are addressed and the procedures used to improve the die forging quality and increase the process output by controlling the forging process parameters, i.e., the flat die configuration, relative feed, unit reduction, and tilting angle, are considered. The effect of the above forging process parameters on the quality of titanium alloy blanks is analyzed in two forging experiments whereby commercial ingots from the VT1 alloys with 750 mm dia. by 1,875 mm dimensions and VT3-1 alloy with 560 mm dia. by 1,400 mm dimensions are forged. The mechanical properties of the pilot forgings are consistent with the mechanical properties of the metal produced by drawing in flat dies with subsequent multiple upsetting and drawing. The principal patterns of the accumulated strain distribution in the cross section as a function of the die forging process parameters are established; the results indicate that upsetting operations may be eliminated from the production process thus lowering the labor outlays and increasing the yield of the process without sacrificing the blank quality. References 4.

Experimental Investigation of Backward Extrusion by Rotating Embossing Punch

927D0112B Moscow
KUZNECHNO-SHTAMPOVOCHNOYE PROIZVODSTVO in Russian No 9, Sep 91 pp 5-6

[Article by M.K. Sergeyev]

UDC 621.777.44.001

[Abstract] Methods of producing hollow blanks—bushings, tubes, liners, and H-shaped parts—and extending the tool servic life by various means are discussed and the effect of the face surface of the punch relief and its straining pattern on the backward extrusion pressure of hollow blanks or H-shaped parts is investigated. The study is conducted on a specially designed test unit with a hollow-part extrusion die. A schematic diagram of the test unit is presented and the dependence of the experimental values of pressure and shearing strain on the torsion angle during the reverse extrusion of lead, soft aluminum, and copper is plotted. An analysis demonstrates that the use of the die with a rotating embossing punch makes it possible to lower the axial force and contact stress intensity as well as reduce the sticking zone in the central area due to an additional tangential stress of the radial metal flow; the method also makes it possible to equalize the strain during the metal transition from the bottom section to the vertical wall and reduce energy outlays and increase the die strength and reliability. Figures 2; references 4.

Weldability of High-Strength Steel 12GN3MFAYuDR-SSh

927D0064B Kiev AVTOMATICHESKAYA SVARKA in Russian No 11(464), Nov 91 pp 12-16

[Article by L.I. Mikhoduy, A.K. Yushchenko, V.D. Poznyakov, T.A. Korniyenko, V.I. Panov, I.M. Izyuryev, Yu.I. Baryshnikov, Electric Welding Institute imeni Ye.O. Paton at the Ukrainian Academy of Sciences and Uralmash Production Association]

UDC [621.791.011:669.14.018.295].001.5

[Abstract] The effect of the high nickel content as well as copper and boron alloying additives in cold-resistant steel 12GN3MFAYuDR on its structure and properties, especially weldability, is discussed the properties of steel 12GN3MFAYuDR are investigated, and the effect of the thermal welding cycle on its structure is estimated. In addition, the resistance to cold cracking during welding is determined. To this end, 16 mm thick sheets of steel 12GN3MFAYuDR-SSh were tested to determine its strength and ductility. The dependence of tensile strength, ductility and impact toughness under impact bending of steel 12GN3MFAYuDR-SSh on temperature is plotted and compared to similar characteristics of steels 12GN2MFAYu and 12GN2MFAYu-U; a continuous cooling austenite transformation diagram of steel 12GN3MFAYuDR-SSh is plotted and the microstructure of arc-welded joints from steel 12GN3MFAYuDR-SSh is studied. The effect of the cooling rate and diffusion hydrogen concentration on the rupture strength of implant-type specimens from steel 12GN3MFAYuDR-SSh is considered. An analysis demonstrates that steel 12GN3MFAYuDR-SSh performs well at temperatures up to -70°C and that under the effect of thermal welding cycles, austenite transformation in the heat affected area (ZTV) of welded joint in steel 12GN3MFAYuDR-SSh occurs in the bainite and martensite areas whereby structural transformations are generally completed within a 200-250°C range. An increase in the heat affected area cooling rate in steel 12GN3MFAYuDR-SSh welds increases the strength of the metal but has virtually no effect on its ductility; the optimum rate is 3-19°C/s. It is recommended that diffusion hydrogen concentration in the surfaced metal be kept under 100 ml/100 g. Figures 8; references 6.

Joint Structure of Electron-Beam-Welded Dissimilar Steels

927D0064C Kiev AVTOMATICHESKAYA SVARKA in Russian No 11(464), Nov 91 pp 17-21

[Article by V.M. Nesterenkov, D.Yu. Novikov, I.P. Kirpach, Electric Welding Institute imeni Ye.O. Paton at the Ukrainian Academy of Sciences]

UDC [621.791.72.052:669.14]:620.18.001.5

[Abstract] The need to improve the operating properties of machines and the resulting need to use dissimilar steels in the same assembly and welded joints are identified and structural characteristics of dissimilar joints from steels 20Kh12VNFM and 20KhN3MFA produced by electron beam welding are studied. Electron beam welding was selected because it makes it possible to minimize the weakness zone. Micro- and macrosections of the welded joints are examined on both sides of the fusion boundary. The hardness distribution in the joints after welding and after tempering and the alloying element distribution in the fusion zone are plotted. An analysis of study data makes it possible to draw the conclusion that joints of steels 20Kh12VNFM and 20KhN3MFA must be heat treated in order to decrease their structural heterogeneity and reduce and equalize their hardness. The presence of a light strip in the welded joint's heat affected area on the side of steel 20KhN3MFA in which the concentration of alloying elements changes sharply and impact strength decreases at subzero temperatures imposes additional stringent requirements on the welded joint structure from the safety margin viewpoint. Figures 8; tables 1; references 2.

On Intermediate Layer Formation Mechanism During Welding of Titanium to Steel

927D0064D Kiev AVTOMATICHESKAYA SVARKA in Russian No 11(464), Nov 91 pp 22-24

[Article by O.G. Bykovskiy, I.V. Pinkovskiy, V.R. Ryabov, Zaporozhye Mechanical Engineering Institute imeni V.Ya. Chubar and Electric Welding Institute imeni Ye.O. Paton at the Ukrainian Academy of Sciences]

UDC 621.791.4:[669.295+669.15.194.56/.57]:539.4

[Abstract] The processes occurring during the resistance spot welding of titanium to steel at the moment when the welding current is disconnected are discussed and it is speculated that the interaction of molten steel with solid titanium in the contact occurs in two successive stages: adsorption and the formation of intermetallic compounds—first by means of a chemical reaction, then by diffusion. The mechanism of the intermediate layer formation during the welding of titanium to steel is investigated; to this end, the heat of formation, entropy, and change in Gibbs energy of the intermetallic compound formation during welding, the dependence of the Ti-F system alloy diffusivity on the alloy composition, and the intermediate layer composition and thickness as a function of welding method are examined. Friction welding, resistance spot welding, and diffusion welding in a vacuum are considered. The results show that during resistance spot welding, the intermediate layer forms due to reactive diffusion whereby the TiFe intermetallic compound is mode "favorable" from the energy viewpoint; moreover, the intermediate layer thickness is determined by the character of the thermal diffusion action; rapid hammering makes it possible to reduce the layer thickness. Tables 3; references 15: 10 Russian; 5 Western.

Assessment of Technological Strength of Multipass Welded Joints by X-Ray Method

927D0064G Kiev AVTOMATICHESKAYA SVARKA in Russian No 11(464), Nov 91 pp 41-43

[Article by V.I. Panov, T.M. Novoselova, V.Ye. Solomatin, Uralmash Production Association]

UDC [621.791.75.052-413:539.4]:621.386

[Abstract] An attempt to assess the technological strength of multipass welded joints by portable X-ray units in order to determine the probability of brittle failure and take timely measures to prevent it is described. In the experiments, steel 14Kh2GMR was used as the base metal and APN-1 (E-70) and UONI-13/55 (E-50A) electrodes were used to make a control beaded weld. The beveling for the deformation seam was filled using OZL-6 austenite electrodes which ensure the highest angular deformation level. The change in angular deformation and stress within and without the concentrator as a function of the number of deformation weld beads is plotted. An analysis shows that the stress distribution in the welded joint metal with a stress concentrator is nonuniform and changes as the beveling becomes filled from pass to pass. The weld strength and the brittle failure probability can be tentatively assessed by the change in the stressed state and the diffraction line broadening while the critical state of the welded joint metal can be evaluated by the termination of the physical diffraction line broadening. Figures 3; references 3.

Copper and Silicon Diffusion in Welded Joint of Silicon Bronze and Steel

927D0064E Kiev AVTOMATICHESKAYA SVARKA in Russian No 11(464), Nov 91 pp 25-28

[Article by A.Ye. Vaynerman, Prometey Science Research Institute]

UDC 621.791.75:[669.35'6+669.141.24]:548.526:[546.56+546.28]

[Abstract] The effect of the depth of the intermediate diffusion layer forming in the fusion zone during the welding of bronze BrKMts3-1 to steel or its surfacing upon steel on the mechanical properties of welded joints is investigated; the diffusion layer metal is brittle and very hard (HV≥350) and has a relatively low ultimate rupture strength (320 MPa) and impact strength (20 kJ/m^2). Samples for the study were cut from clad metal blanks produced by plasma jet surfacing of bronze BrKMts3-1 on steel VSt3, 20, and 35KhNMA, as well as by coating steel by molten bronze. The microstructure of diffusion layers on samples made by plasma jet surfacing after homogenizing annealing is examined and the element concentration variation in the layer is plotted. The parameters of copper and silicon diffusion into steel are summarized and the diffusion layer growth in the BrKMts3-1-steel 20 system and in So-Fe and Cu-Fe systems is plotted. The study reveals that during the welding of silicon bronze with steel or its plasma jet surfacing on steel, copper and silicon diffuse jointly from bronze into steel while the depth of joint diffusion is considerably greater than that of copper alone; conversely, the joint diffusion activation energy is much lower than that of copper diffusion alone. Figures 3; tables 1; references 11: 10 Russian, 1 Western.

Investigation of Zr Alloy and Ti Alloy Joint Formation Process During Vacuum Brazing

927D0064F Kiev AVTOMATICHESKAYA SVARKA in Russian No 11(464), Nov 91 pp 29-32

[Article by A.A. Chularis, M.M. Mikhaylova, L.A. Derbaremdiker, Rostov na Donu Institute of Agricultural Machinery Industry]

UDC 621.791.36.052:[669.295.5+669.296.5].005

[Abstract] The use of titanium, zirconium and their alloys in chemical and aerospace engineering and the difficulties of joining these materials by sharp edge projection welding are discussed; an attempt to use vacuum brazing to produce joints of titanium and zirconium or their alloys is described. An analysis of possible joining methods shows that silver, zirconium, or titanium brazing solders are the most likely to produce dissimilar joints of titanium and zirconium alloys. The N-2.5 zirconium alloy containing 2.5% niobium and the PT-3V pseudo-α-alloy of titanium were used in the study. The alloys' compositions, mechanical properties, and wettability at normal conditions are summarized. The microstructure of a brazed joint of the above two alloys is examined. An investigation of the phase structure, chemical, and mechanical inhomogeneities of the brazed joints shows that the alloys do not display any phase structure anomalies in the heat affected area and that the brazed seam also displays no abnormalities. The seam metal composition corresponds to the solid solution of the alloying elements in α-Zr and intermetallic compounds of Zr and Ti with Co; consequently, the brazed seam's mean microhardness is 5,600-7,500 N/mm^2. It is recommended that the above joints be used in machine- and instrument-building but not used in structural members of nuclear power plants due to the high thermal neutron capture cross section of Co atoms and long-lived strong ^{60}Co γ-radiation. Figures 4; tables 2; references 6: 5 Russian; 1 Western.

Friction Welding of Bronze Br012 and Silumin to Steels Through Intermediate Copper and Aluminum Layers

927D0064H Kiev AVTOMATICHESKAYA SVARKA in Russian No 11(464), Nov 91 pp 56-57, 63

[Article by I.A. Chernenko, A.G. Zakharov, I.A. Tsirul, B.A. Forostovets, Electric Welding Institute imeni Ye.O. Paton at the Ukrainian Academy of Sciences]

UDC 621.791.14:[669.35'6+669.14]

[Abstract] The possibility joining antifriction bronze Br012 to steel 40Kh through a copper layer as well as joining silumin to steel St3 through an aluminum layer using a machine with a rotating insert is investigated. To this end, friction welding was performed in an ST-104 friction welding machine with a rotating insert developed at the Paton Institute; the machine is capable of rotating the insert at two different speeds in both directions. Microsections of bronze and silumin welded joints with steel are examined and the microhardness distribution in 40Kh+M2+Br012 and St3+AD1+silumin joints is plotted. An analysis demonstrates the adequacy of the method for obtaining the above types of joints by friction welding and shows that it takes less than half the time required for successively welding two butt joints; the method of friction welding through an intermediate layer makes it possible to joint together incompatible materials and ensures a good quality of joint. Figures 4; references 4: 3 Russian; 1 Western.

Selecting Optimum Process Parameters of Underwater Cutting by Flux-Cored Wire

927D0064I Kiev AVTOMATICHESKAYA SVARKA in Russian No 11(464), Nov 91 pp 61-63

[Article by M.Ye. Danchenko, Yu.N. Nefedov, Electric Welding Institute imeni Ye.O. Paton at the Ukrainian Academy of Sciences]

UDC 621.791.94.042.004.13(204)

[Abstract] The characteristics of mechanized underwater flux-cored wire cutting (RPP) method are discussed and the need to find the optimum energy parameters of the process, i.e., correctly select the power supply source and determin the optimum ratio of cutting arc parameters allowing for the process factors affecting the arc burning stability, in order to ensure a high technological efficiency of the method is identified. The dependence of the cutting current on the flux-cored wire feed rate at a 10 m immersion depth, the domain of optimal arc voltage values at various immersion depths, and the dependence of the cutting speed on the immersion rate are plotted. Process conditions of underwater flux-cored wire cutting are summarized for a depth of 10, 20, and 30 m. Formulas for the specific flux-cored wire consumption and specific electric power consumption of the underwater flux-cored wire cutting method are calculated; based on these calculations, one can assess the technological efficiency of the method allowing for the change in hydrostatic pressure. For mechanized cutting of up to 10 mm thick steel at a 30 m depth, it is expedient to use flux-cored wire with a 2.0 mm diameter while for 20 mm thick metal at a 60 m depth, flux-cored wire with a 2.4 mm diameter is more efficient. Figures 2; tables 1; references 3.

Weldability of Magnetic Steels With Nonmagnetic Alloys

927D0064A Kiev AVTOMATICHESKAYA SVARKA in Russian No 11(464), Nov 91 pp 7-11

[Article by L.M. Lobanov, L.P. Shatalov, V.M. Klepov, A.A. Borzunov, Electric Welding Institute imeni Ye.O. Paton at the Ukrainian Academy of Sciences and Energiya Scientific Production Association, Voronezh]

UDC 621.791.75.011:[669.15-194.53+669.14.018.584]

[Abstract] The poor weldability of pearlitic magnetic steel, primarily 20Kh3MVF (EI415), and nonmagnetic alloys is discussed and the weldability of magnetic steel 20Kh3MVF with nonmagnetic alloys 36NKhTYu, 40KhNYu, KhN55MBYu (EP666-VD) is investigated. The study reveals the the use of welding for the 20Kh3MVF+36NKhTYu pair is inefficient due to cracking in the weld while the 40KhNYu and KhN55MBYu alloys lend themselves to argon arc welding with steel 20Kh3MVF and produce a good welded joint. Furthermore, the strength of 20Kh3MVF+40KhNYu welded joint is lower than that of the 20Kh3MVF+KhN55MBYu; this fact must be taken into account in developing specifications for the specific products. The welding conditions and methods suitable for each specific pair of pearlitic steel and nonmagnetic alloy are identified and microstructures of the fusion zones of various pairs are examined. Figures 4; tables 7; references 7.

Welding Characteristics of Radionuclide Source Bodies From Dissimilar Materials

927D0092A Moscow SVAROCHNOYE PROIZVODSTVO in Russian No 12(686), Dec 91 pp 2-3

[Article by Ye.M. Tabakin]

UDC 621.791.72:621.375.826

[Abstract] The need to change the body design of radionuclide sources with a cobalt core used in medicine and other fields is identified and an attempt is made to select a metal most compatible with cobalt from the weldability viewpoint from among a series of nonactivatable metals (nickel, titanium, and vanadium), choose a welding metal, develop a welding technology, and select a method of estimating the welded joint quality. The optimum combination of welded metals is selected on the basis of general approaches to the welding of dissimilar materials. Radionuclide source designs are presented and the microstructure of the welded joint of the cobalt core with a nickel slab is examined under a microscope. The procedure of surface preparation for welding is outlined. An analysis shows that it is expedient to use nickel for producing a welded joint of the cobalt rod with the slab for producing a ^{60}Co radioactive source and that laser welding makes it possible to ensure the necessary

welded joint quality. No intermetallic phase is detected in the Ni-Co weld whose microhardness reaches 220-230 given a cobalt and nickel microhardness of 230-240 and 130-140, respectively. Figures 2; references 2.

Quantitative Strength Assessment of Joints From Dissimilar Metals

927D0092B Moscow SVAROCHNOYE PROIZVODSTVO in Russian No 12(686), Dec 91 pp 9-11

[Article by V.N. Dubrov, D.I. Vasilevich, L.I. Novikov, Vyatka Polytechnic Institute]

UDC 621.791.052-192

[Abstract] The difficulty of testing joints made from dissimilar materials due to a difference in their ductility and plasticity, the need for reliable methods of quantitatively assessing the fracture strength of the contact surface between the materials, and the inadequacy of known published sources are discussed and an attempt is made to determine the optimum method of assessing the technological stability of pressure welding of aluminum-steel and steel-zirconium joints and selecting a loading method while taking into account the character of the load and sample configuration. Samples with a pressure welded joint of steel 1Kh19N9 with technical aluminum AD1 and with an alloy of Zr with 2% Nb cut by milling are studied. The general configuration of test billets and the loading diagram are presented; the fatigue endurance distribution at a 150 MPa load is plotted. The experiments confirm that the strength of welded joints from dissimilar materials may be reliably determined only to the extent of the fracture strength along the contact surface; as a result, it is possible to differentiate only joints with equally satisfactory qualities. In testing the strength of welded joint made from materials with widely differing mechanical properties it is expedient to use a combination of cyclical torsion and bending tests with precision stress concentration in the soft material. Figures 3; references 7.

Effect of Dimensional Chemical Pickling on Fatigue Endurance of Butt Welded Joints From Alloy 1420

927D0092C Moscow SVAROCHNOYE PROIZVODSTVO in Russian No 12(686), Dec 91 pp 12-13

[Article by A.A. Movchan, S.A. Kazarina, M.L. Lyapunov, V.V. Ovchinnikov, Moscow Aviation Institute imeni S. Ordzhonikidze and MAPO imeni Mendeleyev]

UDC 621.791.052:539.43:669.7.018

[Abstract] The effect of decomposition products of the lithium compound in the surface layer of aluminum-lithium alloys and the hydrogen gas release on the development of pores during welding which serve as stress concentrators and lead to the formation of premature fatigue cracks is discussed and the effect of the dimensional chemical pickling depth on the fatigue endurance of butt welded joints from sheets of alloy 1420 is investigated. To this end, fatigue tests of pickled and untreated samples are conducted and the results are compared. The automatic argon-arc butt welding procedure is outlined and testing methods are described. Experimental data are statistically processed and the results are summarized. The conclusion is drawn that double-sided 0.2 mm-deep chemical pickling before welding leads to a four- to fivefold increase in the fatigue endurance of butt welded joints from alloy 1420 due to lowering the pore formation intensity as a result of removing the offending lithium compound layer. Tables 2; references 7: 6 Russian; 1 Western.

Nondestructive Testing of Welded Wiring Quality During Electronic Device Assembly

927D0092E Moscow SVAROCHNOYE PROIZVODSTVO in Russian No 12(686), Dec 91 p 29

[Article by V.G. Sizov, A.A. Gulyayev, Z.M. Slavinskiy, A.V. Poduvaltsev, NIITOP, Nizhniy Novgorod]

UDC 621.791.05:620.179:621.37

[Abstract] Three methods of quality control of the welded wiring used in the electronics and semiconductors industry today and their shortcomings are outlined and the advantages of nondestructive testing of welded wiring during the assembly process are discussed. The need to develop an optimum testing check force applied to microelectronics components in order to guarantee the necessary product strength and increase the proportion of serviceable products is identified and a formula for computing this force is derived. The proposed method can be used during the assembly of wire terminals and guarantees their quality in ready products.

Individual Screening From Optical Radiation and Aerosol During Welding

927D0092D Moscow SVAROCHNOYE PROIZVODSTVO in Russian No 12(686), Dec 91 pp 26-28

[Article by I.S. Alekseyeva, E.A. Kolodnin, V.N. Belov, All-Union Scientific Research Institute of Work Safety, Leningrad]

UDC 621.791:658.34:628.83

[Abstract] The effect of optical radiation and aerosol on the respiratory system and sight and relevant shielding devices, mostly foreign made, are discussed and a classification of welding and protective device types developed at the All-Union Scientific Research Institute of Work Safety is summarized. The results of lab tests of Swedish Speedglass Fresh Air welder masks made by the Hernall company are presented. They show that the masks ensure class 2 protection pursuant to GOST 12.4.034—85; over an extended period of operation, the mask is superior to other individual protection devices in that it does not change in color or shape and is resistant to sparks, drops, and mechanical impacts. It also provides complete facial protection and is pressurized, thus avoiding aerosol suction from the work environment. Proper use ensures 1,000 h of air filter operation on one battery. Together with a turbine unit, the mask meets the specifications of regulatory acts and GOST's. Tables 4; references 7.

Microencapsulation of Metallic Powders to Prevent Explosions and Dusting During Their Production and Processing: III. Gas Evolution Kinetics

927D0088F Kiev POROSHKOVAYA METALLURGIYA in Russian No 10(346), Oct 91 pp 96-100

[Article by O.V. Yefremov, O.D. Neykov, P.B. Rabin, M.F. Salomatkina, Institute of Materials Science Problems at the Ukrainian Academy of Sciences]

UDC 613.6

[Abstract] The fire and explosion hazard posed by small fractions as well as the gaseous products resulting from the metallic powder interaction with the corrosive products present in the production environment necessitated an investigation of the effect of microencapsulation on the gas evolution kinetics during said interactions. A Rekord-3F recording complex capable of automatically and continuously monitoring the gas evolution kinetics within a broad range and recording them is used to examine the reaction of metal and alloy powders with liquid media, e.g., water and solutions of acids and alkali. The experimental procedure is outlined and a block diagram of the Rekord-3F complex is presented. The composition of gaseous products of aluminum and rare earth metal alloying composition powders with water is examined and the interaction kinetics of untreated and microencapsulated powders of various contents with water are plotted. The microencapsulation process—treatment with a film-forming composition during the atomizing—is explained. An analysis demonstrates that kinetic components of reactions are dominant over the diffusion components. Microencapsulation makes it possible to reduce the dusting factor by 10-40 times. Figures 3; tables 1; references 5.

Classification of Foundry Working Condition Evaluation Criteria: Discussion

927D0083E Moscow LITEYNOYE PROIZVODSTVO in Russian No 12, Dec 91 pp 19-20

[Article by D.M. Kukuy, A.M. Lazarenkov, Belarus Polytechnic Institute]

UDC 621.74:658.382

[Abstract] The totality of factors which determine the foundry working conditions—the dust content, gas content, noise, vibration, thermal emission, illumination, electromagnetic radiation, and microclimate—is summarized and a classification of foundry working condition evaluation criteria developed on the basis of the above factors and its underlying principles are described. The classification makes it possible to evaluate alternate foundry designs and select the most appropriate version for each casting foundry type from the health viewpoint. A process chart listing all working condition parameters for the specific foundry processes, e.g., core-making machines, knocking out, etc., is compiled. Maximum permissible levels (PDU) and maximum permissible concentrations (PDU) and their excess ranges are established for various factors. The evaluation system was tested in Belarus foundries and revealed a good consistency of experimental and theoretical data. Tables 1.

END OF FICHE DATE FILMED

5 May 1992